

RIGA TECHNICAL UNIVERSITY
Faculty of Civil Engineering
Institute of Building Production

Sanita Rubene

Doctoral study programme „Civil Engineering”

**METHODOLOGY FOR DETECTION
OF MOISTURE DISTRIBUTION THROUGHOUT
THE CROSS SECTION OF AUTOCLAVED
AERATED CONCRETE MASONRY
CONSTRUCTIONS BY APPLICATION
OF EIS METHOD**

Doctoral Thesis

to Obtain the Degree of *Dr. sc. ing.* in Construction Science,
Subfield of Construction Materials and Technology (P-06)

Scientific supervisors

Dr. sc. ing., Associated Professor

M. Vilnitis

Dr. sc. ing., Professor

J. Noviks

Riga 2016

Annotation

In the thesis, there are included results of comprehensive research of application of electrical impedance spectrometry (EIS) for determination of moisture content in autoclaved aerated concrete (AAC) constructions. The research results display correlation between EIS and moisture content rate in AAC masonry constructions. As a result of the research correlation formulas between moisture content rate of the material and EIS measurement result have been established. A methodology for application of EIS for non-destructive detection of moisture distribution throughout a cross section of AAC masonry constructions has been developed and described in these thesis.

The thesis consists of 112 pages, 107 figures, 4 tables, 114 references.

Anotācija

Promocijas darbā ir atspoguļoti pētījuma rezultāti elektriskās impedances spektrometrijas (EIS) metodes pielietošanai mitruma satura noteikšanai gāzbetona (AAC – autoclaved aerated concrete) konstrukcijās. Pētījuma rezultātā ir noteiktas matemātiskas sakarības starp mitruma saturu gāzbetonā un EIS mērījumu rezultātiem. Promocijas darba ietvaros ir izstrādāta negraujoša pārbaužu metodika EIS metodes pielietošanai mitruma satura un tā sadalījuma noteikšanai pa gāzbetona konstrukcijas šķērsriezuma laukumu.

Darbā iekļautas 112 lapaspuses, 107 attēli, 4 tabulas, 114 literatūras avoti.

Table of contents

Annotation.....	2
Anotācija	3
Table of contents	4
General Description of the Doctoral Thesis	7
<i>Actuality of the Research and Formulation of the Problem</i>	7
<i>The Aim of the Research</i>	7
<i>The Tasks of the Research</i>	8
<i>Scientific Novelty of the Research Results</i>	8
<i>Application of the Research Results</i>	9
<i>Methodology of the Research</i>	9
<i>Theoretical and Methodological Basis of the Research</i>	10
<i>Scope of the Study</i>	11
<i>Results Presented for Defence</i>	11
<i>Approbation of the Results</i>	11
<i>List of International Conferences</i>	12
<i>List of Scientific Publications on the Subject of the Doctoral Thesis</i>	13
<i>Structure and Contents of the Doctoral Thesis</i>	16
INTRODUCTION.....	17
<i>Statement of problem and aim of the research</i>	17
<i>The aim of the research</i>	17
<i>The tasks of the research</i>	18
<i>Scientific novelty of the research results</i>	18
1. MATERIALS AND METHODS.....	19
1.1. <i>Structure and main properties of aerated concrete</i>	19
1.2. <i>Direct measurements of moisture content in autoclaved aerated concrete constructions</i>	24
1.3. <i>Non-destructive methods for detection of moisture content in autoclaved aerated concrete constructions</i>	25
1.3.1. <i>Radiological non-destructive methods for detection of moisture content in autoclaved aerated concrete constructions</i>	25
1.3.2. <i>Non-destructive methods for detection of moisture content in autoclaved aerated concrete constructions based on heat flow measurements</i>	28
1.3.3. <i>Detection of moisture content in autoclaved aerated concrete constructions by materials hygrometric performance</i>	31
1.3.4. <i>Electrical non-destructive methods for detection of moisture content in autoclaved aerated concrete constructions</i>	33

1.4.	<i>Method of electrical impedance spectrometry</i>	35
1.4.1.	<i>Previous researches on application of electrical impedance spectrometry for moisture distribution in concrete and porous materials</i>	37
1.4.2.	<i>Frequency analysis in EIS</i>	40
1.4.3.	<i>Application of EIS on autoclaved aerated concrete masonry constructions</i>	42
1.5.	<i>Z-meter III device for electrical impedance spectrometry measurements</i>	43
2.	EXPERIMENTS	46
2.1.	<i>Frequency analysis for the AAC material</i>	46
2.1.1.	Description of the experiment.....	46
2.2.	<i>Correlation between the moisture content and EIS measurement values in AAC masonry constructions</i>	54
2.2.1.	Description of the experiment.....	54
2.2.2.	Results.....	56
2.3.	<i>Measurements of moisture distribution throughout the cross section of single AAC masonry block</i>	59
2.3.1.	Description of the experiment.....	59
2.3.2.	Results	63
2.3.3.	<i>Impact of the bore diameter on measurement results</i>	65
2.3.4.	<i>Impact of the silicone filling on the measurement results</i>	66
2.3.5.	<i>Impact of the liquid silicone on the measurement results</i>	67
2.3.6.	<i>Impact of measurement direction vs the expansion direction of AAC on the results of EIS measurements</i>	69
2.4.	<i>Impact of the pore distribution throughout the volume of the AAC masonry blocks on its hygrometric properties</i>	70
2.4.1.	Description of the experiment.....	71
2.4.2.	Results.....	73
2.5.	<i>Impact of masonry joints on the results of moisture distribution measurements in AAC masonry constructions by EIS</i>	79
2.5.1.	Description of the experiment.....	80
2.5.2.	Results.....	81
2.6.	<i>Monitoring of the drying process of AAC masonry constructions by EIS</i>	84
2.6.1.	Description of the experiment.....	84
2.6.2.	Results.....	85
2.6.2.1.	Monitoring of moisture distribution changes in the wall fragment within single block	85
2.6.2.2.	Monitoring of moisture distribution changes in the wall fragment containing masonry joint between blocks	87
2.7.	<i>Impact of finishing works on drying of AAC masonry constructions</i>	89
2.7.1.	Description of the experiment.....	89

2.7.2. Results.....	91
3. SUMMARY OF RESULTS	94
Conclusions	96
Annexes.....	99
References	100
List of publications.....	109
DECLARATION OF ACADEMIC INTEGRITY.....	112

General Description of the Doctoral Thesis

Actuality of the Research and Formulation of the Problem

Contemporary construction trends are sustainable construction and effective use of construction materials; therefore, load bearing construction materials with high heat insulation parameters tend to become more popular. As an opposite trend, there are short construction terms, which fail to comply with all nuances of the material installation technology. Therefore, non-destructive testing methods have become more and more popular during the past years.

Autoclaved aerated concrete (AAC) masonry blocks are construction material with high heat insulation parameters. In the time of sustainable construction, this material can be used as a load bearing construction material for a range of buildings where it is necessary to obtain high heat insulation parameters of external delimiting constructions. The main problem of AAC masonry constructions is significant influence of moisture content and its gradient on heat resistivity properties of the AAC. It is important to monitor the drying process of AAC masonry constructions in order to avoid sealing of moisture inside the masonry by early application of finishing layers on the construction. Therefore, testing methods, which allow for credible determination of moisture distribution throughout the cross section of the AAC masonry construction as well as moisture migration throughout the cross section of the construction, have to be developed. The drying process of the masonry is a long-term process; therefore, it is preferable to use non-destructive testing methods because a number of measurement series have to be performed in order to provide credible data of the changes in moisture content throughout the cross section of the masonry construction.

There is a variety of manufacturers who offer AAC masonry blocks, and the manufacturing process of the blocks slightly differs as well as the ingredients used for the manufacturing of the blocks. Thus, the porous structure, density as well as chemical composition of the AAC slightly differ. This research has been done to determine the possibility of application of electrical impedance spectrometry for in-situ non-destructive determination of moisture distribution throughout the cross section of AAC masonry constructions.

The Aim of the Research

The aim of the research is to develop a non-destructive testing methodology for detection of moisture distribution throughout the cross section of AAC masonry constructions

under in-situ conditions. After the analysis of previous studies about non-destructive detection of moisture content and its distribution throughout the cross section in solid materials, the tasks of the research have been set.

The Tasks of the Research

1. To determine the correlation between EIS measurement results and moisture content in AAC.
2. To determine the impact of contact surface between measurement probe and AAC masonry construction on the accuracy of the obtained results.
3. To determine the impact of the coating on measurement contact surface on the accuracy of the measurement results.
4. To determine the impact of measurement distance on accuracy of measurement results.
5. To determine the impact of cracks and masonry joints on accuracy of EIS measurement results.

Scientific Novelty of the Research Results

Misunderstanding of the physical processes in construction materials can lead to misuse of effective construction materials and decrease the effectiveness of the properties of constructions designed in compliance with ISO 6946:2007 Building components and building elements - Thermal resistance and thermal transmittance - Calculation method. Therefore, a credible on-site control methodology of moisture distribution in AAC is necessary in order to reach the designed material properties and avoid mistakes during the installation stage of the material.

Previous studies have been focused on non-destructive detection of moisture content and its distribution in solid materials such as concrete. Non-destructive detection of moisture distribution in AAC has not been widely researched due to the uneven and porous structure of the material, which causes problems with repeatability of the measurement results and, therefore, excludes common use of the methodology. Therefore, in the present research an EIS methodology, which is usually applied for moisture detection of bulk materials (such as soil), has been adapted for application on AAC and has reached the aims stated in this research.

Application of the Research Results

The research results can be applied for on-site non-destructive detection of moisture distribution in AAC constructions as a part of quality control activities of the construction process.

Methodology of the Research

The research is based on determination of moisture distribution throughout the cross section of autoclaved aerated concrete (AAC) constructions with Z-meter III device. As a reference material, most commonly used AAC blocks of Latvian construction market were used (Table 1).

Table 1

Type of AAC	Thermal conductivity in dry state stated by manufacturer λ W/mK	Bulk density stated by manufacturer kg/m ³
AEROC Universal	0,090	375
Ytong PP2/0,4	0,105	375
Rocklite	0,11	500
Texoblock classic	0,12	500
Texoblock Lite	0,096	400

At the Laboratory of Water Management Research of the Institute of Water Structures at the Civil Engineering Faculty of Brno University of Technology, a measuring instrument with a Z-meter III device has been developed within the solution of an international project E!4981 of programme EUREKA.



Fig. 1. Z-meter III device with measurement probes.

For control measurements with gravimetric method, electronic scales with precision of ± 5 g were used.

The results were operated by computer software MS Excel and Z-meter III software.

An example of Z-meter III output data has been displayed in Table 2.

Table 2

Z Meter III Output Data

Start at 12.11.2014 9:12:30							
No	f [Hz]	date [dd.mm.yyyy]	time [hh:mm:ss]	ch	range	Rx [ohm]	Xx [ohm]
1	1000	12.11.2014	09:12:30	0	1	101,3	-47,4
2	1000	12.11.2014	09:12:30	1	1	101,4	-47,3
3	1000	12.11.2014	09:12:30	2	1	101,3	-47,3
4	1000	12.11.2014	09:12:31	3	1	101,3	-47,2
5	1000	12.11.2014	09:12:31	4	1	101,4	-47,2

Theoretical and Methodological Basis of the Research

The Thesis has been based upon the following disciplines:

- Construction physics;
- Construction materials and technologies;
- Theoretical base of electrotechnics;
- Materials science;
- Environmental science.

Scope of the Study

The methodology developed for detection of moisture distribution throughout the cross section of AAC by EIS with Z-meter III device as well as the developed correlation equations are valid if the following criteria are met:

1. The EIS measurements are performed within borders of one masonry block, no cracks exceeding 0.1 mm thickness are present in the measurement distance;
2. The distance between measurement probes does not exceed 300 mm;
3. The distance between the measurement probe and AAC does not exceed 1 mm;
4. The measurements are performed in frequency of 8000 Hz.

Results Presented for Defence

- A following methodology for non-destructing detection of moisture distribution throughout the cross section of AAC masonry constructions with Z-meter device has been established:
 1. Choice of measurement points within the AAC masonry construction;
 2. Preparation of measurement bores, cleaning of internal surface of the measurement bores by compressed air;
 3. Frequency analysis of the AAC material (if high accuracy of the EIS measurement results is required);
 4. EIS measurements of the moisture distribution with Z-meter device;
 5. Processing of the measurement results.
- Correlation between EIS measurement results and moisture content in AAC is equal to: $y = a \ln(x) + C$;
- Distribution of pores throughout the volume of AAC has impact on the accuracy of EIS measurement results; therefore, it is advisory to detect expansion direction of the AAC prior the EIS measurements.

Approbation of the Results

The results of the Doctoral Thesis have been reported and discussed in 14 international conferences. The main results of the study have been presented in 16 scientific publications. Five of them have been indexed in SCOPUS database.

List of International Conferences

1. EUREKA 2013, 1st conference and working session, Karolinka, Czech Republic, Brno University of Technology, GEOTest. 30 October – 1 November 2013 (Rubene, S., Vilnītis, M. Application of Electrical Impedance Spectrometry for Determination of Moisture Distribution in Aerated Concrete Constructions);
2. “Innovative Materials, Structures and Technologies”, Riga, Latvia, 28 November – 30 November 2013 (Rubene, S., Noviks, J., Vilnītis, M. Determination of Humidity Level In Aerated Concrete Constructions by Non Destructive Testing Methods);
3. The 18th International Student Scientific and Practical Research Conference “Cilvēks.Vide.Tehnoloģijas”, Rezekne Higher Education Institution, Rezekne, Latvia. 23 April 2014 (Rubene, S., Noviks, J. Frequency Analysis of Electrical Impedance Spectrometry);
4. The 4th International Conference “Advanced Construction”, Kaunas, Lithuania, Kaunas University of Technology, 9–10 October 2014 (Rubene, S., Vilnītis, M., Noviks, J. Monitoring of the Aerated Concrete Construction Drying Process by Electrical Impedance Spectrometry);
5. EUREKA 2014, 2nd conference and working session, Pasohlavky, Brno, Czech Republic, Brno University of Technology, GEOTest. 30 October – 1 November 2014 (Rubene, S., Vilnītis, M. Monitoring of Humidity Distribution Changes in Aerated Concrete Masonry Construction by EIS);
6. 5th European Conference of Civil Engineering, Florence, Italy, 22–24 November 2015 (Rubene, S., Vilnītis, M. Correlation between EIS Measurements and Relative Humidity Distribution in Aerated Concrete Masonry Constructions);
7. 1st International Conference on Civil Engineering, Water Resources, Hydraulics and Hydrology (CEWHH 2014), Athens, Greece, 28 November – 1 December 2015 (Rubene, S., Vilnītis, M., Noviks, J. Impact of Contact Surface on Accuracy of Humidity Distribution Measurements in Autoclaved Aerated Concrete Constructions by EIS);
8. 17th International Conference on Civil, Structural and Geoenvironmental Engineering, London, United Kingdom, 19–20 January 2015 (Rubene, S., Vilnītis, M., Noviks, J. Impact of Masonry Joints on Detection of Humidity Distribution in Aerated Concrete Masonry Constructions by Electric Impedance Spectrometry Measurements);

9. “Vide.Tehnoloģija.Resursi”, Rezekne Higher Education Institution, Rezekne, Latvia, 18–19 June 2015 (Rubene, S., Vilnītis, M., Noviks, J. Impact of Density and Special Features of Manufacturing Process on Drying of Autoclaved Aerated Concrete Masonry Blocks);
10. The 7th Scientific and Technical Conference on Material Problems in Civil Engineering (MATBUD’2015), Crakow University of Technology, Krakow, Poland, 22–24 June 2015 (Rubene, S., Vilnītis, M., Noviks, J. Frequency Analysis for EIS Measurements in Autoclaved Aerated Concrete Constructions);
11. Creative Construction Conference 2015, Krakow, Poland, 21–24 June 2015 (Rubene, S., Vilnītis, M., Noviks, J. Frequency Analysis and Measurements of Moisture Content of AAC Masonry Constructions);
12. The 2nd International Conference “Innovative Materials, Structures and Technologies” (IMST 2015), Riga, Latvia, 30 September – 2 October 2015 (Rubene, S., Vilnītis, M., Noviks, J. Impact of External Heat Insulation on Drying Process of Autoclaved Aerated Concrete Masonry Constructions);
13. EUREKA 2015, 3rd conference and working session, Jaromerice nad Rokytinou, Brno, Czech Republic, Brno University of Technology, GEOTest. 15–16 October 2015 (Rubene, S., Vilnītis, M. Accuracy of Humidity Distribution Measurements in Autoclaved Aerated Concrete Constructions by Electrical Impedance Spectrometry);
14. The 6th European Conference of Civil Engineering, Budapest, Hungary, 12–14 December 2015 (Rubene, S., Vilnītis, M. Monitoring of Water Infiltration in Autoclaved Aerated Concrete Masonry Construction Blocks by Electrical Impedance Spectrometry).

List of Scientific Publications on the Subject of the Doctoral Thesis

1. Rubene, S., Vilnītis, M. Application of Electrical Impedance Spectrometry for Determination of Moisture Distribution in Aerated Concrete Constructions. In: EUREKA 2013: 1st Conference and Working Session: Proceedings, Czech Republic, Karolinka, 30 October – 1 November 2013. Brno: VUTIUM, Brno University of Technology, 2013, pp. 124–131. ISBN 978-80-214-4735-6.
2. Rubene, S., Vilnītis, M., Noviks, J. Impact of Contact Surface on Accuracy of Humidity Distribution Measurements in Autoclaved Aerated Concrete Constructions by EIS. In: Proceedings of 1st International Conference on Civil Engineering, Water Resources, Hydraulics and Hydrology (CEWHH 2014), Greece,

- Athens, 28–30 November 2014. Athens: EUROPMENT, 2014, pp. 99–104. ISBN 978-1-61804-253-8.
3. Rubene, S., Vilnītis, M. Correlation between EIS Measurements and Relative Humidity Distribution in Aerated Concrete Masonry Constructions. In: *Recent Advances in Civil Engineering and Mechanics. Mathematics and Computers in Science and Engineering Series 35*, Italy, Florence, 22–24 November 2014. Florence: WSEAS Press, 2014, pp. 67–72. ISBN 978-960-474-403-9. ISSN 2227-4588.
 4. Rubene, S., Vilnītis, M. Monitoring of Humidity Distribution Changes in Aerated Concrete Masonry Construction by EIS. In: *EUREKA 2014: 2nd Conference and Working Session Proceedings*, Czech Republic, Brno, 30–31 October 2014. Brno: VUTIUUM Brno University of Technology, 2014, pp. 124–130. ISBN 978-80-214-4883-4.
 5. Rubene, S., Vilnītis, M., Noviks, J. Monitoring of the Aerated Concrete Construction Drying Process by Electrical Impedance Spectrometry. In: *Proceedings of 4th International Conference “Advanced Construction 2014”*, Lithuania, Kaunas, 9–10 October 2014. Kaunas: Kaunas University of Technology, 2014, pp. 216–220. ISSN 2029-1213.
 6. Rubene, S., Noviks, J., Vilnītis, M. Determination of Humidity Level in Aerated Concrete Constructions by Non Destructive Testing Methods. In: *Proceedings of the International Conference “Innovative Materials, Structures and Technologies”*, Latvia, Riga, 28-30 November 2013. Riga: RTU Press, 2014, pp. 141–146. ISBN 978-9934-10-583-8. e-ISBN 978-9934-10-584-5. Available from: doi:10.7250/isconstrs.2014.23
 7. Rubene, S., Vilnītis, M., Noviks, J. Impact of Masonry Joints on Detection of Humidity Distribution in Aerated Concrete Masonry Constructions by Electric Impedance Spectrometry Measurements. *International Journal of Civil, Architectural, Structural and Construction Engineering*, 2015, Vol. 9, No. 1, pp. 1089–1094. e-ISSN 1307-6892.
 8. Rubene, S., Vilnītis, M., Noviks, J. Impact of External Heat Insulation on Drying Process of Autoclaved Aerated Concrete Masonry Constructions. *IOP Conference Series: Materials Science and Engineering*, 2015, Vol. 96, conference 1, pp. 1–8. ISSN 1757-8981. e-ISSN 1757-899X. Available from: doi:10.1088/1757-899X/96/1/012059 (SCOPUS indexed).

9. Rubene, S., Vilnītis, M., Noviks, J. Frequency Analysis and Measurements of Moisture Content of AAC Masonry Constructions by EIS. *Procedia Engineering*, 2015, Vol. 123, pp. 471–478. ISSN 1877-7058. Available from: doi:10.1016/j.proeng.2015.10.096 (SCOPUS indexed).
10. Rubene, S., Vilnītis, M., Noviks, J. Frequency Analysis for EIS Measurements in Autoclaved Aerated Concrete Constructions. *Procedia Engineering*, 2015, Vol. 108, pp. 647–654. ISSN 1877-7058. Available from: doi:10.1016/j.proeng.2015.06.194 (SCOPUS indexed).
11. Rubene, S., Vilnītis, M. Application of Electrical Impedance Spectrometry for Measurements of Humidity Distribution in Aerated Concrete Masonry Constructions. *International Journal of Mechanics*, 2015, Vol. 9, pp. 213–219. ISSN 1998-4448. (SCOPUS indexed).
12. Rubene, S., Vilnītis, M., Noviks, J. Impact of Density and Special Features of Manufacturing Process on Drying of Autoclaved Aerated Concrete Masonry Blocks. In: *Environment.Technogogy.Resources*. Rezekne, Latvia: Rezekne Higher Education Institution, 2015, pp. 186–192. ISSN 1691-5402. (SCOPUS indexed).
13. Rubene, S., Vilnītis, M. Frequency Analysis and Measurements of Moisture Content of AAC Masonry Constructions by EIS. In: *Proceedings “Creative Construction Conference 2015”*. Budapest, Hungary: Diamond Congress Ltd., 2015, pp. 147–147. ISBN 978-963-269-491-7.
14. Rubene, S., Vilnītis, M. Monitoring of Water Infiltration in Autoclaved Aerated Concrete Masonry Construction Blocks by Electrical Impedance Spectrometry. In: *Recent Advances in Mechanical Engineering Series 17 “Fluids, Heat and Mass Transfer, Mechanical and Civil Engineering”*, Hungary, Budapest, 12–14 December 2015. Budapest: WSEAS Press, 2015, pp. 106–111. ISBN 978-1-61804-358-0. ISSN 2227-4596.
15. Rubene, S., Vilnītis, M. Impact of Porous Structure of the AAC Material on Moisture Distribution throughout the Cross Section of the AAC Masonry Blocks. *WSEAS Transactions on Heat and Mass Transfer*, 2016, Vol. 11, pp. 13–20. ISSN 1790-5044. e-ISSN 2224-3461.
16. Rubene, S., Vilnītis, M. Accuracy of Humidity Distribution Measurements in Autoclaved Aerated Concrete Constructions by Electrical Impedance Spectrometry. In: *EUREKA 2015 Proceedings*, Czech Republic, Jaromerice nad Rokytinou, 15–16 October, 2015. Brno: 2015, pp. 156–164. ISSN 2464-4595.

Structure and Contents of the Doctoral Thesis

The Doctoral Thesis consists of abstract in English and Latvian, introduction, three main chapters, which have been divided into paragraphs, conclusion, bibliography comprising 114 reference sources and one appendix.

The volume of the Thesis is 112 pages. It has been illustrated by 107 figures and 4 tables.

In the introduction, the issue has been stated as well as the aims and have been defined. The scientific novelty and application of the results has been also stated in the introduction.

In the first chapter, the main properties of the AAC as well as the technology of its manufacturing process have been described. Review on existing non-destructive techniques of detection of moisture distribution throughout the cross section of solid materials has been provided in the first chapter.

In the second chapter, the author describes the experiments performed in order to reach the aims set in the Thesis. The procedure of approbation of the developed methodology for non-destructive detection of moisture distribution throughout the cross section of the AAC has been described in the second chapter.

In the third chapter, the author has provided a summary and brief analysis of the obtained results.

In the conclusion, the main results and finding have been summarized. Thesis statements to be defended have been stated.

INTRODUCTION

Statement of problem and aim of the research

Contemporary construction trends are sustainable construction and effective use of construction materials, therefore load bearing construction materials with high heat insulation parameters tend to become more popular. As an opposite trend are short construction terms, which fail to comply with all nuances of the material installation technology. Therefore, non-destructive testing methods become more and more popular during the past years.

Autoclaved aerated concrete (AAC) masonry blocks are construction material with high heat insulation parameters. In time of sustainable construction, this material can be used as a load bearing construction material for a range of buildings where it is necessary to obtain high heat insulation parameters of external delimiting constructions. The main problem of AAC masonry constructions is the significant influence of moisture content and its gradient on heat resistivity properties of the AAC. It is important to monitor the drying process of AAC masonry constructions in order to avoid sealing of moisture inside the masonry by early application of finishing layers on the construction. Therefore, testing methods, which allow credible determination of moisture distribution throughout the cross section of the AAC masonry construction as well as moisture migration throughout the cross section of the construction have to be developed. The drying process of the masonry is a long term process therefore, it is preferable to use non-destructive testing methods because a number of measurement series have to be performed in order to provide credible data of the changes in moisture content throughout the cross section of the masonry construction.

There is a variety of manufacturers who offer AAC masonry blocks and the manufacturing process of the blocks slightly differ as well as the ingredients used for the manufacturing of the blocks. Thus, the porous structure and density as well as chemical composition of the AAC differ slightly. This research has been done to determine the possibility of application of electrical impedance spectrometry for in-situ non-destructive determination of moisture distribution throughout the cross section of AAC masonry constructions.

The aim of the research

The aim of the research is development of non-destructive testing methodology for detection of moisture distribution throughout the cross section of AAC masonry constructions in in-situ conditions. After analysis of previous researches about non-destructive detection of

moisture content and its distribution throughout the cross section in solid materials tasks for the research have been set.

The tasks of the research

1. Determination of correlation between EIS measurement results and moisture content in AAC;
2. Determination of impact of contact surface between measurement probe and AAC masonry construction on the accuracy of the obtained results.
3. Determination of impact of the coating on measurement contact surface on the accuracy of the measurement results.
4. Determination of the impact of measurement distance on accuracy of measurement results.
5. Determination of the impact of cracks and masonry joints on accuracy of EIS measurement results.

Scientific novelty of the research results

Misunderstanding of the physical processes in construction materials can lead to misuse of effective construction materials and decrease the effectiveness of the properties of constructions designed in compliance with ISO 6946:2007 Building components and building elements - Thermal resistance and thermal transmittance - Calculation method. Therefore, a credible on site control methodology of moisture distribution in AAC is necessary in order to reach the designed material properties and avoid mistakes during the installation stage of the material.

Previous researches have been focused on non-destructive detection of moisture content and its distribution in solid materials such as concrete. Non-destructive detection of moisture distribution in AAC has not been widely researched due to the uneven and porous structure of the material which cause problems with repeatability of the measurement results and therefore exclude common use of the methodology. Therefore, in this research an EIS methodology, which is usually applied for moisture detection of bulk materials (such as soil), has been adapted for application on AAC and has reached the aims stated for this research.

1. MATERIALS AND METHODS

1.1. *Structure and main properties of aerated concrete*

Aerated concrete is basically a mortar with pulverized sand or industrial waste like fly ash as filler, in which air is entrapped artificially by chemical (metallic powders like Al, Zn, and H₂O₂) or mechanical (foaming agents) means, resulting in a significant reduction in density [71].

Aerated concrete falls into the group of cellular concrete (microporite being the other one). The main advantage of aerated concrete is its lightweight, which optimises the design of supporting structures including the foundation and load bearing walls. Aerated concrete provides a high degree of thermal insulation and considerable savings in material due to the porous structure. Aerated concrete can be obtained with a wide range of densities e.g. 300±1800 kg/m³, thereby offering flexibility in manufacturing products for specific applications (structural, partition and insulation grades) [57].

Aerated concrete can be manufactured by several methods; one of them is *air-entraining method*:

Gas-forming chemicals are mixed into lime or cement mortar during the liquid or plastic stage, resulting in a mass of increased volume and when the gas escapes, it leaves a porous structure. Aluminum powder, hydrogen peroxide/bleaching powder and calcium carbide liberate hydrogen, oxygen and acetylene can be used as aerating agents. Aluminum powder is the most commonly used aerating agent. Efficiency of application of aluminum powder is influenced by its fineness, purity and alkalinity of cement, along with the means taken to prevent the escape of gas before hardening of mortar. In the case of Portland cements with low alkalinity, addition of sodium hydroxide or lime supplement the alkali required.

The second method applied for manufacturing of aerated concrete is *foaming method*:

Foaming method is considered the most economical and controllable pore-forming process [88,101] as there are no chemical reactions involved. Introduction of pores is achieved through mechanical means either by pre-formed foaming (foaming agent mixed with a part of mixing water) or mix foaming (foaming agent mixed with the mortar). The various foaming agents used are detergents, resin soap, glue resins, saponin, hydrolysed proteins such as keratin etc.

There also exists *combined pore-forming method*: Production of cellular concrete by combining foaming and air-entraining methods has also been adopted using aluminum powder and glue resin [88].

Based on the method of curing aerated concrete can be non-autoclaved (NAAC) or autoclaved (AAC). The compressive strength, drying shrinkage, absorption properties etc. directly depend on the method and duration of curing. The strength development is rather slow for moist-cured products. Autoclaving initiates reaction between lime and silica/alumina bearing ingredients [57].

Physical properties, especially isolative and hygrometric properties, of aerated concrete depend on its microstructure and macrostructure.

In aerated concrete, the method of pore formation (gas release, foaming or combined) has significant impact on the microstructure, and thus on its properties. The material structure of aerated concrete is characterised by its solid microporous matrix and macropores. The macropores are formed due to the expansion of the mass caused by aeration and the micropores appear in the walls between the macropores [4]. Macropores have been envisaged as pores with a diameter of more than 60 μm [65]. The orientation of the products of hydration of cement is significantly altered due to the presence of voids.

The porous system of aerated concrete is also classified in terms of pore size distribution functions as artificial air pores, inter-cluster pores and inter-particle pores. The distribution of pores in the matrix has influence on its properties [70].

Figs. 1.1-1.3 display the typical pore systems in aerated concrete [56]. Although the air void system remains largely identical, there exists difference in the structure of AAC and NAAC, caused by the variation in the hydration products, which explains the variation in properties of NAAC and AAC. On autoclaving, a part of the fine siliceous material reacts chemically with calcareous material like lime and lime liberated by cement hydration, forming a microcrystalline structure with much lower specific surface. Tada and Nakano [99] points out that NAAC has a larger volume of fine pores due to the presence of excessive pore water. However, it has been observed that macropore size distribution does not have significant influence on compressive strength of autoclaved concrete [4].

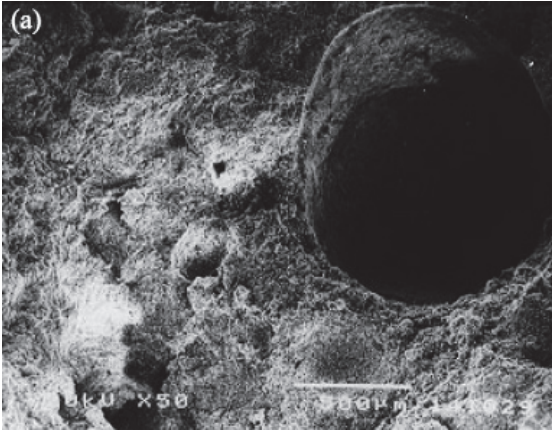


Fig. 1.1. Pore systems in aerated concrete: artificial air pore[57]

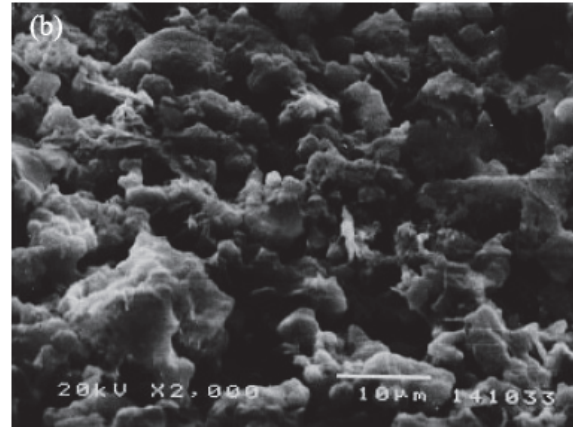


Fig. 1.2. Pore systems in aerated concrete:inter-cluster pore[57]

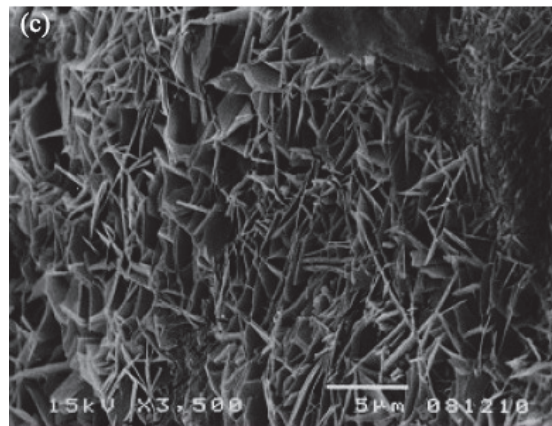


Fig. 1.3. Pore systems in aerated concrete: inter-particle pore[57]

Porosity, pore size distribution and permeability:

Properties of concrete such as strength, permeability, diffusivity, shrinkage and creep are intimately related to its porosity and pore size distribution. Thus, the characterization of the pore structure is extremely important, especially in case of aerated concrete where the porosity may be as high as 80%. Porosity and pore size distribution of aerated concrete varies considerably with the composition and method of curing. Higher porosity of aerated concrete has been established to be the consequence of increase in macropore volume [4], which results in thinner pore walls, thereby reducing the share of micropore volume. Although the porosity varies considerably between aerated concrete made with foaming and gas forming methods, the permeability is not found to vary much. The artificial air pores were found to have little influence on permeability [32].

However, the most important functional properties of AAC are water absorption and capillarity.

Aerated concrete is porous and there is a strong interaction between water, water vapour and the porous system, therefore, there exists various moisture transport mechanisms. In the dry state, pores are empty and the water vapour diffusion dominates, while some pores are filled in higher humidity regions. Capillary suction predominates for an element in contact with water. These mechanisms make it difficult to predict the influence of pore size distribution and water content on moisture migration [70].

The water vapour transfer is explained in terms of water vapour permeability and moisture diffusion coefficient whereas capillary suction [69] and water permeability characterize the water transfer [70,98]. The moisture transport phenomena in porous materials, by absorbing and transmitting water by capillarity, has been defined by an easily measurable property called the sorptivity, which is based on unsaturated flow theory [30,112]. It has been detected that the water transmission property is better explained by sorptivity than by permeability.

The concept of capillary hygroscopicity [88] also employs the same principle as sorption. These values give a fair indication of the fineness of the pores.

As AAC masonry constructions are porous, composed of solid matrix and pores. In porous materials heat transfer is often coupled strongly with moisture transfer [72]. Accurate prediction of heat and moisture transfer in porous material is essential for optimization of building envelope with respect to energy consumption, hydrothermal performance, and indoor environment [16,53].

Thermal conductivity of aerated concrete depends on its density, moisture content and ingredients of the material [42,44,79,88,102,106]. As thermal conductivity is largely a function of density, it does not really matter whether the product is moist-cured or autoclaved as far as thermal conductivity is concerned. The amount of pores and their distribution are also critical for thermal insulation [10]. In case of aerated concrete the finer are the pores the better is the insulation. As the thermal conductivity is influenced by the moisture content [102] (a 1% increase in moisture by mass increases thermal conductivity by 42% [81]), it should not be reported in oven dry condition. Based on the thermal performance requirements for buildings, an optimum material design has been proposed by Tada [97].

Taking into consideration the previous statements it is important to detect not only the overall moisture content of the construction material but also to detect its distribution throughout the cross section of the respective element.

Humidity content of the AAC masonry constructions has significant impact on its heat resistivity properties. Heat transfer by conduction is affected by transfer of energy through

molecular collision, therefore it follows that the thermal conductivity in liquids and solids is much greater than in gases (i.e. for water vapour at 10°C the conductivity λ is ≈ 0.024 W/mK, while for liquid water, the conductivity λ is ≈ 0.6 W/mK which is a factor 25 times greater) [8]. The Research of Barsotelli et.al [8] provides information that the porosity of the construction material has impact on its hygrometric properties and the research shows a low absorption velocity as a consequence of the large amount of macropores that slow down the capillary forces. Water vapour permeability is enhanced by the degree of connection among the pores and by the absence of condensation phenomena which are favoured by the presence of micropores. Therefore, a higher quantity of micropores should be envisaged favouring the condensation phenomena and hindering the water vapour diffusion.

The water transport phenomena are usually modelled by the diffusion type equation. The equation can have two basic forms. In the first case the driving potential at moisture transport is represented by the capillary pressure and the transport parameters in the equation are moisture capacity and moisture permeability, parameters as the moisture permeability and capacity can be modelled from the pore size distribution. In the second case the water flow driving potential is represented by the moisture content and the material transport parameter is the moisture diffusivity and the equation has so called diffusion form Bruce and Klute [12]. As the water transport parameters depend on the boundary conditions there is a difference between the moisture diffusivity during the water absorption, redistribution and drying.

In a case of drying the diffusivity is smaller [40]. A detailed study on drying diffusivity and its determination is given by Pel and Landman [62-64], which present the approaches to diffusivity determination at the absorption and at the drying during different drying phases. Vu [105] realised the simulation experiments of drying process considering the variability of pore structure parameters expressed by theoretical pore size distributions and modelling the water transport coefficients of building materials represented as a bundle of capillaries, size distribution of which is based on their pore structure [46].

These statements are used and developed in the particular research during the approbation of a non-destructive application of EIS on AAC masonry constructions. During the research, there were determined differences of hygrometric properties between several types of AAC masonry blocks by a non-destructive testing method, which can be applied in-situ conditions.

1.2. Direct measurements of moisture content in autoclaved aerated concrete constructions

The most precise and credible test method is destructive measurement method, which is called gravimetric method. Gravimetric method consist on determining water content through weighting samples upon oven drying, encompassing absorbed and chemically bound water. There are automatic moisture analysers that utilize infrared lamps as a heat resource as well. This technique measures the weight loss of hardened concrete slices or specific portions, by comparing to the original weight of the sample, and then the lost of water can be determined. The results may be expressed by weight as the difference of the mass of water present to the dry weight of the concrete sample or by volume as difference of the volume of water to the total volume of the concrete sample [18]. This method is considered to be the most direct and reliable procedure despite the large number of specimens it is required, since different samples should be used for each measure, and only the average water content of each portion or slice should be obtained. It is also one of the few methods that can be employed at high moisture contents [93].

H. Akita et al. [3] proposed the analysis of prismatic concrete specimens in order to quantify the moisture transfer experimentally and numerically (Fig. 1.4). Variations in water content were measured at European Union Governo da República Portuguesa different depths by splitting the specimens and comparing the mass of each peace before and after oven drying at 105°C [73], Accordingly with RILEM (International union of laboratories and experts in construction materials, systems and structures) technical recommendations for AAC [80].

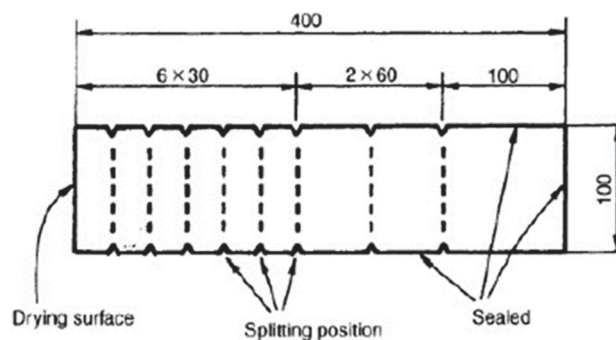


Fig. 1.4. Dimension (mm) of specimens subjected to one-face drying [99]

Such approach can provide credible results about humidity distribution throughout the cross section of the construction but it is long and laborious process, which is hard to repeat in a number of places on construction site. However, this method can be used for controlling of

the non-destructive test results and preparation of correlation equations between moisture content in sample and EIS measurement results.

1.3. Non-destructive methods for detection of moisture content in autoclaved aerated concrete constructions

A number of researches have been performed in order to develop non-destructive test methods for the detection of humidity content in building constructions (mostly in concrete).

These methods can be divided in several sub-groups such as radiological methods, electrical methods, heat flow measurement methods.

1.3.1. Radiological non-destructive methods for detection of moisture content in autoclaved aerated concrete constructions

The gamma densitometry is a non-destructive testing method commonly used to control the density of civil engineering materials [103].

The principle of this method is based on a beam of gamma rays emitted by radioactive source and passing through the concrete (Fig. 1.5). The relative intensity of the transmitted particles is related to the mass of the traversed material m_c , the mass variation of the traversed points can thus be measured. Since chemical evolutions do not lead to significant losses of mass, the mass variation in these beams stem solely from water evaporation; and can be interpreted as the profile of water content variations [73,55].

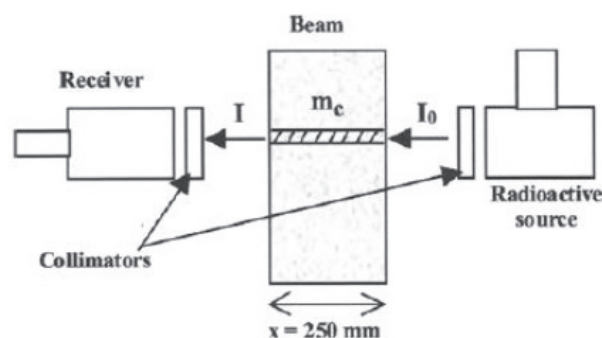


Fig. 1.5. Principle of the gamma densitometry technique [73], [55]

The gamma densitometry is based on absorption of the gamma ray emitted by a radioactive source of Cesium Cs137 [103]. The relation between intensity I of the flow of transmitted particles and traversed mass m_c is as follows is based on the Lambert's Law [55].

The mass variation of the volume intercepted by the gamma ray can be measured at different depths, so water content variation along the height of the concrete beam's cross section can be monitored. The calculation method assumes that at each measurement the flow

intercepts the same volume of material [73,55]. Restrictions on this method are described in [73].

Similar to gamma densitometry, neutron radiography is a non-destructive method using radiation. In contrast to gamma rays, neutrons interact mainly with the hydrogen nuclei. The attenuation of a neutron beam, caused by scattering and absorption of the neutrons, will therefore be directly related to the total water content in the material. The intensity of a neutron beam passing through a specimen is described by an expression similar to Eq. (1.1) [61]:

$$I = I_0 e^{-x(\mu_{mat} + \mu_w \cdot \varepsilon)} \quad (1.1.)$$

where

I is the intensity of a neutron beam after passing through the material [counts/s];

I_0 is the initial intensity of the neutron beam [counts/s];

μ_{mat} is the macroscopic attenuation coefficient of the specific material [m^{-1}];

μ_w is the macroscopic attenuation coefficient of water [m^{-1}];

x is the thickness of the material sample [m];

ε is the water content volume by volume [m^3/m^3].

The coefficients μ_{mat} and μ_w are determined independently by measuring the neutron transmission through pure water, and through the dry material. During the test the specimen is placed between the neutron source and the detector as in Fig.1.6. The neutron beam can be produced by a combination of boron and cadmium and the neutrons can be detected by a 3He proportional detector [61].

As cons of this method can be mentioned the fact that when running a neutron radiography test safety arrangements must be taken and specially trained personnel are necessary. This fact makes this method rather unsuitable for in situ use. Results from measurements with neutron radiography on different materials and experimental arrangements are shown in researches of Pel [61], Adan [1], Dawei et al. [17] and Justnes et al.[33,37].

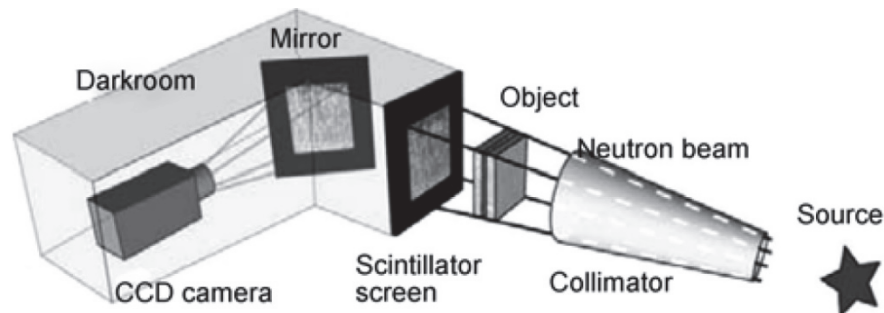


Fig.1.6. Schematic representation of set-up for neutron radiography [114]

Nuclear magnetic resonance (NMR) is a non-destructive method. The accuracy of the water content measurement is approximately 0.5 to 0.1 vol.% according to Kießel et. al.[38]. NMR has a spatial resolution of better than 1 mm according to Kopinga et al.[39]. With NMR, a distinction can also be made among free, physically bound and chemically bound water. Thus, NMR is a very well suited for measuring transient water movements in building materials. A primary disadvantage of NMR is that the equipment needed is rather expensive.

In an NMR measurement the number of hydrogen nuclei are "counted". A magnetic moment is associated with the intrinsic spin of the material's hydrogen nuclei. In a NMR experiment an exterior permanent magnetic field is applied. When an electromagnetic field is applied perpendicular to the constant magnetic field, a part of energy is absorbed. The amount of energy absorbed is proportional to the number of hydrogen nuclei in the measurement volume. It is therefore a value of the water content in the material tested. In addition to water, NMR is suitable for all fluids containing hydrogen atoms.

According to Kopinga et al.[39], NMR offers better sensitivity than gamma-ray densitometry and neutron radiography. Unlike results from the gamma ray method, the NMR results are directly related to the amount of hydrogen nuclei. In de Freitas et al. [22], however, a comparison between gamma-ray attenuation and NMR revealed no significant difference in accuracy. An advantage of NMR compared to gamma-ray attenuation and neutron radiography is that no radioactivity is involved during the experiment [33].

The principle of computer tomography is to measure the intensity loss of a narrow beam of X rays passing through the specimen. The absorption is a measure of the density of the specific material in question. The magnitude of the absorption is measured with a so-called CT-value. The scale is calibrated against distilled water. By definition, water has a CT value of 0. The absorption (CT-value) in air is -1000, which means that there is no absorption (100% less absorption). The absorption of X rays in concrete is 145-150% greater than the absorption in water. The CT-value of concrete consequently is 1450-1500 [11]. The difference in the CT-value between air and water is an indicator for measuring the water content in the material [33].

Non-destructive measurement of the moisture profile can be carried out with a microwave beam. Utilization of electromagnetic microwave radiation (EMWR) for monitoring moisture transport is based on the Lambert-Beer's law that expresses the relation between absorbance, optical length and concentration from the absorbing substance. The empirically derived law itself has the exponential form:

$$A = \log \frac{I_0}{I} = k \cdot c \cdot s \quad (1.2)$$

A is absorbance [-]

I_0 incident radiation intensity

I radiation intensity after passing through the substance

s optical length of material [m]

c molar absorptivity (extinction coefficient) [$\text{m}^2 \cdot \text{mol}^{-1}$]

k coefficient of molar concentration of the substance [$\text{mol} \cdot \text{m}^{-3}$] [95]

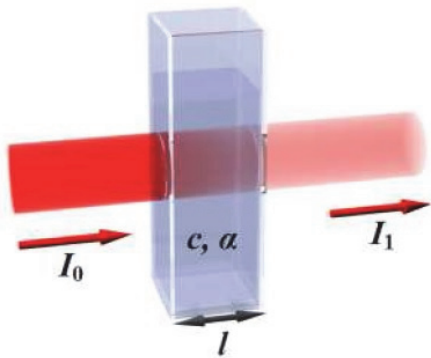


Fig.1.7. Main principle of the EMWR method [95]

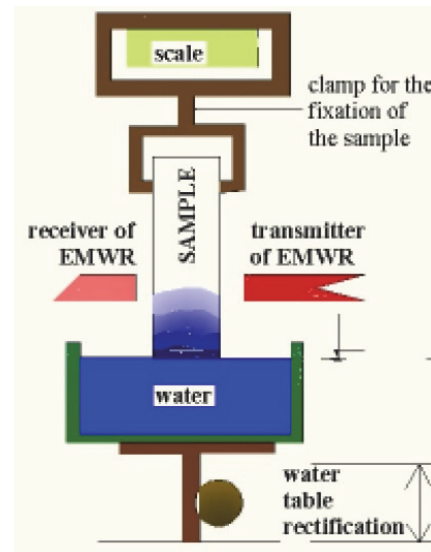


Fig.1.8. Position of sample by measuring [95]

During the measurement the specimen is placed between a transmitter and a receiver and the attenuation of the beam caused by the oscillation of the water molecules is measured. The magnitude of the attenuation corresponds to the water content of the tested material. The equipment must be calibrated against the specific material in question. If the power of the beam is too high, the temperature of the water in the material will strongly increase during the test. Moisture migration caused by the temperature gradient might therefore occur [33].

These methods allow determining humidity distribution throughout the height of the cross section by non-destructible method, but it can hardly be used in on-site conditions and is mostly laboratorial test method.

1.3.2. Non-destructive methods for detection of moisture content in autoclaved aerated concrete constructions based on heat flow measurements

The moisture content on the construction can be performed by measuring its' heat resistivity properties. Heat resistance of the material is directly dependent on its moisture content and its distribution throughout the cross section of the material.

The moisture distribution throughout the cross section of the element has significant impact on the heat conductive properties (equations (1.3) to (1.6)). A number of researches has been conducted on the coupled heat and moisture transfer in porous media [113]. One of the most disseminated and accepted models is the Philip and DeVries model, which uses the temperature and moisture content gradients as driving potentials [66]. However, it is well known that there is discontinuity on the moisture content profile at the interface between two porous media. Luikov proposed a mathematical model for simultaneous heat and mass transfer in building porous materials [45]. The governing partial differential equations to model heat and mass transfer through porous walls are given by equations (1.3) to (1.6). In the porous material, the air humidity ratio is a function of the material moisture content and temperature. The moisture transport process can be described as:

$$\frac{\partial W}{\partial t} = \frac{W_s}{\xi \rho_m} \left(D_v R_v T_m \rho_a + \frac{\xi \rho_m}{W_s} D_w \right) \frac{\partial^2 W}{\partial x^2} + \Phi \frac{\partial W_s}{\partial T} \frac{\partial T}{\partial t} \quad (1.3)$$

At both sides of the wall, the corresponding boundary conditions can be written as:

$$-D_v R_v T_m \rho_a \frac{\partial W}{\partial x} = h_m (W_\infty - W_{surf}) \quad (1.4)$$

where T_m is material temperature, W air humidity ratio (W_s for saturated one), D_v material vapor diffusion coefficient, D_w material liquid water diffusion coefficient, ξ slope of moisture equilibrium curve, ρ_m density of material (ρ_a for air), R_v water vapor characteristic constant, Φ relative humidity, h_m surface mass transfer coefficient, W_∞ ambient air moisture content, W_{surf} surface moisture content.

The thermal transport process can be described as:

$$(\rho_m c_{vm}) \frac{\partial T}{\partial t} = K \frac{\partial^2 T}{\partial x^2} + h_{fg} D_v R_v T_m \rho_a \frac{\partial^2 W}{\partial x^2} \quad (1.5)$$

It displays that the temperature variation is due to heat conduction and the phase change of water. The corresponding boundary conditions can be written as:

$$-k \frac{\partial T}{\partial x} = h_c (T_\infty - T_{surf}) + h_{fg} D_v R_v T_m \rho_a \frac{\partial W}{\partial x} \quad (1.6)$$

where K is the heat conduction coefficient, c_{vm} the material specific heat, h_{fg} latent heat of water vaporization, h_c surface mass transfer coefficient, T_∞ ambient air moisture content, T_{surf} surface moisture content.

This model has been proved valid for the coupled heat and moisture transfer in porous media by experiments, whose results show that the simulation results agree well with field measurements [43,28]. Thus, by measurements of heat conduction coefficient can be

transformed into information about moisture content in the respective material. The heat source will, however, generate a temperature gradient. This will influence the moisture flux and so the temperature gradient is a source of error. According to Vos [104] it is possible to measure the moisture content with a precision of ± 1 vol. % [33].

As it is a laborious process to obtain moisture distribution data from the heat resistance data, therefore it is not widely used for detection of moisture distribution throughout the cross section of construction materials.

Thermal imaging is a simple method to determine the moisture distribution, or the distribution of volatile fluids. The principle is based on the decreasing temperature when liquids evaporate. The method is destructive and one specimen is used every time the moisture profile is to be measured. When the profiles are to be measured the specimen is split into two halves, perpendicular to the exposed surface. The temperature of the split surface is measured with an infrared camera. From the temperature distribution the moisture profile is evaluated. According to Sosoro et al. [96], the moisture profile in a specimen with a constant cross-section over the depth can be calculated by:

$$\varepsilon_x = \frac{(T_0 - T_s(x))^2}{\frac{S}{V_{fl}} \int_0^l (T_0 - T_s(x))^2 dx} \quad (1.7.)$$

where

ε is the water content volume, per volume [m^3/m^3];

T_0 is the temperature of the surrounding air [K];

T_s is the surface temperature [K];

x is the co-ordinate in the direction of water transport [m];

S is the surface area exposed to fluid [m^2];

V_{fl} is the total absorbed test fluid [m^3];

l is the specimen length [m] [44].

Another method is to calibrate the measured temperature of the split surface against the temperature of split surfaces of well conditioned specimens. The calibration is performed on specimens of the specific material with different and known moisture contents. The measuring procedure and conditioning procedure must take place in a climate room with constant relative humidity and temperature, and the image must be taken at the same time after splitting the specimen. This conditioning procedure would be very time consuming, but the accuracy of the measured water content would probably be higher than the water content obtained with Equation (1.7).

Profiles of different liquids and laboratory arrangements are described in Sosoro et al. [33,96].

1.3.3. Detection of moisture content in autoclaved aerated concrete constructions by materials hygrometric performance

There exist some methods to calculate the moisture diffusivity at high moisture levels from the sorption coefficient. Two methods of evaluating the moisture diffusivity at high moisture levels from a series of capillary water uptake tests and results from these methods are described in detail in by Künzel [41] suggests the following equation for calculating the moisture diffusivity D_w from the sorption coefficient:

$$D_w = 3,8 \frac{A^2}{w_{cap}^2} \cdot 1000^{\frac{w}{w_{cap}} - 1} \quad (1.8.)$$

where

A is the sorption coefficient [$\text{kg}/(\text{m}^2 \times \text{s}^{1/2})$];

w is the moisture content [kg/m^3];

w_{cap} is the moisture content at capillary saturation [kg/m^3].

In Eq. (1.8.), the increase of the moisture diffusivity with increasing moisture content is approximated with an exponential function. The theory behind this approach is unclear. Perhaps it is purely empirical [33].

The moisture diffusivity at high moisture levels can also be evaluated from moisture profiles at steady state. The method is based on measurements of the relation between the moisture content and Kirchhoff's flow potential up to capillary saturation. It is described in Arfvidsson [7] and Hedenblad [31]. Instead of measuring moisture profiles as they develop in the specimen during the transient water uptake, profiles are measured only after the flux has reached a steady state. The moisture profile can be measured by the "slice-dry-weigh" – method referred in these thesis as approach by Akita et al [3]. The moisture flow at steady state, $g_{t=\infty}$ must also be known. The profile can be measured in terms of degree of saturation or in terms of moisture content (mass per mass, or mass per volume). Relative humidity is not suitable at the high moisture levels occurring during capillary suction. In the following, the moisture content mass per volume w [kg/m^3] will be used. Using Kirchhoff's flow potential, Fick's law is

$$g = - \frac{\partial \Psi}{\partial x} \quad (1.9.)$$

Here Kirchhoff's flow potential is a function of the moisture content

$$\Psi = \Psi(w) \quad (1.10.)$$

Consider steady state through a specimen $0 \leq x \leq l$. At $x = 0$ there is capillary saturation and at $x = l$ there is a constant value $w(l)$. The steady state moisture profile is $w = w(x)$ and the flux $g_{t=\infty}$. Then we have:

$$g_{t=\infty} = -\frac{d}{dx} [\Psi(w(x))] \quad (1.11)$$

Integration from 0 to x gives

$$g_{t=\infty} \cdot x = -\Psi(w(x)) + \Psi(w_{cap}) \quad (1.12)$$

or

$$\Psi(x) = \Psi(w_{cap}) + (-g_{t=\infty}) \cdot x \quad (1.13)$$

With Eq. (1.13.) the stepwise relation $\Psi(w)$ now can be calculated. A disadvantage of this method is that it will take a considerable time for the specimen to reach steady state. It is also difficult to use the method on materials with very steep profiles. Furthermore, the surface exposed to water will reach a higher moisture content than that corresponding to capillary saturation. This gradual water absorption exceeding w_{cap} is not a flow process described by Fick's law. Therefore, the part of the profile with $w > w_{cap}$ can not be used when calculating the relation between Kirchhoff's flow potential and water content. The process going on at the surface part is a process in which the air enclosed in the specimen pores is solved in the pore water. This process can probably be described with a source term $f(w)$ in the moisture balance equation

$$\frac{\partial w}{\partial t} = \frac{\partial^2 \Psi}{\partial x^2} + f(w) \quad (1.14)$$

It must be observed that this gradual water absorption above w_{cap} is not a moving boundary but a process going on simultaneously across a considerable pore volume. Only the part of the specimen with a water content below w_{cap} should be used when calculating $\Psi(w)$, see Figure 1.9.[44]

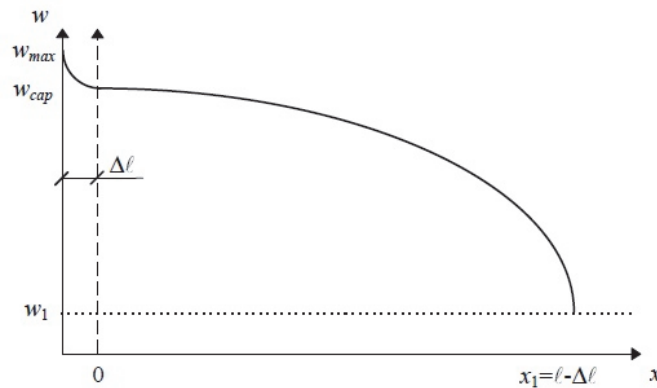


Fig. 1.9. Only the part of the specimen with a water content below w_{cap} can be used when calculating $\Psi(w)$.

The x-axis is moved a distance Δx so that the used fictive length become $l - \Delta l$ [33]

1.3.4. Electrical non-destructive methods for detection of moisture content in autoclaved aerated concrete constructions

There is a number of non-destructive test methods, which are based on measurement of electrical parameters and corresponding them to humidity contents of construction materials.

Electrical techniques [67,82] utilize the relationship between the electrical properties of cement-based materials and their water content. Measurements of resistance, impedance, capacitance, and the dielectric constant of porous materials are influenced by the water content and can be used as the basis of assessing water content. With appropriate attention to the condition of the material, electrical techniques can offer a quick, non-destructive method of identifying the extent of surface moisture by giving comparative measurements.

However, the accuracy and quality of results from these techniques are often affected by local temperature variations, the presence of dissolved salts in the pore solution and the presence of metallic components close to the measurement points [114].

One of electrical methods for detection of humidity content and distribution in construction materials is use of relative humidity sensors. High quality relative humidity sensors are usually made of hair from horses or humans. The movement of the hair is converted into an electrical signal by a strain gauge. Similar sensors are made of a strip cellulose butyrate, a water absorbent polymer that likewise stretches and shrinks according to relative humidity.

There are two main types of relative humidity sensors, capacitive and resistive sensors. The capacitive sensor consists of a thin layer of water absorbent polymeric or inorganic material that is coated onto a conductive base. This layer is then covered with porous conductive layer material. With the increase of the relative humidity, the water content of the polymer increases too. Water has a high dielectric constant, which means that the combination of two electrodes with the water between can store a relatively high electric charge. This electrical capacity is measured by applying rapidly reversing (AC) voltage across the electrodes and measuring the current that passes. The polymer or inorganic material is usually aluminium oxide and just plays an indirect part of the measurement. The change of capacitance of these capacitive sensors is, however, small when even compared with the capacitance of few meters of cable. This means that the electronic process of data acquisition has to be completed close to the sensor. If one data logger is connected to several relative humidity sensors, each sensor will need its own power supply and relatively bulky electronics [68,73].

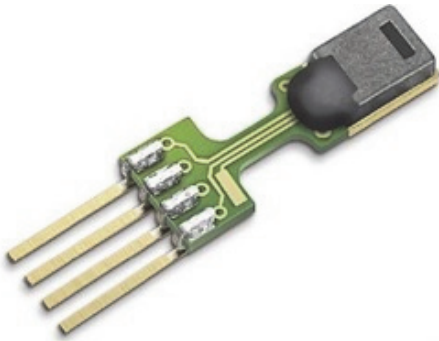


Fig. 1.10 Capacitive sensor [73]

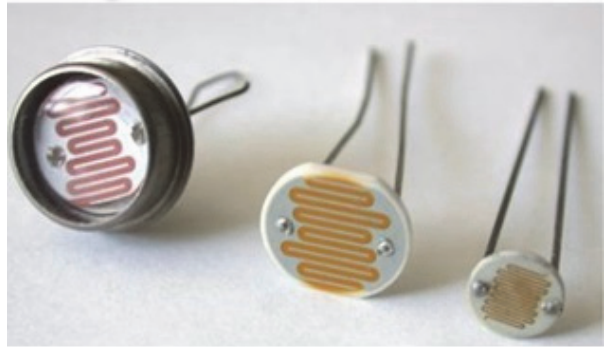


Fig. 1.11 Resistivity Sensor [73]

Although capacitive sensors can have reduced accuracy at relative humidity values exceeding 90%, they typically provide better linearity than resistive sensors.

As stated by Weiss internal water content measurements generally use relative humidity sensors that are placed inside fabricated cavities in a concrete sample. However, the measurements can be inaccurate especially for high relative humidity. At humidity higher than 80% the sensor's response to a change in humidity is inconveniently slow and it may take minutes or even hours for the sensor to respond to a humidity change [60]. This makes the use of humidity sensors inappropriate for water sorption measurements, especially for measurements very near the concrete surface. In addition, the sensors could have a large drift with time (up to 3% RH per week) [77].

This large drift causes major difficulties in evaluating the correct moisture gradient and necessitates continuous calibrations [31]. A newly introduced humidity sensors may be able to lessen some of these problems by having a smaller drift and being able to stabilize more rapidly [25,77].

However, capacitive sensors can take several hours to reach equilibrium and provide valid readings [111]. They cannot also be directly exposed to fresh concrete. To solve this problem in the experiment, the sensors are mounted in plastic tubes with Gore-tex® caps and then embedded in fresh concrete. This material, protect the sensor from liquid water but allows vapour transmission. The vapour pressure within the airspace around the sensor and in the concrete pores will always be equal. This allowed the sensor to be permanently embedded in the concrete reaching its equilibrium and obtaining valid readings [25,73].

Relative humidity sensors has a significant disadvantage against the measurement methods, which allow to detect moisture content in the material. The previously described sensors allow to detect the relative humidity in the construction material while in the

equations ((1.3) and (1.8)) for the coupled heat and mass transfer use values of the moisture content in the construction material. Therefore, such sensors are not suitable for detection of moisture content and further use of the data for evaluation of coupled heat and mass transfer.

This method in its base is similar to the EIS method with the exception that the sensors should be left inside the structure, so it requires large amount on sensors which have to be embedded in constructions during the construction phase and left there for further measurements. EIS method with Z-meter allows using only one probe pair for all measurements because probes can be withdrawn from the construction after the measurement.

1.4. Method of electrical impedance spectrometry

Method of electrical impedance spectrometry (EIS) enables detection of the distribution of impedance or other electrical variables (such as resistivity, conductivity etc.) inside a monitored object, and thus the observation of its inner structure and its changes [20,51]. This method ranks among indirect methods for detection of materials' properties through electrical measurements and it is used in measuring properties of organic and inorganic substances. So far, EIS is widely used in medicine as one of the most common testing methods in diagnostics where any kind of tissues are involved. It constitutes a very sensitive tool for monitoring phenomena that take place in objects (e.g. changes occurring in earth filled dams when loaded by water, in wet masonry sediments etc.), electrokinetic phenomena at boundaries (e.g. electrode/soil grain, between soil grains) or for describing basic ideas about the structure of an inter phase boundary (e.g. electrode/water) [94].

Electrical impedance is a basic property characterizing the AC electrical circuits. It is always greater than or equal to the real electrical resistance R in the circuit. Imaginary resistance, i.e. inductance - reactance of inductor X_L and capacitance - reactance of capacitor X_C , creates variable and therefore frequency - dependent part of the impedance. Electrical impedance is evidently made up of real and imaginary parts. Resistance R creates real part and is frequency-independent. Imaginary part is created by reactance X , which is frequency-dependent. Electrical impedance can be expressed by Ohm's equation for AC circuits, i.e. by the ratio of electric voltage phasor U and electric current phasor I

$$Z = \frac{U}{I} \tag{1.15}$$

Impedance values are, as well as resistance R values in case of DC circuits, expressed in ohms (Ω).

Frequency characteristic of impedance Z can be expressed as a function of complex variable in the algebraic (component) form

$$Z = R + jX \quad (1.16)$$

where R is resistance forming the real part of impedance independent of frequency, X is reactance, the imaginary component of impedance and the magnitude of which changes with frequency.

Absolute value, i.e. the modulus of the vector of the impedance $|Z|$ is expressed by the formula

$$Z = \sqrt{R^2 + X^2} \quad (1.17)$$

and the phase shift is expressed by the relation [70]

$$\varphi = \arctg\left(\frac{X}{R}\right) \quad (1.18)$$

The impedance is usually plotted in the Nyquist diagram, as imaginary part versus real part, providing a convenient tool for determining various electrical response behaviour of the system [2].

As stated by Barsoukov and McDonald [9] from the theory of physics capacitances and inductances are generally associated with space charge polarization regions and with specific adsorption and electrocrystallization processes at an electrode. Ordinary circuit elements, such as resistors and capacitors, are always considered as lumped-constant quantities, which involve ideal properties. All real resistors are of finite size and thus are distributed in space; they therefore always involve some inductance, capacitance, and time delay of response as well as resistance. These residual properties are unimportant over wide frequency ranges and therefore usually allow a physical resistor to be well approximated in an equivalent circuit by an ideal resistance, one which exhibits only resistance over all frequencies and yields an immediate rather than a delayed response to an electrical stimulus.

The physical interpretation of the distributed elements in an equivalent circuit is somewhat more elusive. However, they are essential in understanding and interpreting most impedance spectra. There are two types of distributions with which needs to be concerned. Both are related, but in different ways, to the finite spatial extension of any real system. The first is associated directly with nonlocal processes, such as diffusion, which can occur even in a completely homogeneous material, one whose physical properties, such as charge mobilities, are the same everywhere. The other type, exemplified by the constant-phase element (CPE), arises because microscopic material properties are themselves often

distributed. For example, the solid electrode–solid electrolyte interface on the microscopic level is not the often presumed smooth and uniform surface. It contains a large number of surface defects such as kinks, jags, and ledges, local charge inhomogeneities, two- and three-phase regions, adsorbed species, and variations in composition and stoichiometry. Such state can be referred to the situation of AAC sample and Z-meter measurement probe. Reaction resistance and capacitance contributions differ with electrode position and vary over a certain range around a mean, but only their average effects over each channel of measurement probe surface can be observed. The macroscopic impedance, which depends on the reaction rate distribution across such an interface, is measured as an average over each channel of the electrode. Such averaging is usual in one-dimensional treatments (with the dimension of interest perpendicular to the electrode property distributions occur throughout the frequency spectrum) [9].

1.4.1. Previous researches on application of electrical impedance spectrometry for moisture distribution in concrete and porous materials

Electrical measurements have shown promise as non-invasive methods to evaluate the material properties of concrete. For example, a range of microstructural properties can be evaluated including porosity, pore connectivity, water permeability, and ion diffusivity [15,24]. Also, electrical measurement procedures have been suggested to monitor water and ionic penetration inside concrete [47,50,77, 90, 91,108].

One potential drawback associated with the use of electrical measurements is that several factors can simultaneously influence the measurement results and this may complicate the interpretations [74]. It has been shown that the electrical properties of concrete vary due to hydration [15], changes in pore solution composition [47,50,74], moisture variations[47,50,74,91,108], and temperature variations [19,54,110]. To differentiate between these concurrent contributions, the way by which each parameter influences the results must first be understood. Subsequently, experimental measurements can be modified to allow distinction between the simultaneous influences, thereby enabling reliable data interpretations. For example, several methods have been presented to utilize electrical measurements for monitoring moisture transport inside concrete [47,50,77,90,91,108].

These methods often establish an empirical correlation between the electrical properties of concrete and its moisture content (or internal humidity). To avoid complications caused by hydration (and other microstructural changes), these methods rely on calibration techniques, which may limit the applicability of the method to specific materials, specimen age, or

exposure history. To enable the development of a comprehensive procedure that would be applicable to a concrete member in service. Rajabipour [76] has investigated how the electrical conductivity of cement paste is influenced by moisture variations. The research [76] of electrical conduction in cement paste occurs through its liquid phase (i.e., the liquid filled capillary and gel pores) since the conductivity of solid and vapour phases are several orders of magnitude lower than the liquid phase [75]. It is argued that the electrical conductivity of cement paste is a function of the volume, connectivity, and electrical conductivity of the liquid phase. Drying causes a reduction in the volume and connectivity of the liquid phase while increasing the ionic concentration (and the conductivity) of the pore solution. In work of Rajabipour and Weiss [76], two types of cement paste and a natural porous rock have been studied to determine the mechanism of electrical conduction in a porous material when the material experiences moisture variation. To provide an estimation of the pore size and surface area distributions of each material, mercury intrusion porosimetry (MIP) was performed. Also, pore solution was extracted from each cement paste to determine its ionic composition and electrical conductivity. Finally, mass and electrical conductivity isotherms were obtained for each material (at $23 \pm 0.5^\circ\text{C}$) by progressively drying specimens to constant relative humidity from 100% down to 10% and then allowing the specimens to absorb moisture by gradually increasing the humidity back to 100%. From this information, a quantitative analysis was performed to determine the volume, connectivity, and electrical conductivity of the liquid phase at each stage of drying [76].

Another objective of the research by Rajabipour and Weiss [76] is to quantify the contribution of surface conduction on the overall conductivity of paste specimens. It has been shown that in porous materials, electrical conduction along the solid-pore surfaces might be considerably higher than conduction in the bulk of the pores due to the presence of an electrical double layer at the solid-pore surface [35,78]. Depending on the material, this effect may be dominant to the point that the overall conductivity of the material is governed by the surface characteristics rather than the volume and connectivity of the pores. To ensure that microstructural properties such as porosity and pore connectivity can be reliably estimated from electrical measurements, the contribution of surface conduction to the overall conductivity of cement paste should be evaluated [76].

Rajabipour and Weiss have made statements that the overall information of total moisture content in construction materials is not sufficient if the moisture gradients is unknown. These authors [77] have performed series of humidity detection and moisture gradient researches by application of EIS method [77].

In Figure 1.12, the resistance is normalized by the resistance that was measured before introducing the water to the specimen's surface (R_0), when R_t is the resistance that was measured across the same electrode pair at some time (t) after the introduction of water. As the resistance was measured over a period of time, an S-shaped response is obtained. These S-shape curves correspond to an initial flat response that correlates to negligible measured change in the electrical resistance when the water front is far away from the electrode pair, a rapid decrease in resistance as the water front approaches and passes the electrodes, and a flat portion that corresponds to the fact that the moisture front is passed and sufficiently far away from the electrode pair. McCarter et.al. [49] proposed that the maximum slope on each S-curve corresponds to the moment that the water front passes that electrode level. Using this technique, the time at which the water front passes the electrode level can be obtained from a series of resistance measurements [77].

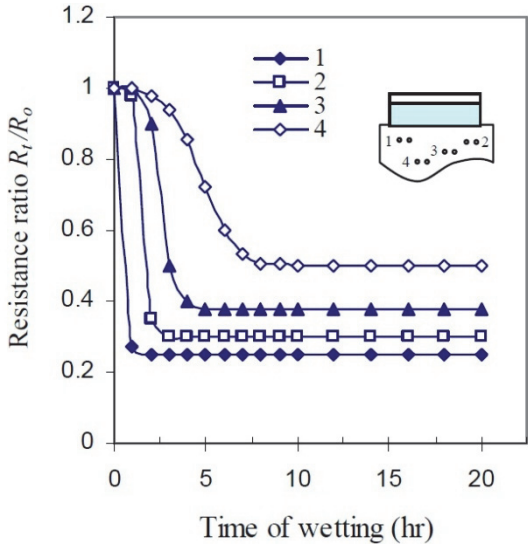


Fig.1.12. Variations in the electrical resistance of a concrete specimen as measured by several electrodes during the 24 h absorption period [49]

This approach uses a series of electrodes that are placed at different depths from the exposed surface to measure the depth of water penetration over time and introduces an approach whereby a single measurement of electrical conductivity measured between any two electrodes in concrete can be used to determine the position of the moisture front inside specimen after rewetting (note that this also assumes that the conductivity of the wet and dry concretes are known). Rajibapour and Weiss [77] have observed the effect of specimen size on the measured conductivity, the specimen's dimensions ($a \times a$) were varied from 16 x 16 to 100 x 100 millimetres while the electrode spacing (d_{elec}) was kept constant and equal to 10 mm. The specimen was then meshed into 1 x 1 mm square elements. The electrodes were

placed at the centre of the plate (in both x and y directions) to maintain a biaxial symmetry. It can be observed in both the conductivity and the derivative graphs that the S curves are not symmetric with respect to the electrodes level. The degree of asymmetry is observed to decrease as the ratio of the dry and wet concrete conductivities (σ_1/σ_2) increases. The electrodes sense the water front only when it is within a specific neighbourhood of the electrodes level. For example, for the case of $\sigma_1/\sigma_2 = 0.01$, this sensitive zone is observed when the depth of the moisture front reaches a distance of approximately $0.2d_{elc}$ of the electrodes level and is no longer sensed when the water front passes to approximately $0.6d_{elc}$ pass the electrodes centreline (it should be mentioned that, in this research, the sensitive zone is defined as the collection of the points at which the slope of the S-curve is greater than 10% of the slope that is measured at the inflection point.). Using these simulations, the electrical conductivity between the two electrodes was calculated for different positions of the moisture front within the defined sensitive zone ($-0.4d_{elc}$ to $+0.6d_{elc}$) [77].

The EIS method is based on the principle that a change in the water content of concrete alters the electrical response of the concrete (McCarter and Garvin [52], Weiss et al. [109]). On the other hand, Schießl and his team [90] have researched the moisture gradients that develop in drying concrete. Using a series of embedded stainless steel electrodes, they measured the electrical resistance of drying mortar samples as a function of distance from the drying surface [77]. This approach is based on the principle that a change in the water content of concrete alters the electrical response of the concrete [51,107]. Figure 1.12 is a schematic representation of the electrical resistance measured by McCarter and co-workers [49] from a series of electrodes placed at different levels inside a concrete specimen as the specimen was allowed to absorb water.

As it is known from the approach of Matiasovsky, Mihalka, Pel, Landman [40,46,62-64] the water absorption, absorption after rewetting and the drying process have slightly different kinetics and should be considered separately.

1.4.2. Frequency analysis in EIS

Prior beginning of moisture distribution measurements on autoclaved aerated concrete construction by EIS, a frequency analysis must be performed in order to determine, which frequency is most suitable for the respective material. Selection of a correct measurement frequency has a significant impact on the measurement results. Researches of author [86] prove that if unsuitable frequency is selected, the monitored changes of humidity distribution can be minimal or cannot be monitored at all. It is important to pay attention not only to a

single frequency, which seems to be suitable for the measurements but also to a range of frequencies around the selected frequency.

According to Jonscher [36], the origin of the frequency dependence of the conductivity was due to relaxation of the ionic atmosphere after the movement of the particle. This idea have been developed into a quantitative model suitable for solids by Funke [23]. It is assumed that immediately after an ion hops to a new site (a new minimum in lattice potential energy) it is still displaced from the true minimum in potential energy, which includes a contribution from other mobile defects. At long times the defect cloud relaxes, until the true minimum coincides with the lattice site. The model predicts upper and lower frequency-limiting conductivities and a region in between of power law (the constant-phase distributed response element) behaviour This is an important fact because the most suitable frequency tend to change its value along with changes of AAC structure during its drying process [9].

Furthermore, Tamtsia et al. [100] have discovered that analysis of the spectra provides pore structure information. Their studies allowed to obtain real-time descriptions of microstructural change during creep and shrinkage of cement paste through the coupling of time-dependent deformation and impedance measurements. Impedance spectra recorded over a wide range of frequencies (from 15 MHz to 1 Hz) have provided information and insight on cement paste microstructure and hydration. Cement based materials generally contain a broad size distribution of conducting pores. The network of these conducting pores continuously changes during the drying process. This change can also be detected in AC impedance spectra.

In the objective of predicting the corrosion of reinforced concrete structures over aging process, various studies were performed by using the electrochemical impedance spectroscopy (EIS) as a non-destructive tool. The general aim was to monitor corrosion of reinforcing steel embedded in cement-based materials [2].

This method, introduced in 1980's in reinforced concrete studies [34], allows determining the specimen response on a large frequency domain. Indeed, the EIS was used to study both:

- the low frequency domain (LF) of the impedance response to characterize the reinforcing steel behaviour in relation to the corrosion [5,6,27,29];
- the high frequency domain (HF) to monitor the hydration process of cement-based materials [14,26,48,92]. In addition, the HF arc can be related to the rebar surface adsorbed species such as Cl and OH in the case of chloride corrosion [2].

Therefore, taking into consideration the findings of Barsoukov and McDonald [9] and Tamtsia et al. [100] it is important to consider possible changes of the ACC material structure. The chemical properties of each AAC type have to be taken into consideration as well to proceed to EIS measurements on the material in order to determine humidity distribution throughout the cross section of the material.

1.4.3. Application of EIS on autoclaved aerated concrete masonry constructions

Experiments on application of EIS method for the detection of humidity distribution throughout cross section of aerated concrete constructions have been performed in Riga Technical university by Z-meter III device. The development of methodology for measurement process is a subject of these PhD thesis.

EIS method can be applied for non-destructive detection humidity level throughout AAC masonry constructions. It is easily applicable for testing of changes of humidity level in construction in relative means. In such cases no prior calibration of the Z-meter III device is necessary. As there are several types of probes which can be used as sensors for fully non-destructive testing and probes which require prior drilling of holes in construction in order to make accurate measurements the method gives opportunity to apply it for different constructions and situations. The most efficient and convenient type of probes is type 1 (probes, which are inserted in the construction, Fig. 1.13).



Fig. 1.13. Type 1 probes inserted in autoclaved aerated concrete block

With such probes it is not necessary to access construction from both sides which is rather difficult for in situ testing.

It is also possible to determine the moisture distribution in absolute means within construction with the EIS method. In such case calibration work in laboratory must be done before the in situ testing in order to determine the correlation of the electric impedance value and absolute humidity content of the construction. The advantage of EIS method against commonly used method of determination the material humidity rate by weight differences in dry and saturated conditions is that EIS can show the distribution of the humidity throughout the cross section of the construction. Other commonly used methods do not allow obtaining such data.

1.5. Z-meter III device for electrical impedance spectrometry measurements

In the Laboratory of Water – Management Research of the Institute of Water Structures at the Civil Engineering Faculty of Brno University of Technology, a measuring instrument with a Z-meter III device has been developed within the solution of an international project E!4981 of programme EUREKA. This instrument has been verified in laboratory experiments and measurements on objects in situ for moisture measurements in earth filled dams [59]. A prototype of the Z-meter III has been applied for all EIS measurements described in these thesis.

Z-meter III device consists of an electronic block and detachable measurement probes. With this measurement device, it is possible to perform measurements with use of one probe or a pair of probes and it is possible to expand the measurements up to 256 channels in a probe.

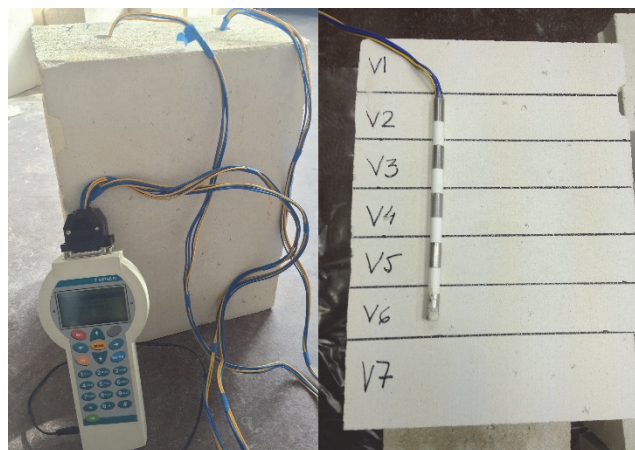


Fig.1.14. Z-meter III device and measurement probes with five active measurement channels
(stainless steel elements on measurement probe)

The measurement probe consists of active channels from stainless steel and insulator channels from plastics. The measurements are performed between the active channels of the measurement probes.

In case of single probe measurements the measurements are taken between active channels of the probe as in Fig.1.15.

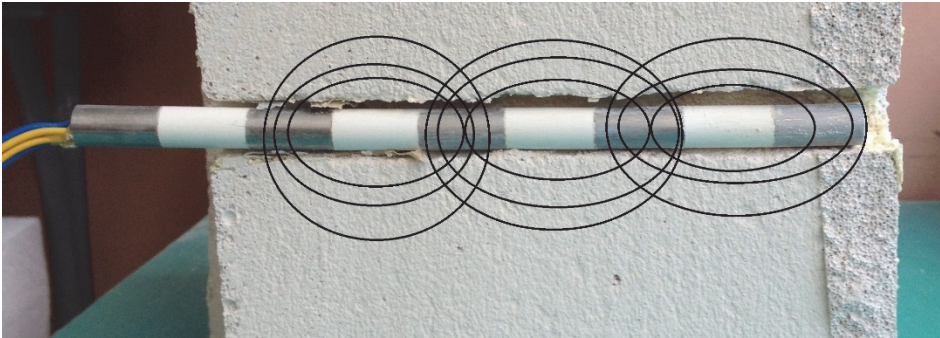


Fig.1.15. Schematic picture of measurements with one probe of Z-meter III

In case of a probe pair the measurements are taken between the corresponding active channels of each probe as in Fig.1.16. The quantity of active channels is variable depending on the probes, which are attached to the Z meter device. The probes can be customized to achieve the best fit for the circumstances of each construction type.

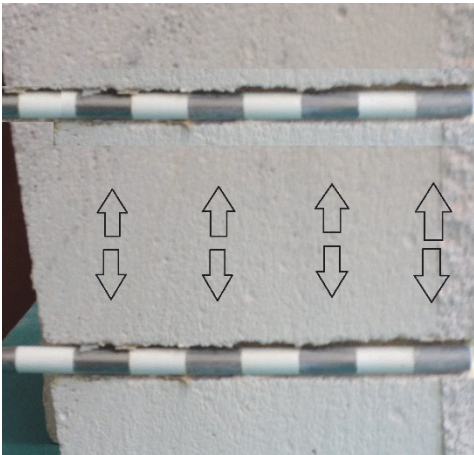


Fig.1.16. Schematic picture of measurements with a probe pair of Z-meter III

The output data of EIS measurements is divided into the main components of electrical impedance – the R and the X parts are separated in the output data (see table 1.1), which brings more opportunities for data interpretation.

The model of interaction between Z-meter device and porous media (in particular case AAC) can be described with an electrical circuit displayed in Fig.1.17 where the AAC material is the resistor of the electrical chain.

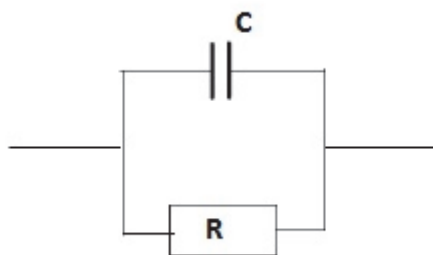


Fig.1.17. Schematic model of measurement circuit

Table 1.1

Z meter III output data

Start at 12.11.2014 9:12:30							
No	f [Hz]	date [dd.mm.yyyy]	time [hh:mm:ss]	ch	range	Rx [ohm]	Xx [ohm]
1	1000	12.11.2014	09:12:30	0	1	101,3	-47,4
2	1000	12.11.2014	09:12:30	1	1	101,4	-47,3
3	1000	12.11.2014	09:12:30	2	1	101,3	-47,3
4	1000	12.11.2014	09:12:31	3	1	101,3	-47,2
5	1000	12.11.2014	09:12:31	4	1	101,4	-47,2

EIS method with Z-meter [58] device allows using only one probe pair for multiple in-field measurements because the probes can be withdrawn from the construction after the measurement. Experiments with EIS method for the detection of humidity distribution throughout cross section of aerated concrete constructions have been performed by author using Z-meter III device [83-85]. EIS method can be applied for non-destructive detection humidity level throughout the cross section of AAC constructions. It is easily applicable for testing of relative changes of humidity level in construction. In such cases no prior calibration of the Z-meter III device is necessary [87].

2. EXPERIMENTS

These thesis have been based on comprehensive research, which was performed on step-by-step basis taking into consideration all main issues that could affect the possibilities of application of EIS method for detection of moisture distribution in AAC masonry constructions. Every experiment has been performed in order to verify the influence of different issues such as measurement frequency, quality of contact surface between measurement probe and AAC etc. on the accuracy of the obtained results. In further paragraphs description of the experiments as well as the main results have been displayed.

2.1. Frequency analysis for the AAC material

The EIS method is based on measurements of resistance of AC circuit. Therefore, the measurement result is a frequency dependant value, which depends on number of factors that characterize the properties (such as porous structure, density changes, moisture saturation rate etc.) of the material measurements are taken upon.

2.1.1. Description of the experiment

The experiment was based on monitoring of the differences the preferable measurement frequencies in AAC material due to the chemical and structural differences of the material.

For this experiment, five different AAC masonry block specimen were chosen. In order to compare the possibilities of the application of EIS on different types of AAC masonry constructions five different types of specimen of AAC were used for this test. The samples came from different manufacturers and had slightly different densities. Those facts allowed assuming that the porous structure as well as chemical structure of the samples slightly differed.

At first, the material samples were prepared for the experiment. Two full size masonry block elements were taken and cut into two equal parts each. In three samples, which were obtained in such way, there were made bores for embedment of the measurement probes while the fourth sample was cut into slices following the approach of Akita [3] in order to determine the initial moisture content throughout the cross section of the AAC block. All samples were scaled in order to compare the changes of moisture content in elements while the samples were drying in laboratory conditions (+20 °C, ≈80% Rh).

Measurements of moisture distribution by EIS were performed by Z-meter device using one probe pair of type 1 probes, which were inserted in previously prepared bores (Fig. 2.1.).

Each measurement probe, had five measurement channels, which mean that resistance data was obtained in five different depth levels of the specimen.

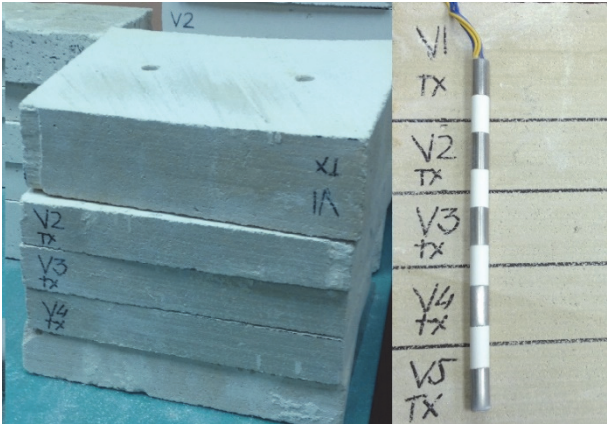


Fig.2.1. AAC masonry block samples for determination of humidity distribution by gravimetric method

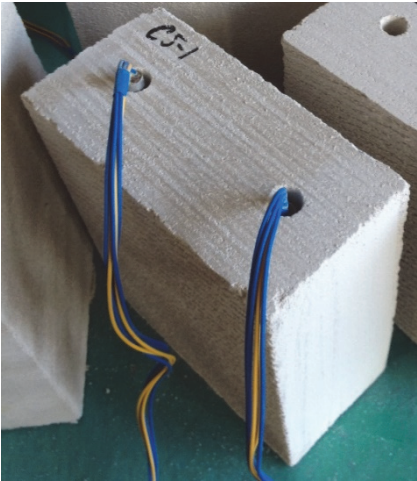


Fig.2.2. Autoclaved aerated masonry block sample with measurement probes

During the measurement phase, several external impact factors on the results of frequency analysis (the frequency analysis was performed in range from 100Hz to 20 000Hz) were observed as well. The external factors were the position of the measurement probes – the tests were performed with horizontal and vertical alignment of the measurement probes in the sample (Fig.2.3 a and b); the settling time between EIS measurements; and the humidity state of the measured material.



Fig.2.3 (a) Vertical placement of measurement probes



Fig.2.3 (b) Horizontal placement of measurement probes

For the detection of impact that is caused by the changes of samples' density due to their drying process the frequency analysis was performed several times during the drying process of the samples. Firstly, the frequency analysis was performed on AAC masonry blocks in the state of uneven humidity throughout the cross section of the AAC masonry blocks (Fig. 2.1.). Such state of moisture distribution in AAC masonry blocks is typical for

the material delivered to the construction site from factory or warehouse storage. The humidity distribution throughout the cross section of the AAC samples was determined by the methodology introduced by Akita [3] and V_0 to V_6 abbreviations stand to number of pieces each part of AAC sample block was cut into.

Therefore, uneven density of the sample due to uneven moisture distribution throughout the cross section of the samples was also evaluated in the results of frequency analysis. The second set of the frequency analysis measurements was performed after the samples had dried for a certain period of time (for 3 months in the particular case) in such way determining the impact of humidity distribution in samples on the results of frequency analysis.

All the way through the drying process of the samples EIS measurements were performed on the samples in order to detect the moisture distribution throughout the cross section of specimen. The correlations between EIS measurement results were established upon comparing the results of EIS measurements for sliced pieces and the measurements of mass change of corresponding samples.

2.1.2. Impact of moisture distribution throughout the cross section of the AAC sample on the results of frequency analysis

For frequency analysis, the X component of resistance is used because the optimal measurement frequency depends on the structure of AAC material. The complex impedance Z of the unsaturated porous material describes its properties - the solid part (grains) is formed by insulating materials characterized by their dielectric constants and represents the imaginary part of the measured impedance, which is taken into consideration during the frequency analysis. Water containing mineral salts is a conductive material. The degree of saturation of the material strongly influences the real part of the measured impedance. However, it is impossible to exclude the impact of moisture on the results of frequency analysis, especially, if the saturation rate of the material is high. In such cases moisture fills pores of the material, increasing overall density of the material and reduces the impact of the pores to the results of frequency analysis. Therefore, it is important to perform frequency analysis on specimen with possibly low saturation rate and even moisture distribution throughout the cross section of the material.

The results of performed frequency analysis display that for all specimen the most suitable frequencies are in range from 6,3 kHz to 20 kHz and vary significantly (Fig. 2.5. to Fig. 2.14.). Therefore, it is possible to conclude that the structure of AAC material has significant impact on determination the preferable measurement frequency for further

monitoring of the material by EIS measurements. Such statements have been also introduced in previous researches performed on porous materials by other non-destructive approaches [46,105].

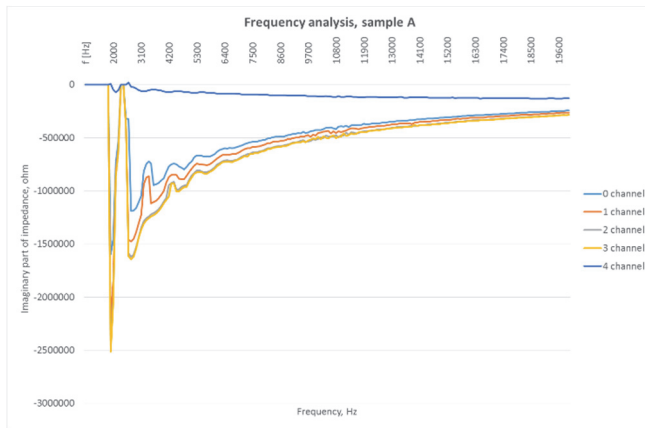


Fig. 2.5. Results of frequency analysis for sample A

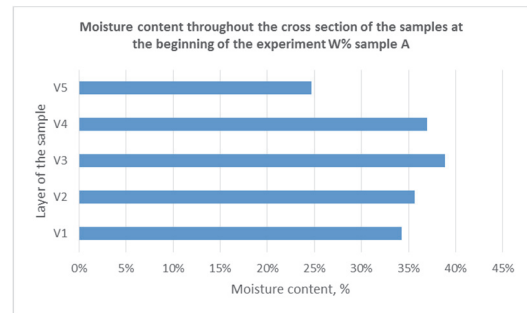


Fig. 2.6. Initial moisture distribution throughout the cross section of sample A, %

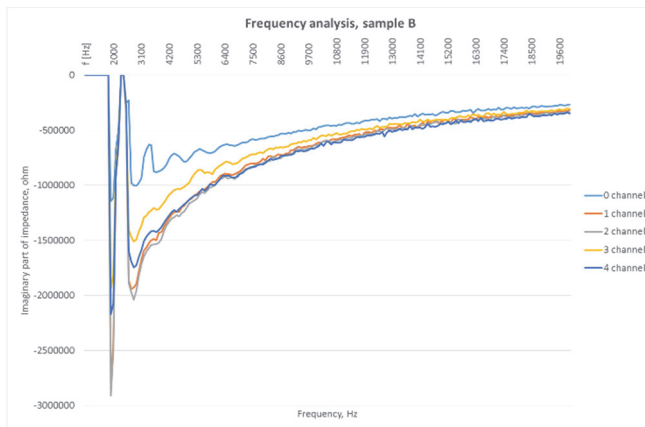


Fig. 2.7. Results of frequency analysis for sample B

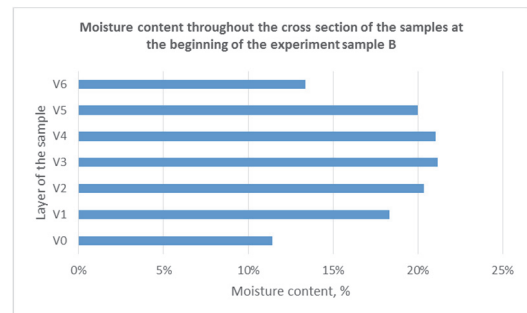


Fig. 2.8. Initial moisture distribution throughout the cross section of sample B, %

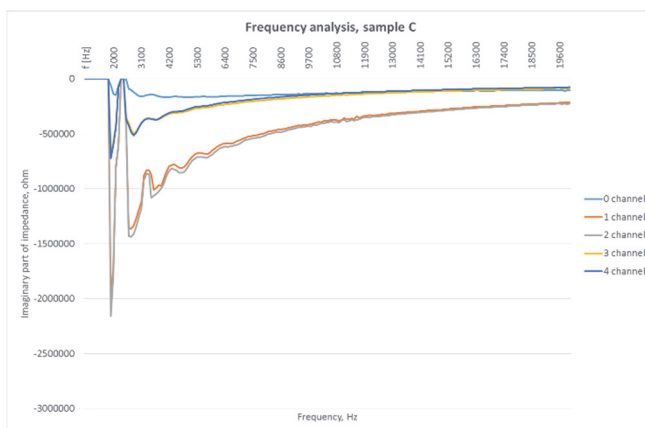


Fig. 2.9. Results of frequency analysis for sample C

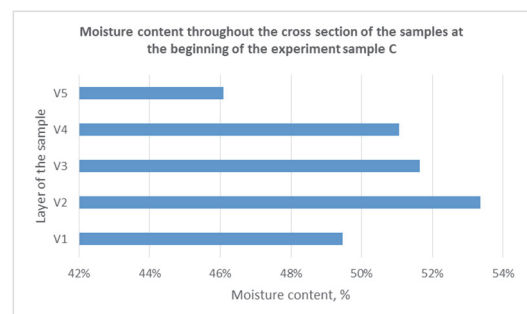


Fig. 2.10. Initial moisture distribution throughout the cross section of sample C, %

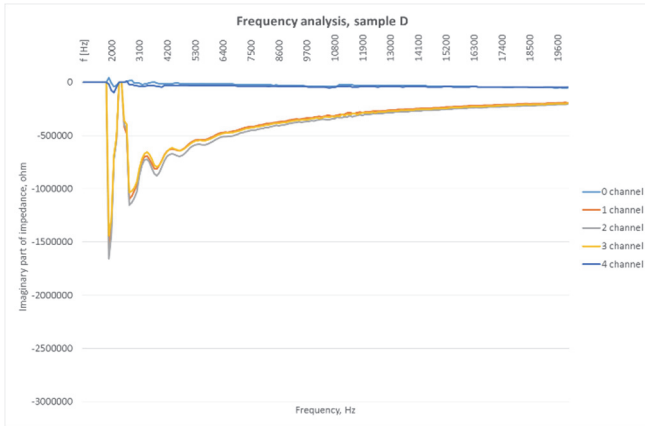


Fig. 2.11. Results of frequency analysis for sample D

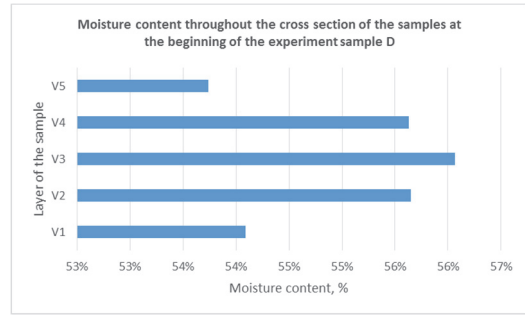


Fig. 2.12. Initial moisture distribution throughout the cross section of sample D, %

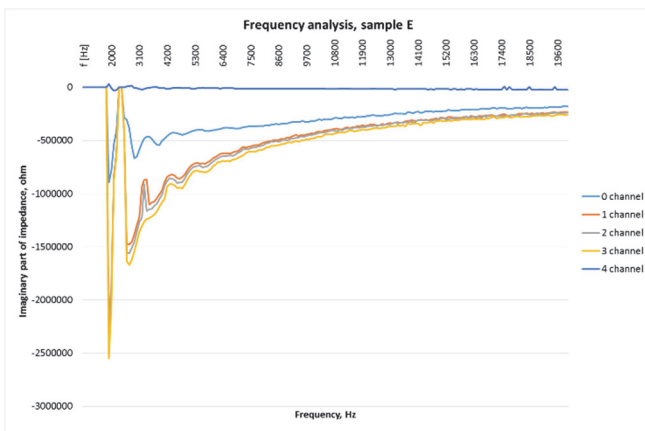


Fig. 2.13. Results of frequency analysis for sample E

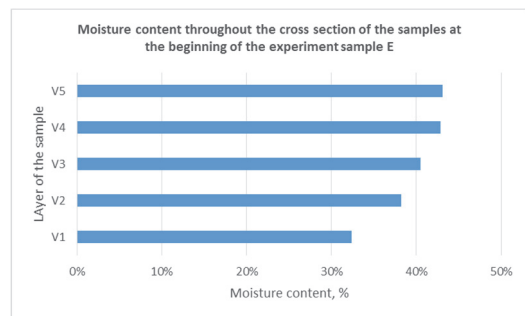


Fig. 2.14. Initial moisture distribution throughout the cross section of sample E, %

After comparing the frequency analysis data with the information (Fig. 2.5-2.14) of moisture distribution throughout the cross section of the samples, it can be concluded that the density changes of the material, which are caused by moisture content of the porous material have significant impact on the results of frequency analysis. It can be observed that the regions of the samples with higher moisture content and thus with higher density have wider frequency ranges, which are suitable for EIS measurements. However, it should be taken into consideration that the samples with large differences of the moisture content throughout the cross section of the sample also had large differences of impedance measurement results. Therefore, the moisture distribution measurements should be performed on the specimen prior frequency analysis in order to determine initial moisture distribution throughout the cross section of the sample in relative means using an average measurement frequency of 8-10 kHz, which has been detected as suitable for moisture distribution measurements in AAC. For more demonstrative comparison of moisture influence on the results of EIS frequency analysis

results, the comparison between frequency analysis graphs for the same block in different humidity states has been displayed in Fig. 2.15-2.22.

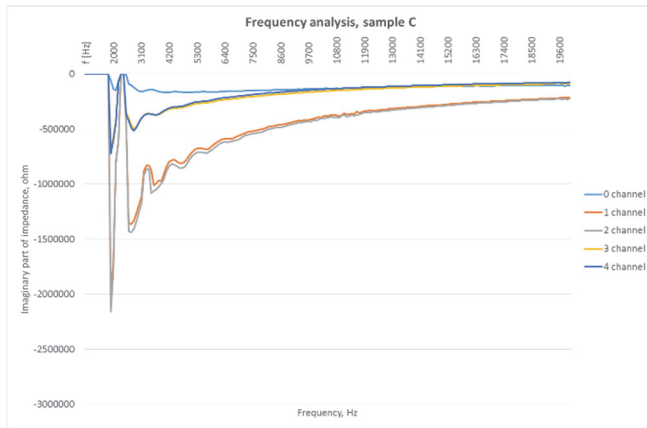


Fig. 2.15. Results of frequency analysis for sample C

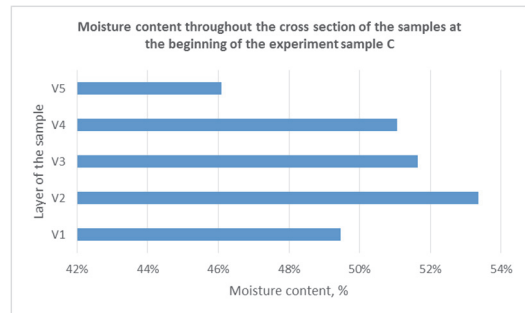


Fig. 2.16. Initial moisture distribution throughout the cross section of sample C, %

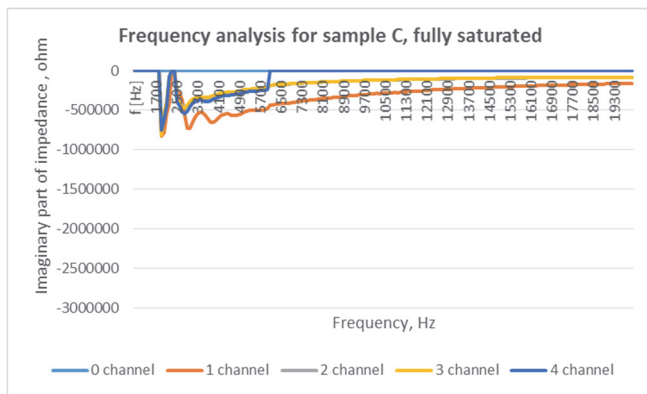


Fig. 2.17. Results of frequency analysis for sample C after full saturation of the specimen

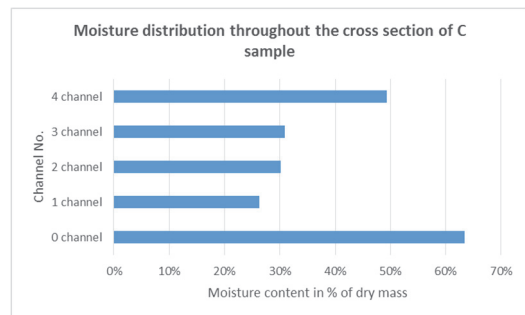


Fig. 2.18. Moisture distribution throughout the cross section of sample C after full saturation, %

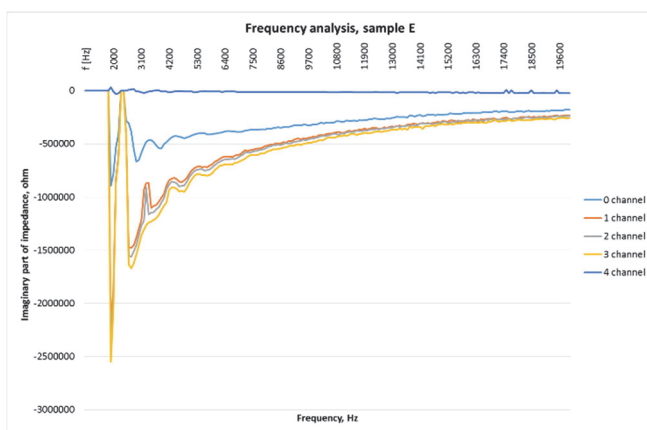


Fig. 2.19. Results of frequency analysis for sample E

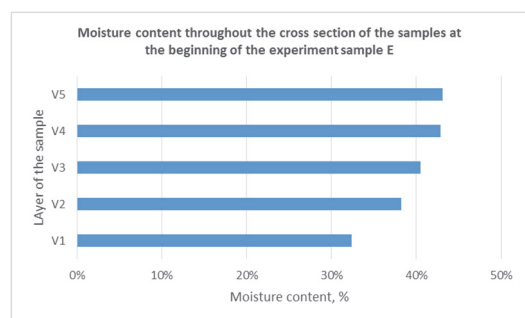


Fig. 2.20. Initial moisture distribution throughout the cross section of sample E, %

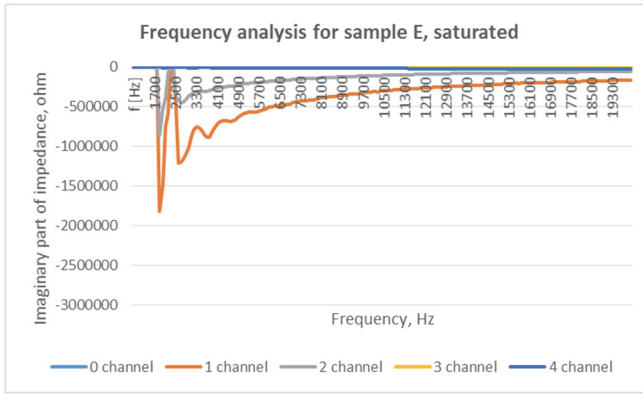


Fig. 2.21 Results of frequency analysis for sample E in saturated state

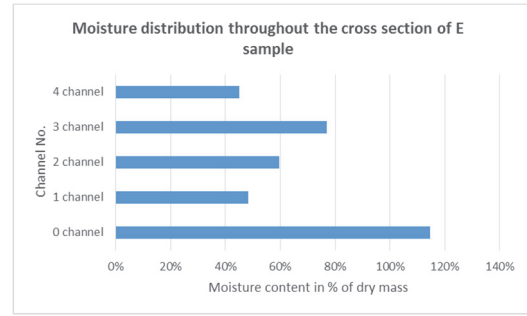


Fig. 2.22 Moisture distribution throughout the cross section of sample E in saturated state, %

While the moisture content of the AAC has significant impact on the results of frequency analysis, the probe placement in space (e.g. vertical vs horizontal placement) does not have significant impact on the EIS measurement results (Fig. 2.23). However, this statement is true only in cases when the probe embedment direction does not change against the direction of expansion of AAC during its manufacturing phase (fig. 2.24) which is described later in this paragraph.

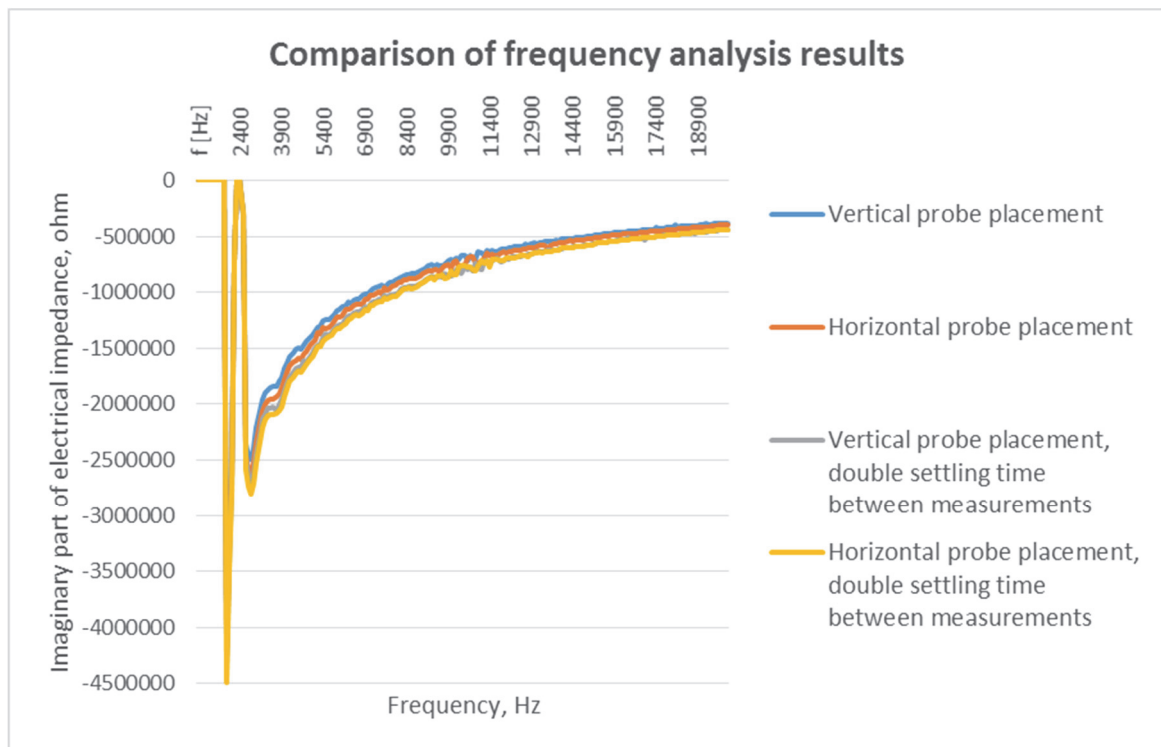


Fig. 2.23 Comparison of frequency analysis results

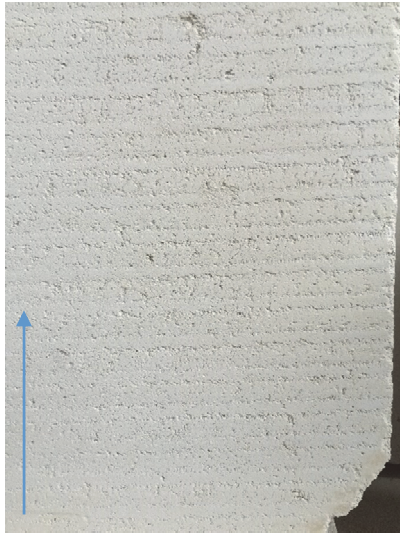


Fig. 2.24 (a) Porous structure of AAC parallel to the expansion direction (displayed with arrow) of AAC

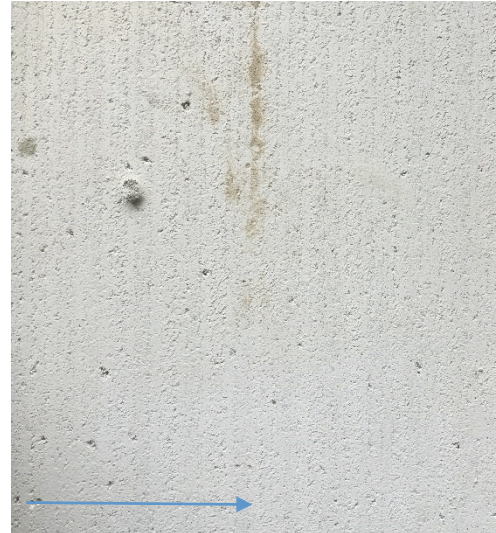


Fig. 2.24 (b) Porous structure of AAC perpendicular to the expansion direction (displayed with arrow) of AAC

AAC

2.1.3. Impact of anisotropy of AAC on results of frequency analysis

In previous paragraph it was stated that the density of the material has impact on the results of frequency analysis. Therefore, a separate frequency analysis was performed in order to determine the impact of the anisotropy of AAC on the results of frequency analysis. For the respective experiment two AAC masonry block specimen were used. EIS measurements of frequency analysis for one specimen was performed in the direction which is perpendicular to the manufacturing direction of the AAC and therefore parallel to the direction of expansion of AAC (A2 block). Meanwhile, the frequency analysis measurements of the other specimen were performed perpendicular to the direction of manufacturing and therefore parallel to the direction of expansion of AAC (A1 block) (fig.2.24 (a), 2.24 (b)).

For frequency analysis the X component of resistance was used because the measurement frequency depends on the porous structure of the material as stated in previous paragraph. As the porous structure of the AAC tends to change with the changes of the moisture content in the material, it is important to consider the anisotropic properties of the AAC within the frequency analysis of the material. The results display that the most suitable frequencies for different measurement directions vary significantly (Fig.2.25 and Fig.2.26).

For the A1 block the most suitable measurement frequency is in range from 8 000 – 13 000Hz while for block A2 it is a range from 5 000 – 9 000Hz. In order to obtain a comparable measurement results there had to be chosen one measurement frequency which in this case was chosen 8 000Hz.

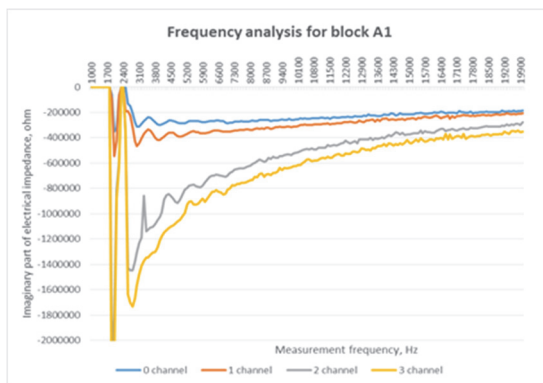


Fig.2.25. Frequency analysis for block A1

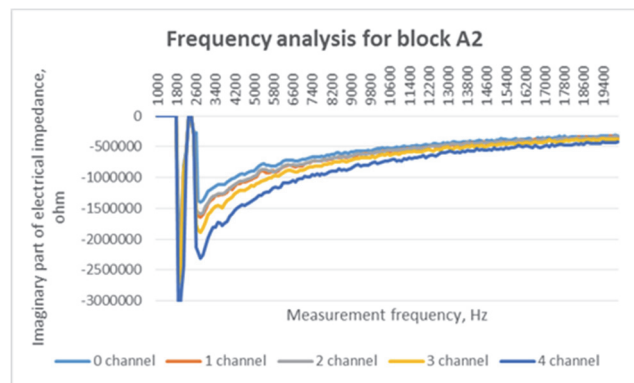


Fig.2.26. Frequency analysis for block A2

Additional attention should be paid to the 2 000Hz frequency in both graphs (Fig.7 and Fig.8) because this frequency show that next to a seemingly suitable measurement frequency can be frequencies which are totally unsuitable for the measurements in particular material. If such unsuitable frequencies are chosen for measurements all test results can be compromised because of the drying process' impact on the application of certain frequencies for EIS measurements.

2.2. Correlation between the moisture content and EIS measurement values in AAC masonry constructions

When a suitable measurement frequency for the EIS measurements in AAC material has been detected it is possible to apply EIS measurements for detection of moisture distribution throughout the cross section of the AAC material. However, these measurements have only relative character if a correlation between the EIS measurement result and a moisture content of the AAC sample is not known. As it is important to be aware of the moisture content in the construction materials in absolute means, a necessity of development of correlation equations between the EIS measurement results and the moisture content of the AAC samples arise.

2.2.1. Description of the experiment

In order to develop correlation equations between the moisture content in AAC masonry constructions (moisture content in % upon an weight of dry mass) and the result of EIS measurement of real part of electrical impedance (ohm), a research with set of experiments has been performed.

For the particular experiment, a set of five different types of AAC masonry blocks with different density and porous structure were used (Table 2.1).

Specimen with density in range from 375 to 500 kg/m³ were chosen for the experiment in order to determine the impact of different AAC properties – such as density, speed of drying, porous structure – on the correlation between the EIS measurement results and moisture content in the AAC.

Table 2.1

Technical data of AAC masonry blocks used for experiment

AAC block figure	Thermal conductivity in dry state stated by manufacturer λ W/mK	Bulk density stated by manufacturer kg/m ³
A	0,090	375
B	0,105	375
C	0,11	500
D	0,12	500
E	0,096	400

For the experiment a set of AAC masonry specimen were prepared, where four blocks of each AAC type were taken. In each specimen, two bores were made for embedment of type 1 measurement probes (Fig.2.1-2.2).

As the first step of the experiment, the frequency analysis was performed on all specimen in order to determine a suitable EIS measurement frequency for all ACC masonry block types. The description of the frequency analysis procedure has been described in chapter 2.1. of these thesis. The results of frequency analysis proved that there are different range of frequencies, which should be used for the EIS measurements on each type of the samples. However, in order to acquire comparable data the same frequency had to be chosen for all samples. So it was determined, that the frequency of 8000 Hz is the most suitable for measurements on all samples.

One of the blocks from each type were split into several pieces according to the approach of Akita et al. [3] in order to determine the moisture content of each segment in the masonry block by gravimetric method (Fig.2.2). The monitoring of the changes in moisture content of each sample was performed by monitoring of mass changes in time for each specimen. Such approach allowed determining the changes of moisture content in the specimen and the relevant changes of EIS measurement results upon the specimen.

The other three specimen from each type of AAC were placed in laboratory premises (20°C, 85% Rh) for drying. Along the drying process, regular EIS measurements were performed on all the samples. Additional EIS measurements were performed on the cut samples in order to secure the obtained data of AAC masonry block moisture content. Monitoring of samples' natural drying process was performed for four months. After the

samples had reached the air dry state they were oven dried in order to determine the weight of samples in absolute dry state.

From the obtained results, it can be concluded that the density of the AAC does not have significant impact on samples` drying speed. The C and D samples (Table 2.1.) had lost approximately the same amount of moisture content (after 3 months of drying time in laboratory storage) in % as the other samples.

2.2.2. Results

At the beginning of the experiment, all samples had similar character of moisture distribution throughout their cross section although the moisture content in the specimen was significantly different (Fig.2.27). The initial moisture content of the AAC blocks depend on the specialties of the manufacturing process and storage conditions prior delivering the blocks to the construction site. Therefore, in in-situ conditions these values cannot be influenced by any party.

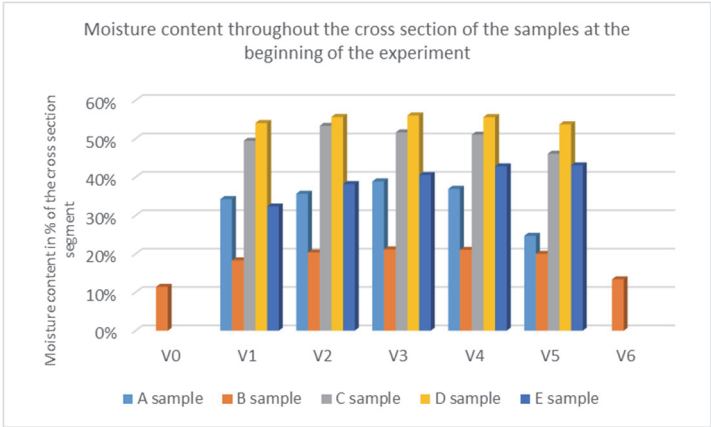


Fig.2.27. Moisture content throughout the cross section of the samples at the beginning of the experiment

The data for Fig.2.27 was obtained by gravimetric measurement method for detection of moisture content in construction materials by the approach described by Akita et.al [3] and moisture content measurements by differences in mass. Further data concerning the moisture distribution throughout the cross section of the samples were obtained by EIS measurements. The gravimetric method was used for overall control of the experiment results and for preparation of correlation equations between the EIS measurement results and corresponding relative moisture content of the AAC.

In order to correlate values of EIS measurements with the absolute values of moisture content in cross section of the sample correlation graphs were prepared for each type of AAC samples (Fig.2.28-2.32).

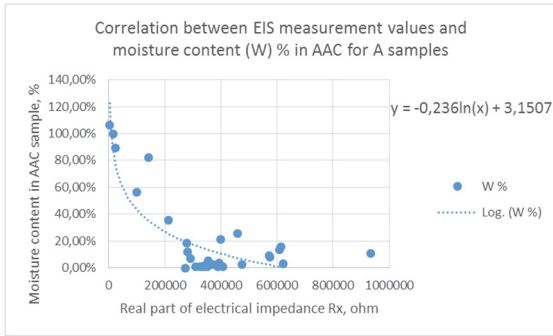


Fig.2.28. Correlation between EIS measurement values and moisture content of the samples of A series in %

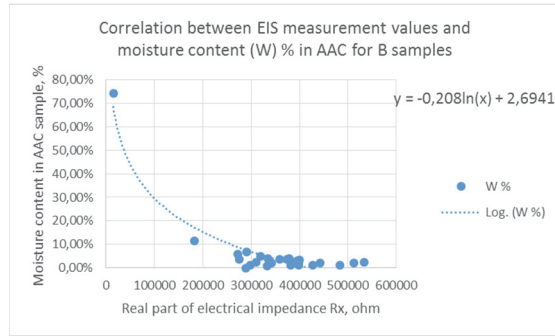


Fig.2.29. Correlation between EIS measurement values and moisture content of the samples of B series in %

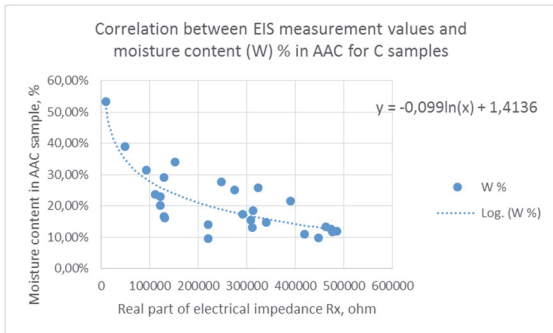


Fig.2.30. Correlation between EIS measurement values and moisture content of the samples of C series in %

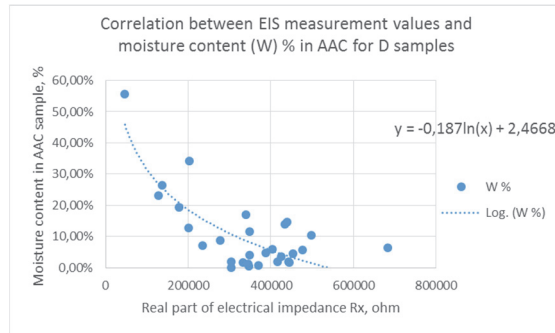


Fig.2.31. Correlation between EIS measurement values and moisture content of the samples of D series in %

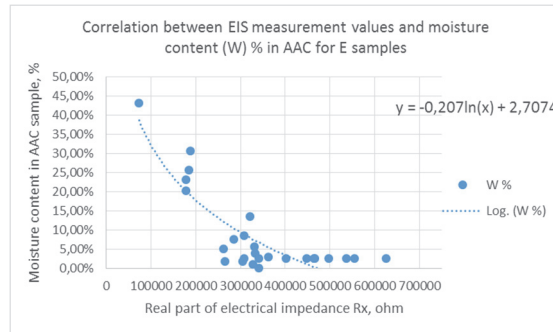


Fig.2.32. Correlation between EIS measurement values and moisture content of the samples of E series in %

The correlation equations have the same basic form:

$$y = a \ln(x) + C \quad (2.1)$$

where “a” varies from -0,099 to -0,236 and constant “C” varies from 1,4136 to 3,1507. A and C values from each particular equation can be used as a describing parameters of the respective type of AAC in aspect of drying speed and interaction of specimen with EIS measurement method.

From all obtained results, an universal equation (2.2.) for all types of AAC has been developed in order to reduce the amount of preparation works for measurements where high accuracy is not required.

$$y = -0,201 \ln (x) + 2,6513 \tag{2.2}$$

The equation data (Fig.2.28-2.32) was used to determine the changes of moisture content throughout the cross section of the AAC samples after 3 months drying time (Fig.2.33).

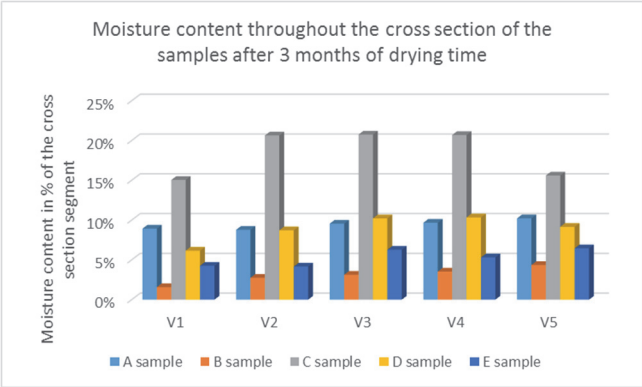


Fig.2.33. Moisture content throughout the cross section of the samples after 3 months of drying time

The measurement results display that the AAC blocks with lower density have more regular moisture distribution throughout the cross section of the block than specimen with higher density.

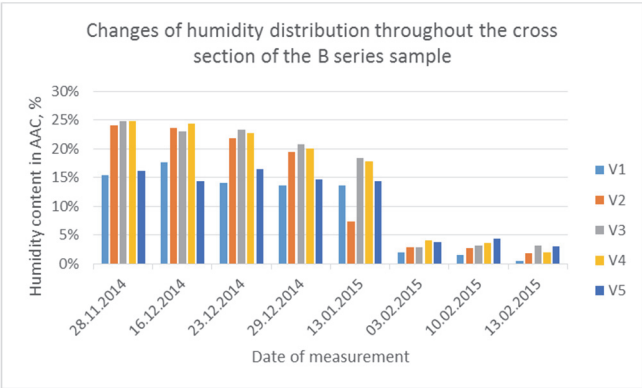


Fig.2.34. Changes of moisture content throughout the cross section of the samples during drying process

EIS measurement results can be transformed into moisture content rate of the AAC material and in such way, the distribution of moisture content in the material sample can be determined by non-destructive method (Fig.2.34).

From the obtained results, it can be concluded that the density of the AAC does not have significant impact on overall speed of samples` drying. It has impact on the speed of drying only in case the sample has high moisture content which is above 40%. In such case

samples with higher density has lower drying speed for the central part of sample's cross section material.

However, the AAC density and structure of pores has significant impact on accuracy of EIS measurement interpretation. Therefore, prior using the EIS method by Z-meter device for humidity content measurements on-site, correlation equations between EIS measurement results and moisture content of the AAC sample should be determined in laboratory.

2.3. Measurements of moisture distribution throughout the cross section of single AAC masonry block

In-situ application of EIS method for detection of moisture content and its distribution throughout the cross section of AAC masonry constructions involve several issues, which should be taken into consideration. One of such issues is the quality of contact surface between the measurement probe and the AAC. The term contact surface involves not only the smoothness of the measurement surface but also the distance between the measurement probe and the AAC as well as the coating material of the measurement surface in order to obtain closer contact surface between the measurement probe and AAC.

In order to determine the impact of contact surface between measurement probe and the AAC material as well as to monitor the drying process of AAC within boundaries of one masonry block there was preformed an experiment described in paragraph 2.3.1. The impact of the measurement probe alignment vs expansion direction of AAC materials (according to the description of the manufacturing process in chapter 1.1.) was also assessed during the experiment.

2.3.1. Description of the experiment

In the experiment two types of autoclaved aerated concrete blocks (AEROC Universal and Texoblock Standart) as in Fig.2.35 were used.

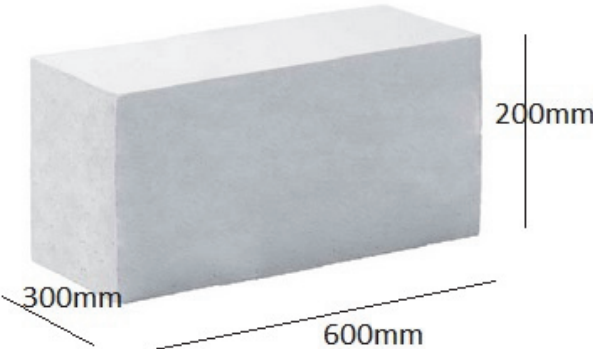


Fig.2.35. Aerated concrete block AEROC Universal

Each of the blocks was cut in three identical parts with part size of 200mm x 200mm x 300mm. In each specimen two bores with 12mm diameter for measurement probes were made as in Fig.2.36 which brings a 2mm gap between diameter of the measurement probe and the embedment bore.

For the measurements of moisture distribution, one pair of type 1 measurement probes with five active channels were used. The probes were embedded into bores as in specimen displayed on Fig.2.37.



Fig.2.36. Specimen of autoclaved aerated concrete blocks bores for measurement probes



Fig.2.37. Example of measurement probe embedment in fragment of autoclaved aerated concrete block

The measurements were made between the active parts of measurement probes as stated in paragraph 1.5. In particular case, all five channels of the probe were used for the measurements in the AAC material.

In order to monitor the drying process of the blocks each time they were scaled, the changes of weight were fixed and the resistivity measurements by EIS performed (Fig.2.38). After the blocks had reached air dry state, they were oven dried in 105°C degree temperature to reach an absolute dry state as stated in the methodology by RILEM for AAC [80]. EIS measurements were performed on AAC blocks in absolute dry state as well. After these measurements, the moisture content rate of the material was calculated using the approach of gravimetric method and equation (2.2).

$$W = \frac{m_w - m_d}{m_d} \cdot 100\% \quad (2.2)$$

W-Moisture content of the material %;

m_w -weight of the material sample in wet state, g;

m_d - weight of the material sample in dry state, g.

As a result of the experiment two independent correlation equations were obtained and it became possible to compare the EIS measurement results and correlation equations for two different types of AAC masonry blocks. This comparison allowed to make conclusions whether the EIS measurement results by Z-meter III display the same deviations in the measurement results due to the slightly different pore structure of the AAC material as it was displayed in [44] tests by sensors used by Rabijapour and Weiss as well as Barsotelli et.al [102] and has been described in chapter 2.4 of these thesis.

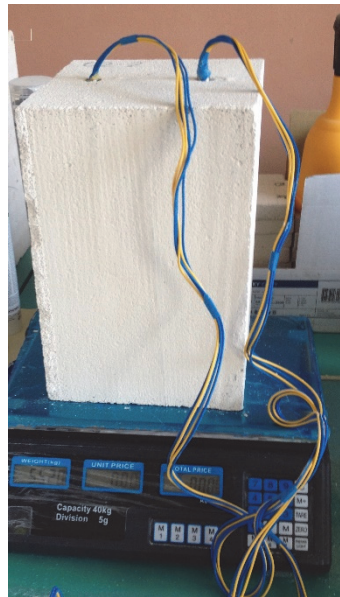


Fig.2.38. EIS measurements in aerated concrete block fragment (C1-1 to C3-3)

The experiment also included application of three measurement series where in each set different type of contact surface improvements were applied. In order to increase the credibility of obtained results each of the series consist of measurements performed on three blocks, which were exposed to identical conditions.

For the first series of the blocks the measurement bores were made with the maximal accuracy for the bore diameter to comply with the diameter of the measurement probe. Thus, the embedment bore was maximally close to the probe diameter. The difference between the probe radius and the radius of the bore was less than 1mm.

Although such precision causes certain inconveniences in measurement process due to difficult insertion of the measurement probe the contact surface in this case was tight and no other contact surface improvements were used.

During the measurement process, there arose a problem of extensive drying process due to additional ventilation of the blocks through the measurement bores and a solution for this

problem was researched during this experiment as well as the problem of contact surface's influence on the accuracy of measurement results.

Therefore, for the second series of experiment specimen in order to prevent fast drying of the block due to additional ventilation of the structure in the measurement bores; the bore surface was covered with liquid silicone and the influence of this material on measurement results was assessed.

In the third series of the specimen the space in the measurement bore between the probe and the surface of the aerated concrete block was filled with universal silicone. The silicone filled all free space between the measurement probe and the AAC so that ideal contact surface between the probe and the block was established. However, a problem arose during the drying process of the block. As the block dried small particles of AAC which were displaced in the pores of the material during the drilling process separated from the material surface and in such way decreased adhesion between the silicone and the AAC block. As the measurement process assumed cyclic embedment and withdrawal of the measurement probes then the decreased adhesion between the materials caused separation of the silicone from the block surface and in such way the integrity of the measurement process was terminated.

The obtained results from all three sets of the specimen were compared within each of the measurement series and afterwards the results were compared between the series.

All blocks were monitored for period of three months during summer of 2014. The average temperature of the surrounding environment during the monitoring process was +22°C and average air humidity rate was 70%.

In order to determine the impact of the AAC expansion direction (see chapter 1.1.) on the EIS measurement results during the drying phase of AAC masonry blocks the experimental series were extended. Therefore, two fragments of the same AAC block were used (AEROC universal AAC masonry block) with density of 375 kg/m³. In both blocks a pair of bores were made for embedment of measurement probes (Fig.2.1.-2.2.). In one block the bores were made parallel to the manufacturing (expansion) direction of the block (block A1) and in the other block perpendicular to the manufacturing (expansion) direction of the block (block A2).

The EIS measurements were performed with 4 channels of probe for A1 block and 5 channels for A2 block. The difference of the channels were caused by the thickness of the blocks and the fact that in A1 block only 4 active channels of the measurement probe could be inserted.

At the first phase of the experiment, the frequency analysis for both blocks was performed according to the procedure described in chapter 2.1. The frequency analysis was performed in range from 1 000Hz to 20 000Hz with measurement step of 100Hz. Based on the results of the frequency analysis all further measurements were performed in frequency of 8 000Hz.

The second phase of the experiment consisted of several parts. At first, both blocks were fully saturated with water and the initial EIS and gravimetric measurements were taken. Afterwards blocks were left for drying in laboratory conditions (+20...+25°C and approx. 70% Rh) and periodically EIS measurements were performed on the blocks. After the blocks had reached an air dry state they were put into a drying oven and dried to absolutely dry condition in compliance with RILEM recommendations for drying of AAC [80]. After the drying procedure another set of EIS measurements was taken. Throughout the time of the EIS monitoring of the blocks they were also scaled so that correlation between the EIS measurement values and the average moisture content ratio in % of the material could be established and the character of the relevant correlation equations could be compared with the character of the developed correlation equations for different types of AAC (see chapter 2.2).

2.3.2. Results

As a result of the experiment six independent correlation equations were determined. The correlations are displayed in Fig.2.39-2.44. Separate correlation equations were established for the specimen with different types of contact surface coating, for specimen without contact surface coating and for the specimen, which were used for the comparison of the impact on AAC anisotropy on the EIS measurement results. The established correlation equations were prepared using average measurement means for the whole specimen, therefore they cannot be used for the determination of the absolute values of moisture content. In the particular case these correlation equations are used to compare the obtained results from different specimen in the frame of the particular experiment.

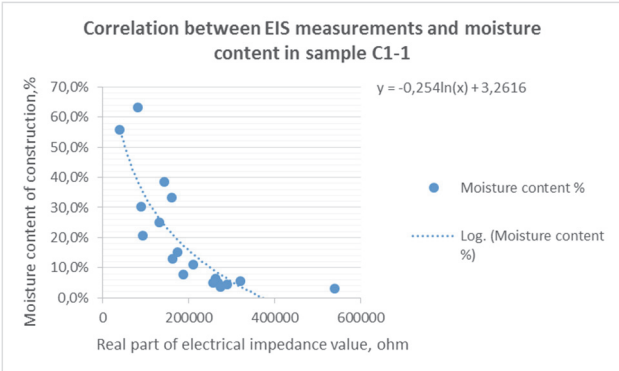


Fig.2.39. Correlation between EIS measurements and moisture content % in aerated concrete block fragment (C1-1)

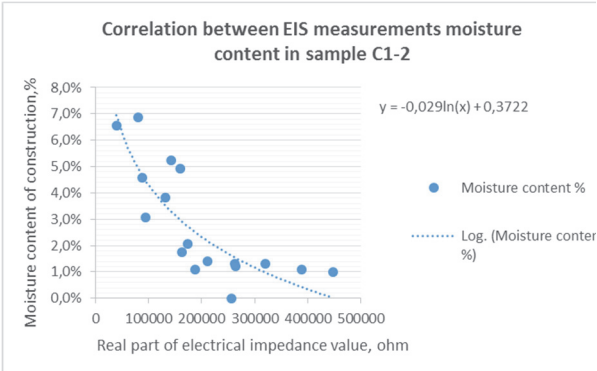


Fig.2.40. Correlation between EIS measurements and moisture content % in aerated concrete block fragment (C1-2)

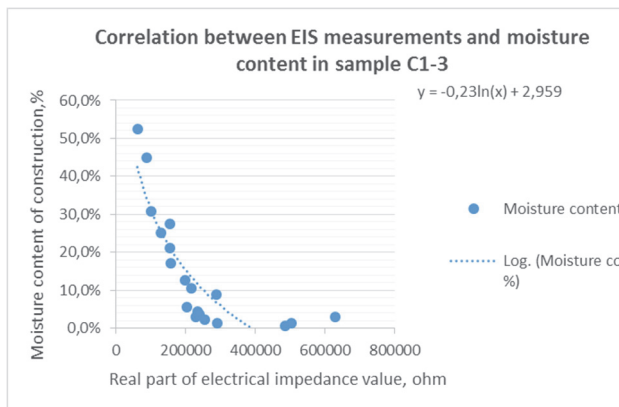


Fig.2.41. Correlation between EIS measurements moisture content % in aerated concrete block fragment (C1-3)

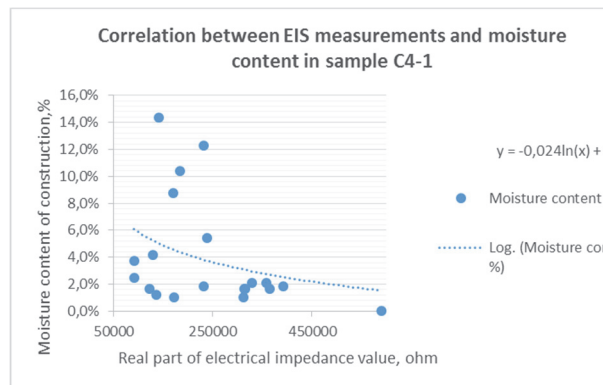


Fig.2.42. Correlation between EIS measurements and relative humidity % in aerated concrete block fragment (C4-1)

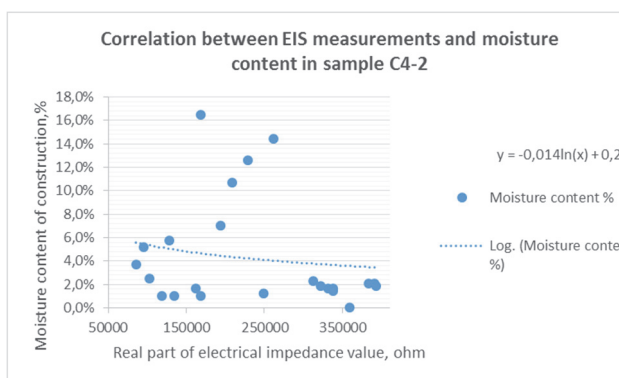


Fig.2.43. Correlation between EIS measurements and moisture content % in aerated concrete block fragment (C4-2)

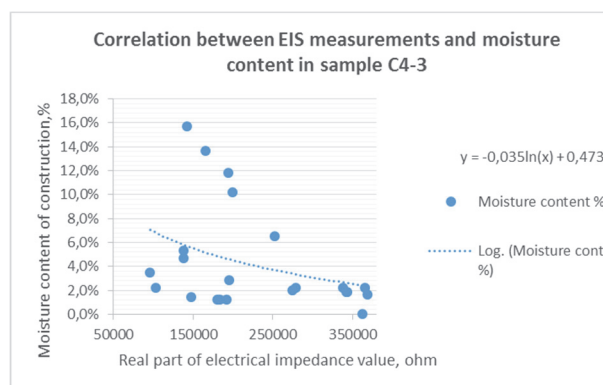


Fig.2.44. Correlation between EIS measurements and moisture content % in aerated concrete block fragment (C4-3)

After comparison of obtained results it is clear that the density and pore structure of the AAC masonry block has significant impact on the measurement results. Correlation between EIS measurement results and the moisture content of the construction has logarithmic character but absolute values can be compared only if the measurement conditions, especially, the structure of measured AAC material is similar. Results in Fig.2.39 to Fig.2.41 show similar character as well as the results on Fig.2.42 to Fig.2.44. As the specimen C1-1 to C1-3 were from one type of AAC masonry block (A in table 2.1) and specimen C4-1 to C4-3 were from another type of AAC masonry block (D in table 2.1) then it is possible to conclude that density and other physical characteristics of the material have significant impact on the electrical measurement results. Therefore, the overall application of the EIS measurements for measurements of humidity distribution is restricted to the types of the AAC, which have previously established correlation equations between EIS measurement results and moisture content rate of the construction.

Therefore, for each type of AAC masonry blocks there should be developed an individual correlation equation between EIS measurement results and moisture content of the material. Moreover, the type of the AAC should be recognized during the EIS measurements in situ, in opposite case it may lead to the situation when wrong correlation equation is chosen and the obtained EIS measurement results do not meet the maximum of possible accuracy. Such situations may lead to the increase of deviation of the measurement results.

2.3.3. Impact of the bore diameter on measurement results

An assumption that the distance between the measurement probe and AAC material has impact on the accuracy of EIS measurement results due to the dielectric properties of the air. Therefore, the impact of the difference between the bore diameter and the diameter of the measurement probe (thus, the free distance between the surface of the measurement probe and the AAC material) has been researched. The data described in this paragraph has relative character for the comparison between the results, obtained from different specimen. The EIS measurement result, which was obtained from the AAC blocks with no filling between the block surface and measurement probe has been considered as a reference result.

The reference chart is displayed in Fig.2.45.

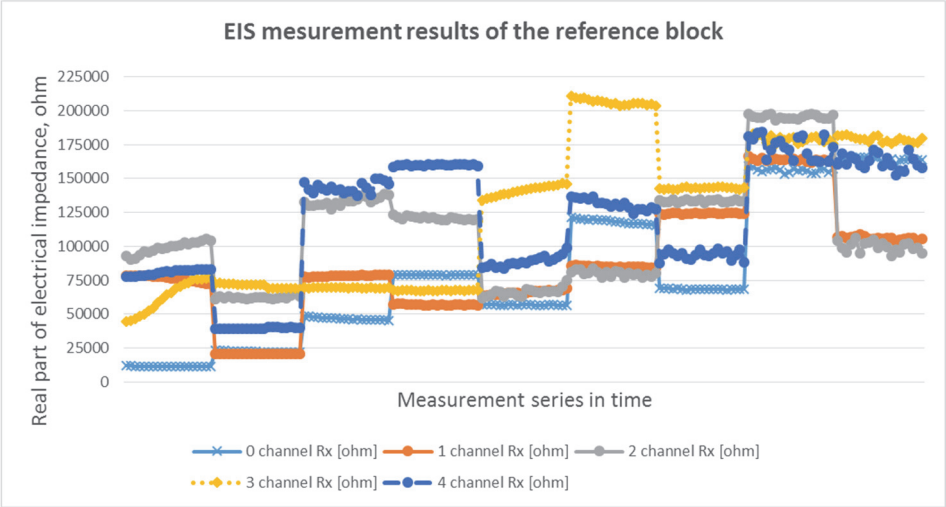


Fig.2.45 EIS measurements during the drying process of the reference block

During the blocks` drying process its` electrical resistivity changes. Fig.2.45 displays that the changes of the electrical resistivity are not equal in all areas of the block and tendencies of moisture migration throughout the cross section of the block can be monitored through the EIS measurement results. From the measurement results it can be concluded that each sector of the block show different speed of drying and moisture transfer. The resistivity measurements of separate channels can change significantly in time from high values (aka

relatively low moisture content rate) to low values (aka relatively high moisture content rate) but the tendency of overall increase of the resistivity can be correlated to overall decrease of the materials' moisture content rate. After series of measurements, where the distance between the measurement probe and contact surface varied in range from 1 to 3mm it was determined that the bore diameter does not have significant impact on measurement results.

2.3.4. Impact of the silicone filling on the measurement results

As the application of universal silicone significantly improves contact surface between the measurement probe and the surface of autoclaved aerated concrete block as well as decreases the surface area where extensive drying can occur, universal silicone was used as the surface coating material in the second set of measurements (Fig.2.46).

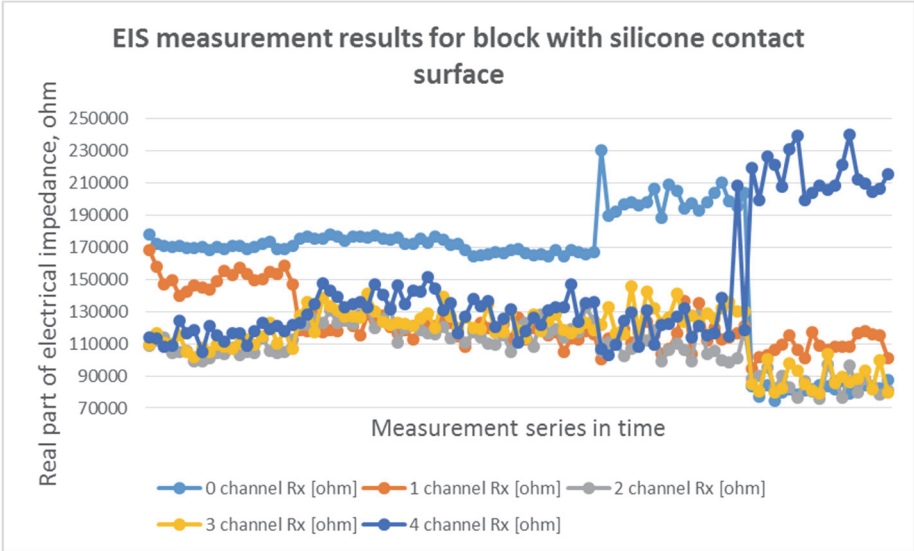


Fig.2.46 EIS measurements during the drying process of the block with silicone filling between the measurement probe and the surface of the aerated concrete block

After comparing results of Fig.2.45 and Fig.2.46 it can be stated that the trend of the results for the measurements where silicone was used as a filling material for space between the probe and the block surface is similar. However, the later measurements results are more even and do not show significant differences between the measurement series, which are taken in different time. In case where universal silicone was not applied, the differences between the measurement series are obvious (Fig.2.45).

Comparison of absolute measurement values between the measurements made without any filling material and using silicone as filling display that the silicone filling works as insulation material which does not allow to monitor detailed changes of moisture migration through the cross section of the material in real time (Fig.2.47).

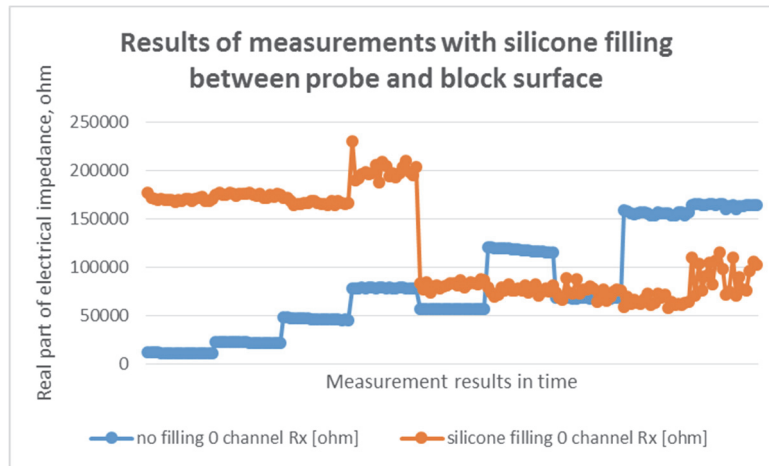


Fig.2.47. EIS measurements during the drying process of the reference block and block with silicone filling between the probe and the measurement surface

These results also display significant differences in absolute values of measurement data, which does not allow to correlate data obtained during different measurement sessions. In fact the measurement results prove that during the drying process silicone layer loses its' adhesion to the measurement surface and then a leap of measurement values can be observed. This brings to a conclusion that due to difficult application of silicone in measurement bores and to the fact that silicone affects measurement results it is not suitable for prevention of measurement surfaces' accelerated drying process or for improvement of the contact surface between the measurement surface and the probe.

2.3.5. Impact of the liquid silicone on the measurement results

The experiment with application of universal silicone in order to prevent accelerated drying processed of the measurement areas due to additional ventilation and exposed drying surfaces proved that universal silicone is not suitable for such purpose.

As an alternative a liquid silicone spray was chosen. After the preparation and cleaning of the measurement bores with compressed air a layer of liquid silicone spray was applied on the surface of the measurement bores. The liquid silicone infiltrated into the aerated concrete for approx.1 cm (Fig.2.38), the block with the measurement probes inserted). After the blocks were infiltrated with water, the area, which was exposed to liquid silicone spray became clearly visible and in such way it can be stated that liquid silicone had covered all area of contact surface between the measurement probe and the AAC material.

Although liquid silicone spray infiltrates into the AAC and thus does not improve the contact surface, it prevents the measurement bore surface from accelerated drying. In such

way, these results can provide more precise data about moisture migration processes throughout the cross section of the construction.

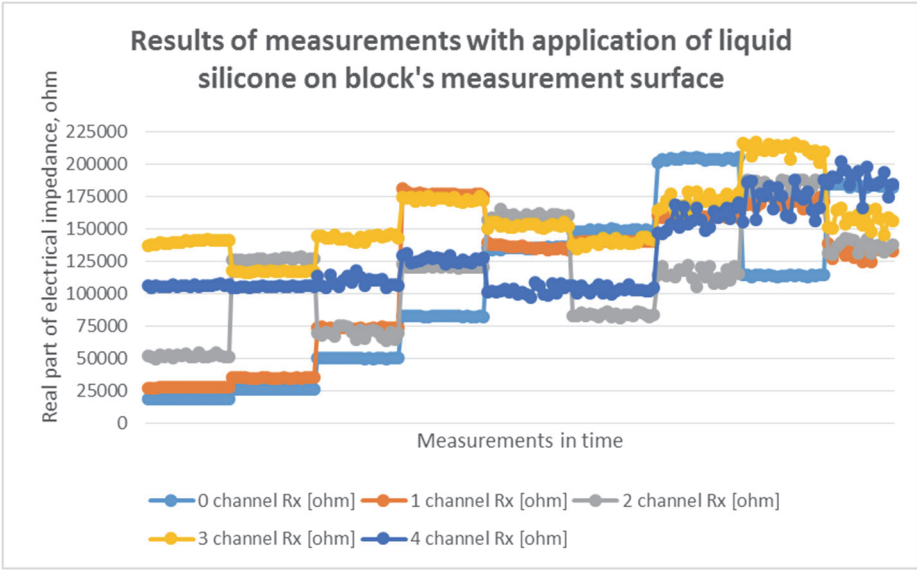


Fig.2.48. EIS measurements during the drying process of block with liquid silicone spray filling between the probe and the measurement surface

The overall character of the measurement results for the reference block and for the block with liquid silicone application of measurement contact surface is similar (Fig.2.45 and Fig.2.48). Exact division into measurement series can be seen in the chart which allow to assume that liquid silicone does not have significant impact on sensitivity of measurement tool as universal silicones does.

Comparing the absolute values of the measurement results (Fig.2.49) from the reference block and the block with liquid silicone filling on measurement bores it can be stated that liquid silicone spray does not have significant impact on absolute values of EIS measurement results.

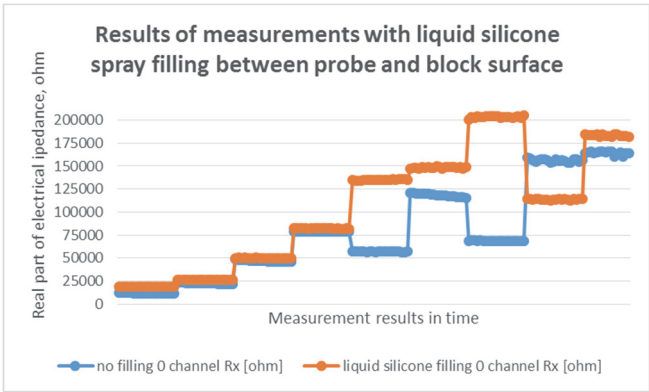


Fig.2.49. EIS measurements during the drying process of the reference block and block with liquid silicone spray filling between the probe and the measurement surface

Furthermore, it can be stated that application of liquid silicone spray on measurement bore surface excludes some influence of surrounding area to the results of the experiment. The barrier, which is made by the silicone coating prevents measurement surface from accelerated drying in warm and dry conditions and increased absorption of air humidity in case of high humidity rate of surrounding environment.

2.3.6. Impact of measurement direction vs the expansion direction of AAC on the results of EIS measurements

In paragraph 2.1. it was defined that the uneven pore distribution throughout the volume of AAC due to the manufacturing technology of the material has significant impact on the results of the frequency analysis.

Therefore, after determination of the most suitable measurement frequency (described in paragraph 2.2) the monitoring process of the AAC blocks begun. The impact of the EIS measurement direction vs the expansion direction of the AAC was assessed. The EIS measurements were taken for four months' period and impact of measurement direction on the accuracy of obtained results was determined (Fig.2.50).

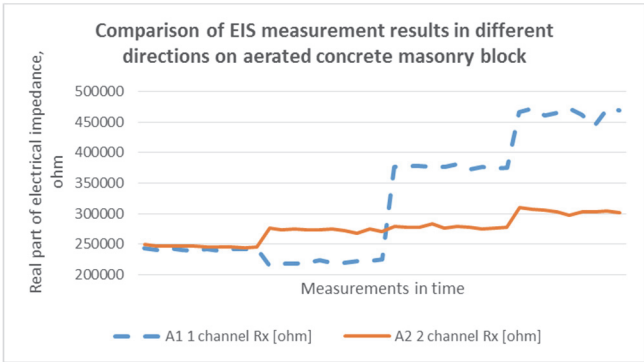


Fig.2.50 Comparison of EIS measurement data on blocks A1 and A2 depending on measurement direction

The measurement results display that at the beginning of AAC masonry blocks' drying phase the measurement values do not significantly differ due to the anisotropy of the AAC but as the drying process progresses the influence of optimal frequency distribution displays its impact on the results and the measurement values start to differ significantly. It means that in situations when comparison of the EIS measurement results is necessary it is important to take into consideration the measurement direction. In opposite case the obtained results can be misinterpreted as increased speed of moisture migration through the cross section of the construction.

In order to compare the application possibilities of EIS monitoring on different types of AAC a correlation between EIS measurements and values of moisture content have been determined (Fig.2.51 and Fig.2.52).

The correlations equations differ depending on measurement direction but overall the trend of the equations is similar and allow to assume that in all cases concerning measurements performed on AAC masonry constructions they would be similar.

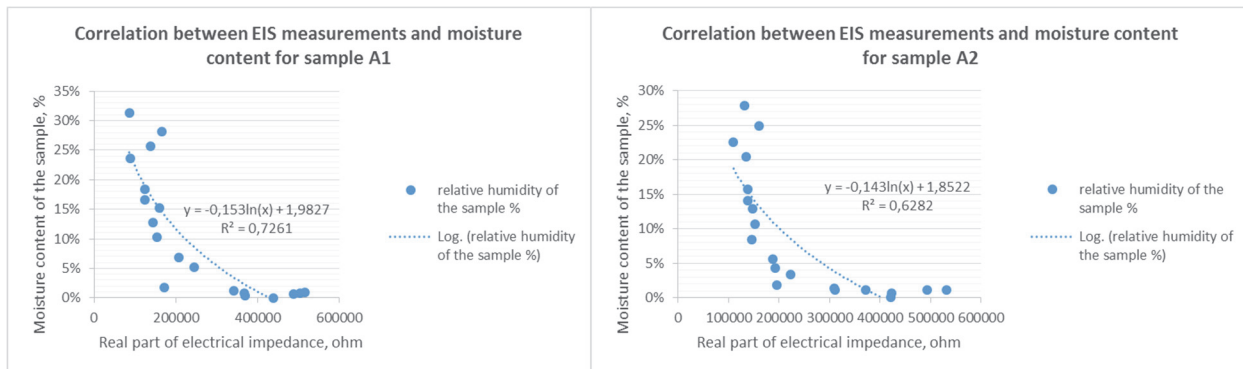


Fig.2.51. Correlation between EIS measurements and value of moisture content in % for sample A1

Fig.2.52. Correlation between EIS measurements and value of moisture content in % for sample A2

The correlation between the EIS measurement values and moisture content value of the construction is logarithmic. The deviation from the average result should not be taken into the consideration for the respective results due to the fact that the graphs were developed for the average moisture content in the specimen.

The results in Fig.2.51 and 2.52 display deviation of 10% between the obtained results in different measurement directions according to the expansion direction of AAC. Therefore, a research of impact of the pore distribution in the AAC on the accuracy of the results was started.

2.4. Impact of the pore distribution throughout the volume of the AAC masonry blocks on its hygrometric properties

The porosity of the construction material has impact on its hygrometric properties and the research shows a low absorption velocity as a consequence of the large amount of macropores that slow down the capillary forces. Water vapour permeability is enhanced by the degree of connection among the pores and by the absence of condensation phenomena which are favoured by the presence of micropores. Therefore, a higher quantity of micropores should be envisaged favouring the condensation phenomena and hindering the water vapour diffusion.

As AAC is anisotropic material, it has uneven pore distribution throughout the cross section of the material, that has significant impact on the moisture migration gradients as well as on EIS measurement results in AAC material. The differences of EIS measurement values depending on the measurement direction have been described in this paragraph. In this section the moisture migration differences depending on the pore distribution have been researched.

2.4.1. Description of the experiment

As it is commonly known there exist several types of moisture transport and liquid transport processes in solid media as stated in table 2.2.

Table 2.2

Heat and moisture transport mechanisms occurring in practice, their causes and driving potentials [41]

	Transport mechanism	Cause and potential of transport
Liquid transport	Capillary conduction	Capillary suction stress
	Surface diffusion	Relative humidity
	Seepage flow	Gravitation
	Hydraulic flow	Total pressure differentials
	Electrokinesis	Electrical fields
	Osmosis	Ion concentration
Vapour transport	Gas diffusion	Vapour pressure
	Molecular transport (effusion)	(temperature, total pressure)
	Solution diffusion	Vapour pressure
	Convection	Vapour pressure gradient

All of the transport processes stated in table 2.2. can be applicable for AAC masonry construction in different occasions. Therefore, a series of experiments by application of EIS measurements for detection of moisture transport throughout the cross section of the AAC masonry blocks have been carried out.

The experiment was divided in three parts: firstly, the infiltration of water was monitored in situation when the blocks were inserted in water as in Fig.2.53. In such way, the capillary suction processes in AAC were monitored by EIS.



Fig.2.53. Monitoring of capillary suction of water in AAC masonry block

There were used two sets of AAC masonry blocks (A and D in table 2.1.) with three blocks in each set. Both sets of the blocks were used for monitoring of capillary suction of water in direction which is parallel to the manufacturing direction of the AAC and perpendicular to the manufacturing direction of the respective AAC masonry blocks due to the uneven distribution of the pores in the AAC material. For the measurements of moisture distribution, one pair of measurement probes with five active channels was used (as described in chapter 1.5). The probes were embedded into the previously prepared bores as in sample on Fig.2.53.

In order to monitor the speed of capillary suction in different directions of AAC masonry blocks, the blocks were inserted into a constant amount of water for a controlled period of time. EIS measurements were taken every hour as well as scaling of the samples was performed in order to determine the average increase of the moisture content in the samples.

For the second part of the experiment the water was applied evenly on the top surface of the AAC samples as in fig.2.54. in order to monitor the seepage flow in the AAC masonry blocks by EIS.



Fig.2.54. Samples with application of water on the top of the samples

In order to monitor the water infiltration speed in different directions of AAC masonry blocks a constant amount of water was applied on the blocks hourly and the EIS measurements were taken every hour as well as scaling of the samples in order to determine the average increase of the moisture content in the samples.

In the third part of the experiment there was monitored the seepage flow of water in the AAC masonry blocks when the water is applied on the top surface of the sample constantly in

a condition of a water droplets as in stand in fig.2.55. In such case a coupled seepage flow and hydraulic flow processes cause the moisture transport throughout the cross section of the AAC.



Fig.2.55. Stand of the water application on the AAC masonry blocks in condition of water droplets

2.4.2. Results

As a result of the experiment information about different liquid transport processes in different directions (parallel and perpendicular direction vs direction of expansion of AAC) of AAC masonry blocks has been obtained.

From the EIS measurements during the first part of the experiment, following results were obtained:

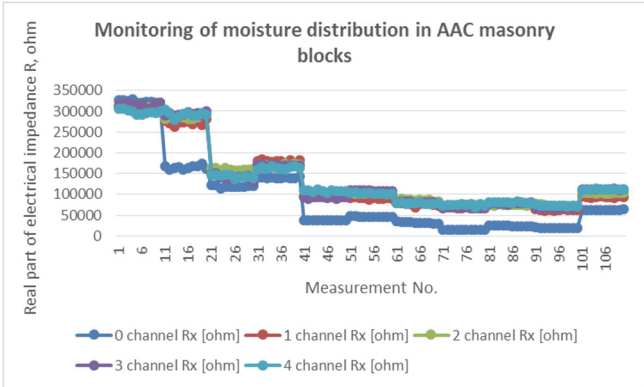


Fig.2.56. EIS measurement results of water infiltration in the first set of the samples [14]

In Fig.2.56. results from moisture distribution measurements throughout the cross section of AAC masonry constructions have been displayed. In this case EIS measurements have been performed in the direction which is parallel to the expansion direction of the AAC. Meanwhile, in Fig.2.57. results from moisture distribution measurements throughout the cross section of AAC masonry constructions which have been performed in the direction which is perpendicular to the expansion direction of the AAC have been displayed.

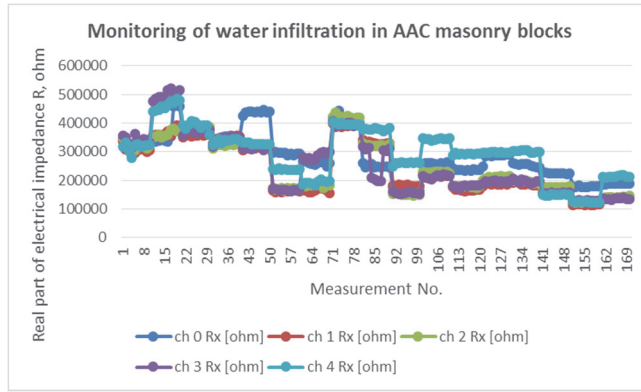


Fig.2.57. EIS measurement results of water infiltration in the first set of the samples [15]

From the obtained results it can be concluded that the capillary suction of the liquid as well as its distribution throughout the cross section of AAC material with higher porosity is more uneven than in the one with lower porosity (Fig.2.56 and Fig.2.57).

The obtained results were compared with the information about pore distribution in the relevant sections of the AAC used for the experiment (fig.2.58 and fig.2.59).

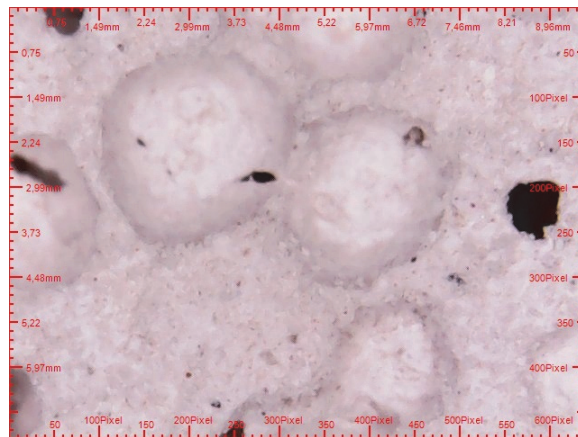


Fig.2.58. Macropore distribution throughout the cross section of the AAC sample (parallel to the manufacturing direction) A type of AAC in table 2.1.



Fig.2.59. Macropore distribution throughout the cross section of the AAC sample (parallel to the manufacturing direction) D type of AAC in table 2.1.

In fig.2.58 and fig.2.59 it can be seen that the AAC material in the direction which is parallel to its manufacturing direction has a number of interconnected pores. Such phenomena is much less typical for the AAC material in the direction, which is perpendicular to the manufacturing direction of the material (fig.9 and fig.10).

Therefore, it can be stated that the capillary suction of the AAC depend on the number and density of layers of different density within its volume. If the material is researched in the direction, which is parallel to its manufacturing direction due to the features of the manufacturing process of AAC then EIS measurement results display that the speed of capillary suction is much lower than in case when the capillary suction happens in the direction which is perpendicular to the expansion direction of AAC.

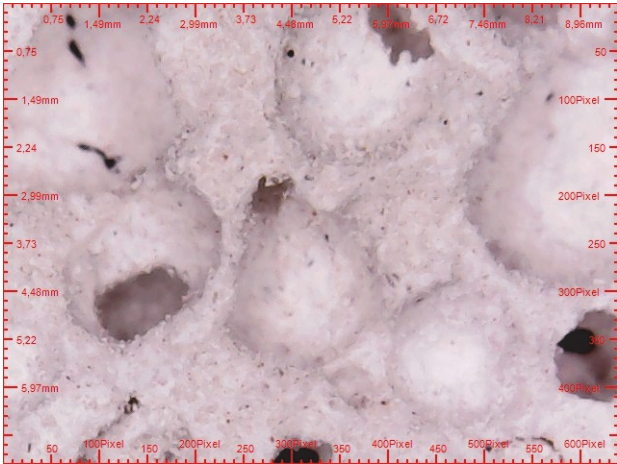


Fig.2.60. Macropore distribution throughout the cross section of the AAC sample (perpendicular to the manufacturing direction) A type of AAC in table 2.1.

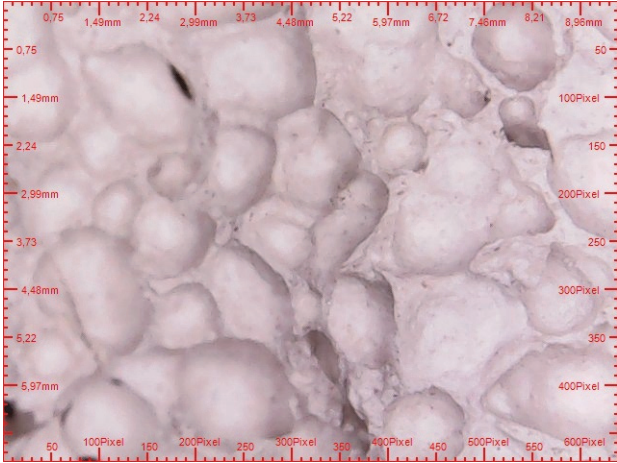


Fig.2.61. Macropore distribution throughout the cross section of the AAC sample (perpendicular to the manufacturing direction) D type of AAC in table 2.1.

However, AAC has more even pore distribution in the direction, which is perpendicular to its expansion direction where the volume of dense areas and less dense areas is approximately even so the cross section has sections with large number of closed pores as well as sections with interconnected pores. This fact brings us to the statement that EIS measurement results in fig.2.56. display more even moisture distribution throughout the cross section of AAC due to equally distributed capillary suction forces throughout the volume of AAC.

The results of the second part of the experiment display the impact of the porous structure of the AAC on moisture migration throughout its volume due to the seepage flow. From the EIS measurements made during the second part of the experiment there were obtained four different result graphs. Fig. 2.62 and Fig.2.63 display the results for the type A AAC while Fig.2.64 and Fig.2.65 display the results for type D AAC.

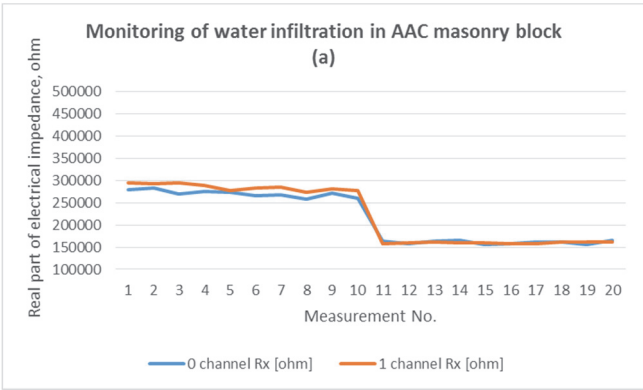


Fig.2.62. EIS measurement results of moisture migration due to the seepage flow in the second set of the samples, measurements taken parallel to the manufacturing direction of AAC

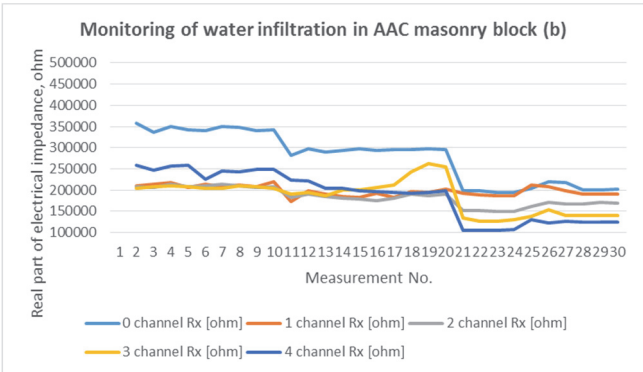


Fig.2.63. EIS measurement results of moisture migration due to the seepage flow in the second set of the samples, measurements taken perpendicular to the manufacturing direction of AAC

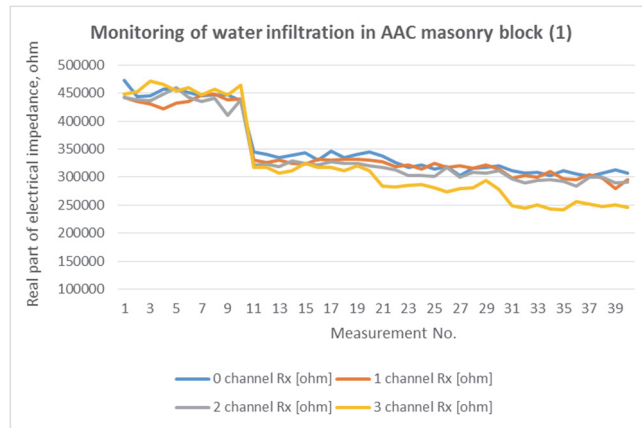


Fig.2.64. EIS measurement results of moisture migration due to the seepage flow in the second set of the samples, measurements taken parallel to the manufacturing direction of AAC

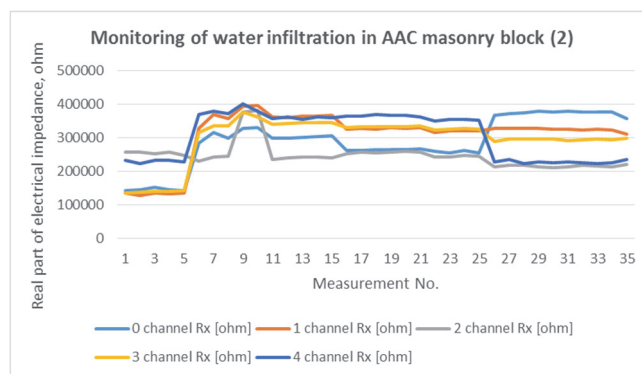


Fig.2.65. EIS measurement results of moisture migration due to the seepage flow in the second set of the samples, measurements taken perpendicular to the manufacturing direction of AAC

The obtained results display correlation between the diversity of porous structure in AAC material and the EIS measurement results of moisture distribution throughout the cross section of the specimen in the respective specimen. In both cases of the AAC the measurements results in the specimen where the EIS measurement probes were inserted parallel to the manufacturing direction (in such case moisture migration is perpendicular to the manufacturing direction) of the AAC, the measurement results display more even distribution of EIS measurement results during the changes of moisture content in the sample. Therefore, it can be concluded that the porous structure itself has significant impact on the speed of moisture infiltration in AAC material which can be substantiated by EIS measurement results.

These conclusions are approved by results of the third part of the experiment. The results obtained from the samples with probe placement parallel to the manufacturing direction of AAC display more even distribution of EIS measurement results than the ones, which were performed with perpendicular probe placement.

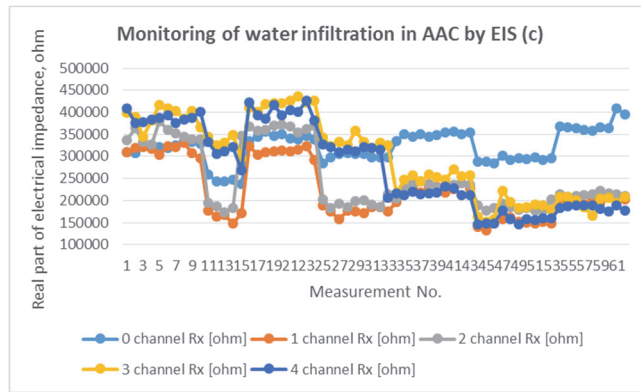


Fig.2.66. EIS measurement results of moisture migration due to the seepage flow in the third set of the samples, measurements taken perpendicular to the manufacturing direction of AAC

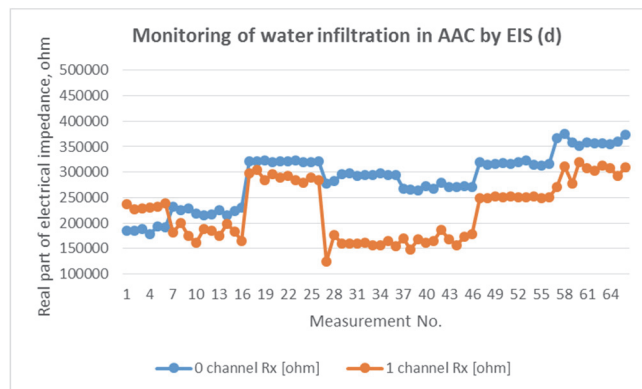


Fig.2.67. EIS measurement results of moisture migration due to the seepage flow in the third set of the samples, measurements taken parallel to the manufacturing direction of AAC

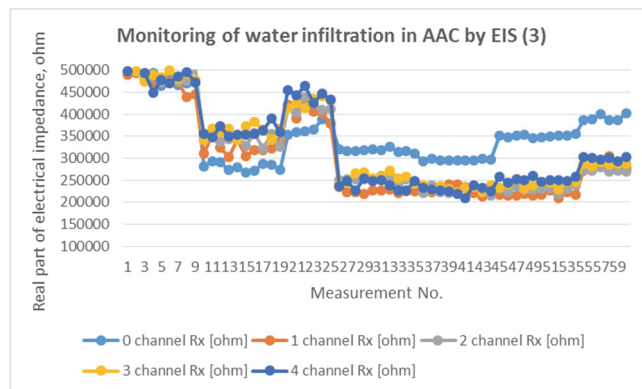


Fig.2.68. EIS measurement results of moisture migration due to the seepage flow in the third set of the samples, measurements taken perpendicular to the manufacturing direction of AAC

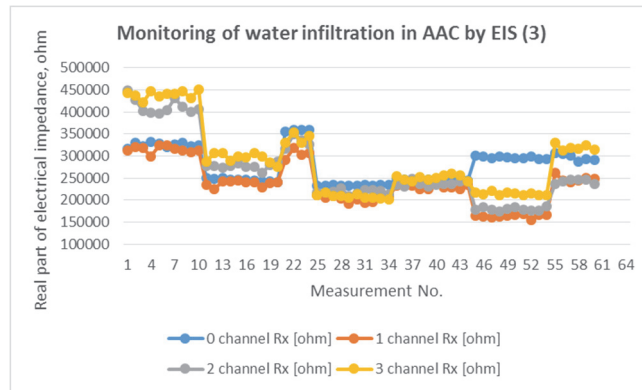


Fig.2.69. EIS measurement results of moisture migration due to the seepage flow in the third set of the samples, measurements taken parallel to the manufacturing direction of AAC

Moisture migration due to the seepage flow in AAC masonry construction is strongly dependent on the orientation of the AAC masonry blocks vs the direction of liquids impact. The research proves, that the mass of liquid transport in all three types of used in this research is lower when the water is applied on the AAC masonry block in direction, which is parallel to its manufacturing direction. This phenomena can be explained with the fact that AAC has uneven pore distribution throughout its volume and the distribution of pores depend on the manufacturing direction of the material.

Therefore, this property of the AAC masonry blocks should be used in situ for better avoiding them excessive moisture accumulation in AAC masonry constructions during the construction stage of the delimiting constructions and assessed during construction stage by application of EIS.

2.5. Impact of masonry joints on the results of moisture distribution measurements in AAC masonry constructions by EIS

Application of EIS measurements for in-situ detection of moisture distribution in AAC masonry constructions can be expanded to the subject of non-destructive detection of moisture content in habitable buildings with finishing layers applied on masonry constructions. Therefore, a question of impact from masonry joints on the accuracy of the EIS measurement results arise. This subject is important because it is difficult to detect the masonry joints beneath the finishing layers without removing of finishing which brings the EIS method out of range of easily applicable non-destructive methods as a number of on-site preparation works (e.g. removal of finishing layers, location of masonry joints) have to be done. The following experiment was performed in order to determine the impact of the masonry joints on the overall accuracy of EIS measurement results in order to determine

whether this impact has significance to be taken into account during the processing of EIS measurement results.

2.5.1. Description of the experiment

The experiment was performed on aerated concrete block masonry wall segment in laboratory of Riga Technical University. AEROC aerated concrete blocks with dimensions 300x200x600mm (width x height x length) (Fig. 2.35) were used for cladding of the experiment specimen. The wall segment consisted of 6 blocks as in Fig. 5 and 23 (twenty three) measurement points were made in this segment as in Fig.2.70. The measurement points were chosen in such way that they were evenly distributed throughout the surface of the specimen and included sections without masonry joints as well as sections with masonry joints between the measurement points.

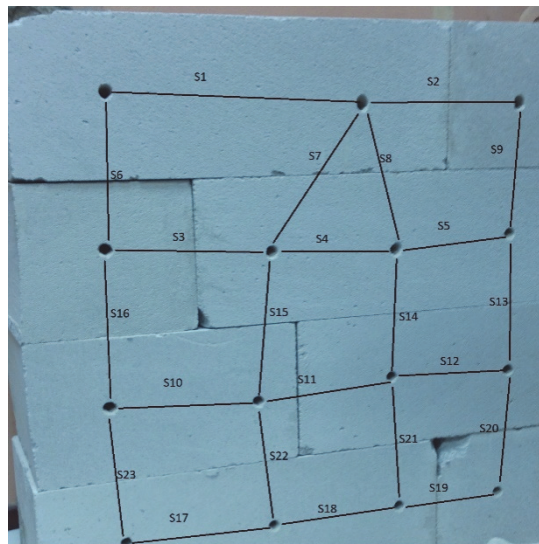


Fig. 2.70 Aerated concrete wall segment and measurement points

The aim of this experiment is to determine the impact of the masonry joints on detection of the humidity distribution by EIS method. Therefore, for the reasons of comparison series of s1-s2; s3-s4; s10-s11-s12 and s18-s19 measurement point will be taken into consideration.

EIS measurements were performed during drying process of newly built AAC masonry wall segment for 3 months in laboratory conditions (+20°C, ≈70% Rh). There were made parallel measurements within one block and within two blocks where a masonry joint is included in the measuring distance. In such way there were obtained 5 pairs of comparable results where the impact of masonry joints can be observed.

2.5.2. Results

During the monitoring of the drying process of the specimen, regular EIS measurements were taken in all measurement points. The obtained EIS measurement data was used for development of the moisture migration graphs, where a separate curve for each channel of the measurement probe was prepared. In such way a range of moisture migration curves was obtained. After evaluation of the prepared charts it can be concluded that EIS measurement results of drying process of AAC without masonry joint in measurement distance in point s1 (Fig. 2.71) and point s2 with masonry joint within the measurement distance (Fig. 2.72) display similar character but the absolute measurement values are significantly different. That means that masonry joints have significant impact on EIS measurement results. Therefore, results, which are obtained in wall segments without joints, are not directly comparable to results, which are obtained in wall segments with masonry joints.

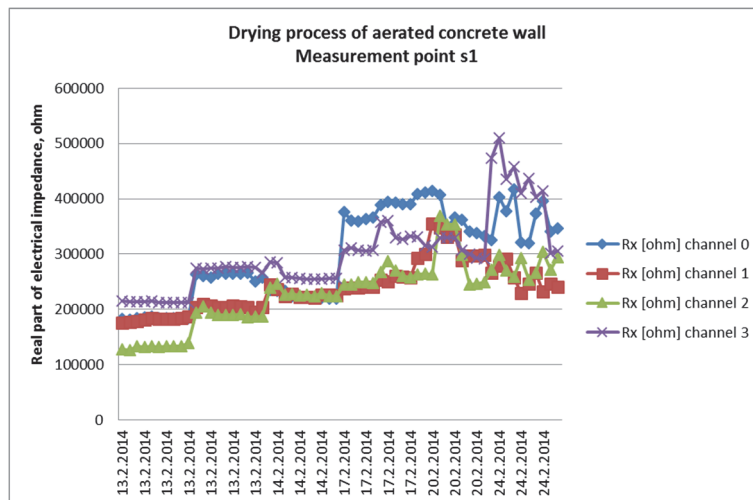


Fig. 2.71. EIS measurements of drying process of the aerated concrete wall fragment without masonry joints

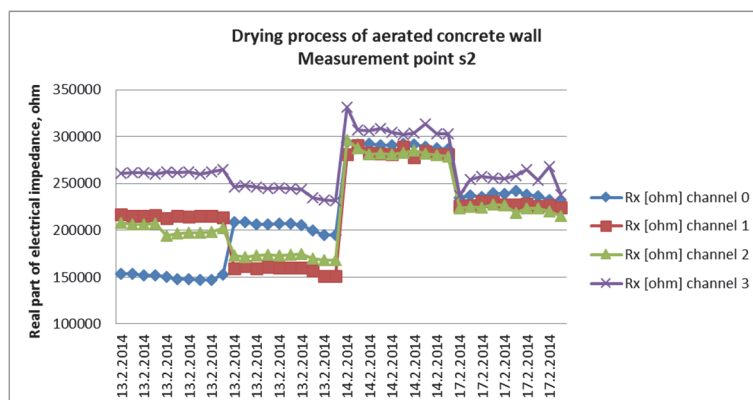


Fig. 2.72. EIS measurements of drying process of the aerated concrete wall fragment with joint between measurement points

The difference in second series of the measurements (Fig.2.72) proves the theory about joint impact on measurement results because the first series of the measurements were

performed prior filling the joints with glue mortar (first 10 measurement results). Filling of the joint with glue mortar affected the results impressively (measurement points 11-20 Fig.2.72.).

The absolute values of EIS measurements in points s1 and s2 for the same measurement series change almost twice in their values so it is clear that the masonry joints have their effect on the final measurement results. Thus, the correlation equations between moisture content and EIS measurement results, which have been developed for AAC and described in paragraph 2.2. cannot be applied for calculations of moisture content in AAC from the measurement results obtained by EIS.

Therefore, using data from five pairs of the comparable result series from the specimen wall, several correlation equations between measurement results with and without masonry joints have been developed.

The results of EIS measurements for the pair of measurement distance s1-s2 have been displayed in Fig. 2.73. As of Fig. 2.73 the impact of masonry joint can be expressed by (1):

$$y = 0,9101x + 20633 \text{ [ohm]} \tag{2.3}$$

where (2.3)-(2.7) x is EIS measurement value in masonry segment without joints and y is EIS measurement value in masonry segment with joints.

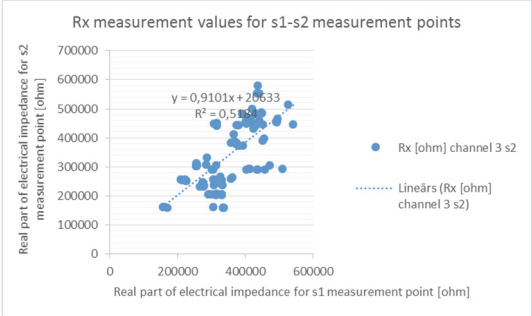


Fig. 2.73. EIS measurement results with masonry joint impact s1-s2

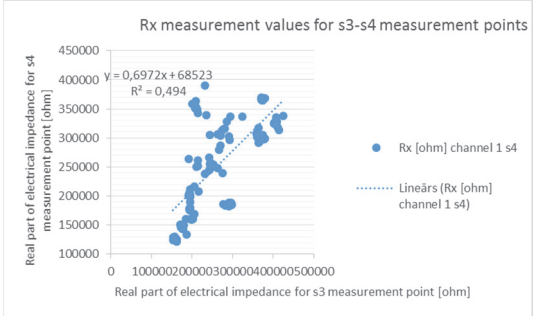


Fig. 2.74. EIS measurement results with masonry joint impact s3-s4

The same results were obtained for measurement points s3-s4, s10-s11, s11-s12 and s18-s19 (Figs. 2.74-2.77).

In this case (Fig. 2.74) the impact of joint is expressed with (2):

$$y = 0,6972x + 68523 \text{ [ohm]} \tag{2.4}$$

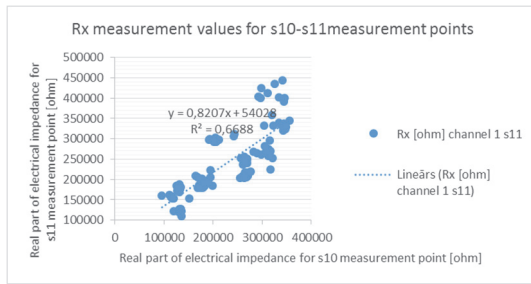


Fig. 2.75. EIS measurement results with masonry joint impact s10-s11

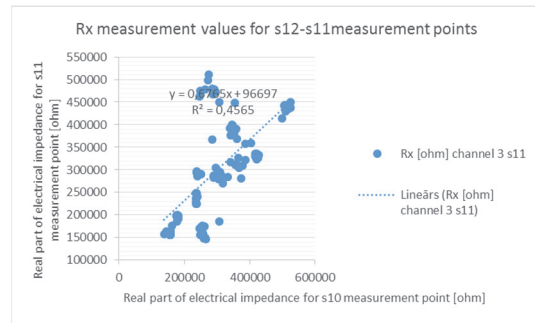


Fig. 2.76. EIS measurement results with masonry joint impact s12-s11

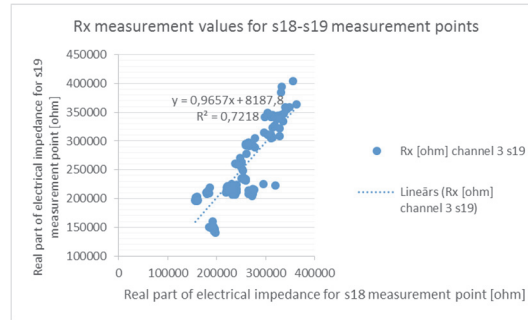


Fig. 2.77. EIS measurement results with masonry joint impact s18-s19

For all examined cases of impact of masonry joints on the results of EIS measurements, the correlation between EIS results obtained from areas with and without masonry joints can be expressed with equations of linear character. However, the absolute values of equations vary significantly.

In case of Fig. 2.75 the impact of joint is expressed with:

$$y = 0,8207x + 54026 \text{ [ohm]} \quad (2.5)$$

In case of Fig. 2.76 the impact of joint is expressed with:

$$y = 0,6765x + 96697 \text{ [ohm]} \quad (2.6)$$

In case of Fig. 2.77 the impact of joint is expressed with:

$$y = 0,9657x + 8187,8 \text{ [ohm]} \quad (2.7)$$

From (2.3)-(2.7) it is obvious that there is a linear correlation between measurements which are made in sectors without joints and sectors including masonry joints which goes to basic equation:

$$y = ax + C \quad (2.8)$$

The quotient is in range of 0,67 to 0,96 therefore the joint impact reduces the EIS measurement value from the measurement value which has been obtained in a section without joints. Hence a quotient varies in range of 30% it never exceeds 1. The “a” quotient has direct correlation to the thickness and density of the masonry joint, which should be researched separately. However, the C constant is different every time and it is difficult to conclude what it depends on. The value of C constant has to be a subject of further research. The C constant

in all obtained equations can reach a value of 70% from the base value of relap part of the electrical impedance measurement result and thus have significant impact on overall accuracy of EIS measurement results. Nevertheless, it has a trend to decrease while EIS measurement results are increasing (during the loss of moisture in the monitored construction) and for the air dry construction the impact of the C constant does not exceed 25% of the base measurement value. Taking into consideration the impact of the masonry joints on the overall accuracy of the measurement results, this method should be applied within the borders of one masonry block.

2.6. Monitoring of the drying process of AAC masonry constructions by EIS

As the main impact factor on the accuracy of the EIS measurement results has been researched and correlations between EIS measurement results and moisture content in AAC constructions has been developed, the approbation of the methodology had to be done. Therefore, a monitoring of drying process of a newly cladded segment of AAC masonry block wall was performed. During the experiment the moisture migration process throughout the cross section of the masonry blocks by EIS was performed.

2.6.1. Description of the experiment

The particular experiment was performed on aerated concrete block masonry wall segment in laboratory of Riga Technical university. For the experiment the wall fragment described in chapter 2.4. was used. The AAC masonry blocks were newly manufactured and delivered to the laboratory in the same state as they are usually delivered to construction sites. Therefore, the conditions of the experiment were made as similar to the on-site conditions as possible.

Z-meter III device with a pair of probes, which have been described in paragraph 1.5 were used for EIS measurements during this experiment. One pair of probes with 4 (four) active channels were used.

The aim of this experiment was to monitor the drying process of AAC masonry construction in different points of the construction, compare the obtained results and prepare the moisture migration charts in different cross sections of the monitored construction.

EIS measurements were performed during the drying process of newly built AAC masonry wall segment where measurements were made within one block as well as within two blocks where a masonry joint is included in the measurement distance. In such way there

were obtained different results, which display the impact of the masonry joints on the accuracy of the obtained results as well as the drying process itself.

The distance between measurement points changes in the range of 174 to 348mm (exact distance between measurement points is given in table 2.3 according to Fig.2.70.). Therefore, it was important to find a frequency during the frequency analysis, which can provide reliable results in the range of distances, where the measurements were performed.

Table 2.3

Distance between measurement points in wall specimen (Fig.2.70)

Marking of the measurement point (according to Fig.2.)	Distance between measurement points, mm
S1	348
S2	258
S3	232
S4	188
S5	186
S6	196
S7	237
S8	215
S9	185
S10	221
S11	208
S12	200
S13	206
S14	187
S15	215
S17	212
S18	215
S19	203
S20	174
S21	198
S22	171
S23	195

2.6.2. Results

2.6.2.1. Monitoring of moisture distribution changes in the wall fragment within single block

During the monitoring process there were performed 7 (seven) series of measurements within the boundaries of one masonry block. The monitoring went on for two months (from February 2014 until April 2014). The results of the measurements have been displayed in Fig.2.78.

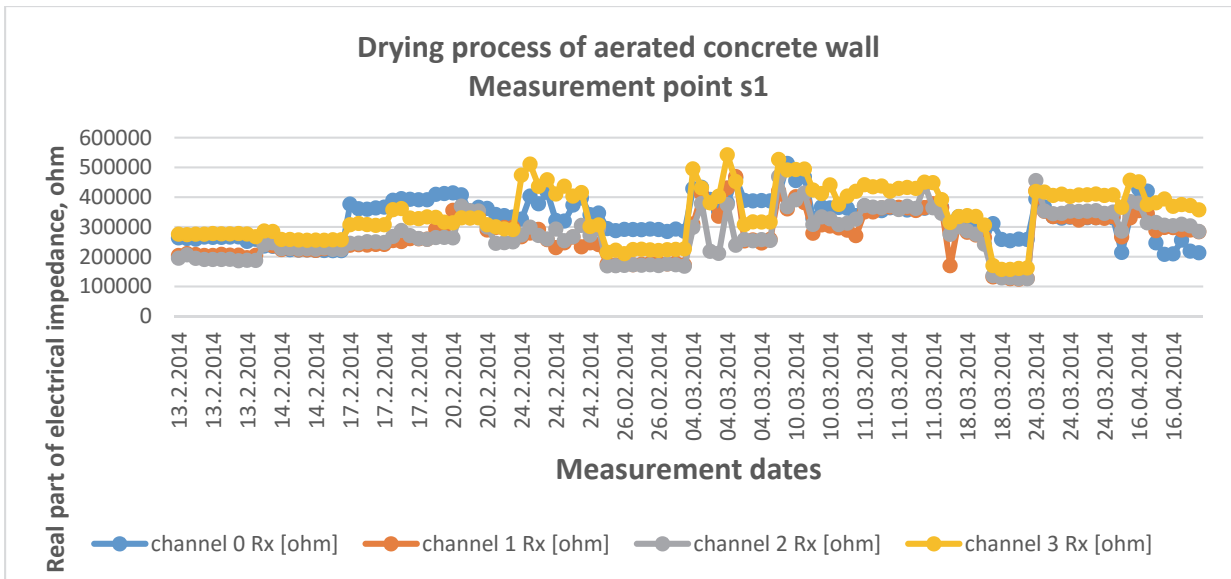


Fig.2.78. Measurement results for point s1

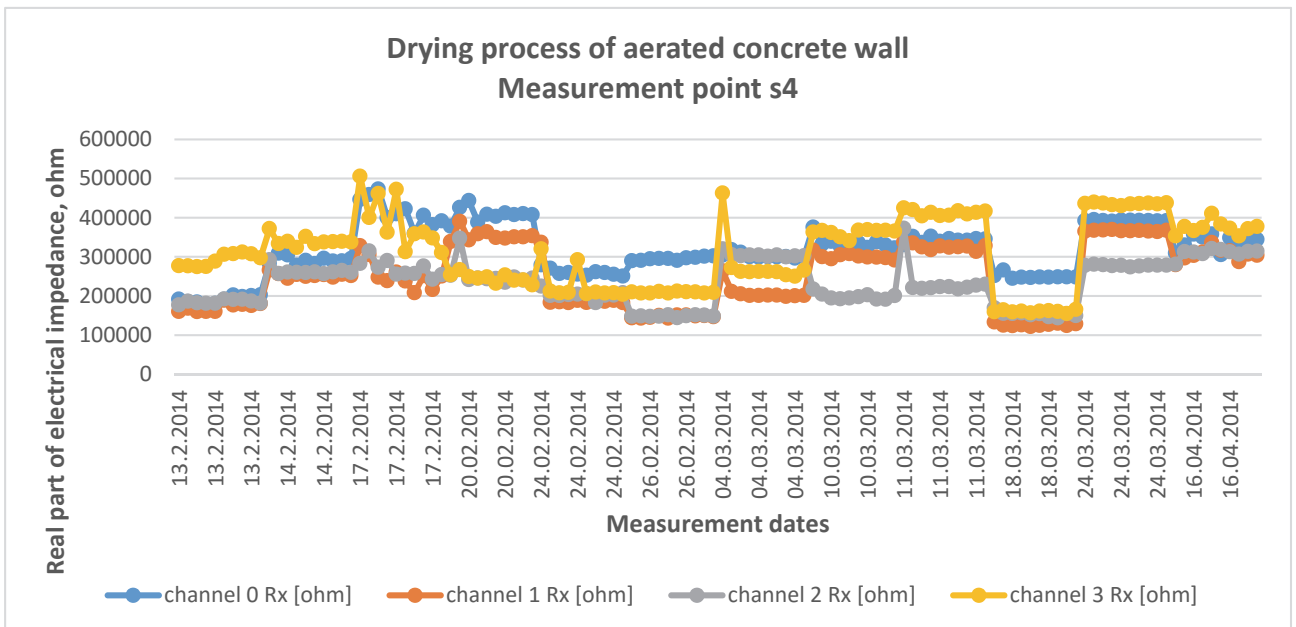


Fig.2.79. Measurement results for point s4

The results for these two measurement points display that moisture consequently drives from the centre of the construction to the side surface of the masonry blocks. Throughout the time when monitoring was performed some irregularities were noticed. As Fig.2.77. measurement results performed on 24.02.2014 and 04.03.2014 or Fig.2.78. measurement results performed on 17.02.2014 when the results performed within one series are significantly different. Such irregularities is an object of further research but as it occurs rarely (in case of measurement points s1 and s4 it is one to two out of twelve measurements) then it can be ignored as it does not have significant influence on overall test results. However, such irregularities could be caused by significant impact of external

electromagnetic sources. Therefore, it is advisable to remove all possible electromagnetic sources from the EIS measurement area.

A comparison of the moisture gradient was performed during this experiment as the measurements for channels 1 and 2 were compared for points s1 and s4 (Fig.2.79).

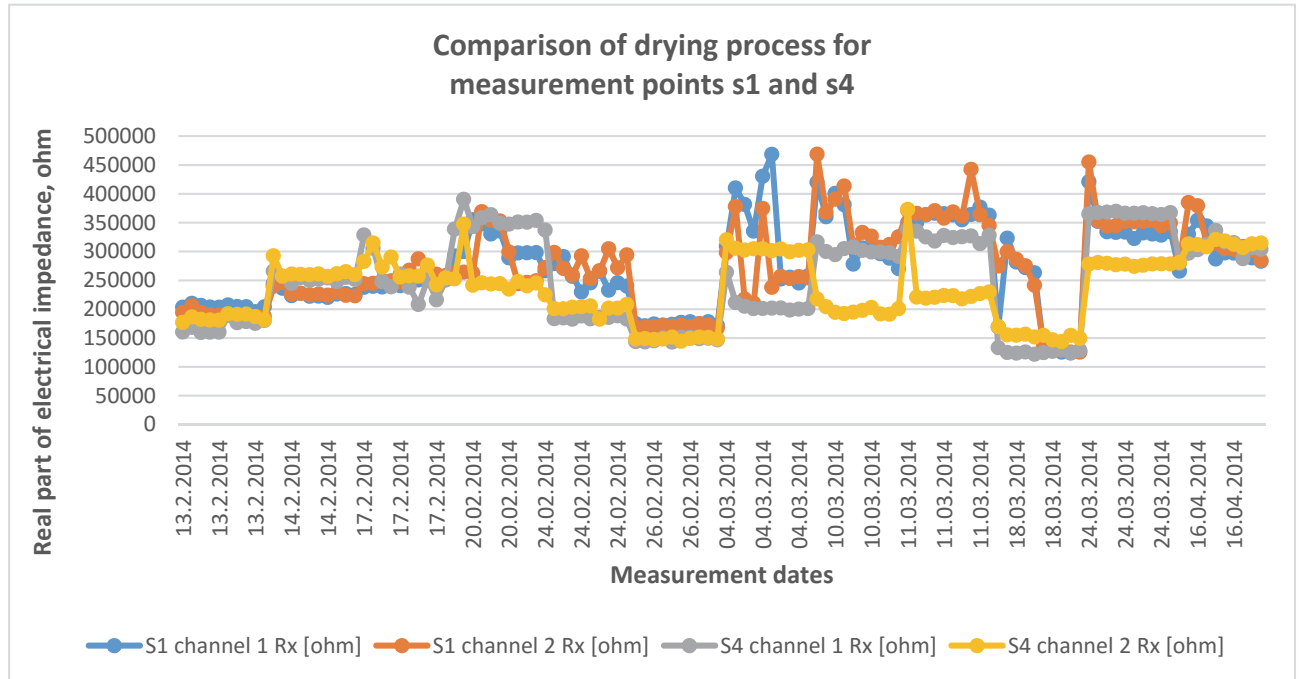


Fig.2.79 Comparison of measurement results for points s1 and s4

Fig.2.79. displays that in the beginning of the drying process there is no difference in speed of moisture migration and moisture content in the measurement points s1 and s4. After one month of drying time the moisture content of the point s1 decreases faster than in point s4 which is expectable as the s1 point has an additional free surface (the top of the wall segment) where moisture can migrate and the drying process is faster than for the block which is in the middle of the masonry construction.

2.6.2.2. Monitoring of moisture distribution changes in the wall fragment containing masonry joint between blocks

Large cracks in masonry constructions and masonry joints have significant impact on the absolute values of EIS measurement results. Therefore the results, which were obtained in measurement points containing masonry joints, were processed according to the approach described in paragraph 2.5.

In order to obtain more detailed data about moisture migration process in the wall construction the measurement points, which contained masonry joints were chosen right next to the points where EIS measurements were made within boundaries of one block.

Thus, the results are assumed to be comparable because the moisture content in the AAC blocks, which were besides each other had the same moisture distribution and drying conditions. Therefore measurement points s2 and s3 (Fig.2.70) were selected.

The measurement results display that the drying process is similar to the one, which was monitored in the blocks without masonry joints (Fig.2.80 and Fig.2.81).

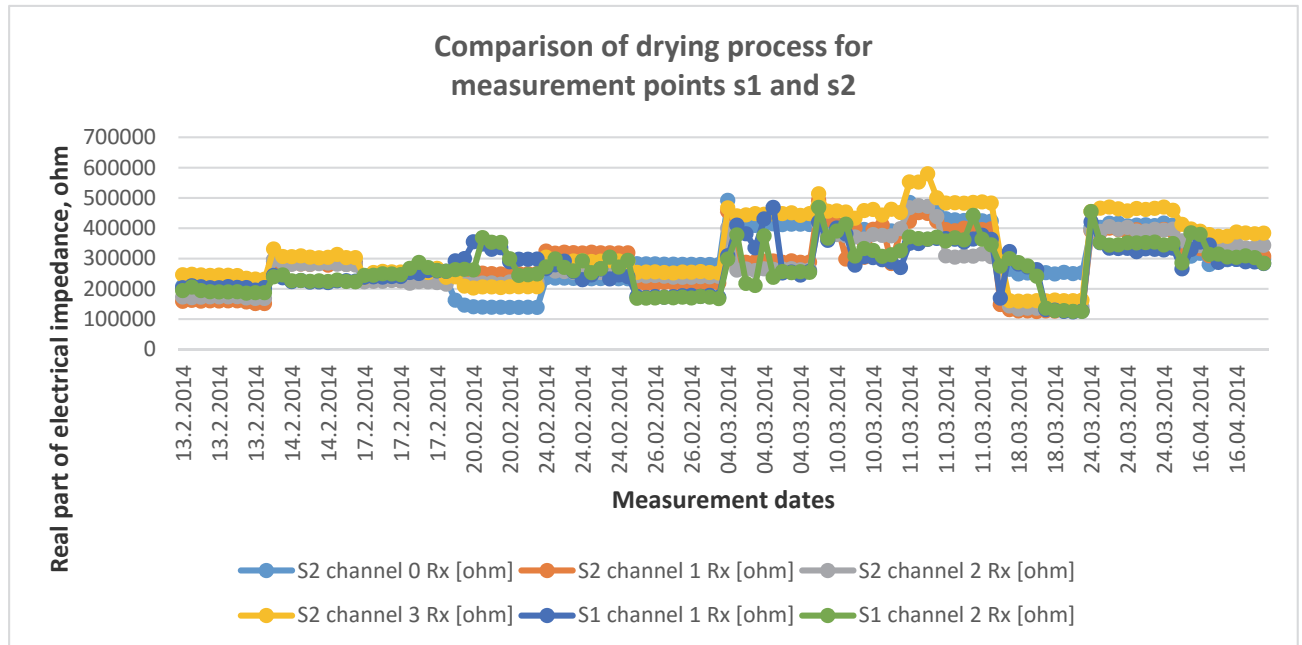


Fig.2.80. Comparison of measurement results for points s1 and s2

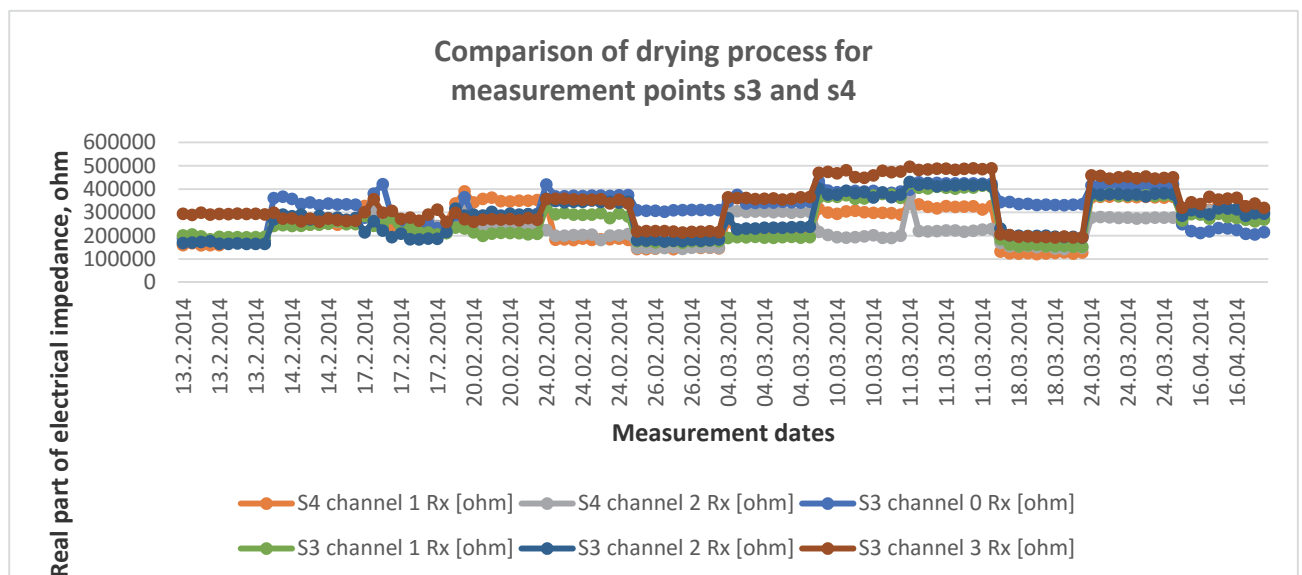


Fig.2.81. Comparison of measurement results for points s3 and s4

Although overall character of the measurement charts between measurements with and without masonry joints have similar character it is important to point out that absolute values of these measurements have significant differences. In order to make obtained data comparable, the equation (2.8), which has been developed during this research can be used.

The moisture migration map for point s1 and s2 from the acquired data has been displayed in fig.2.82.

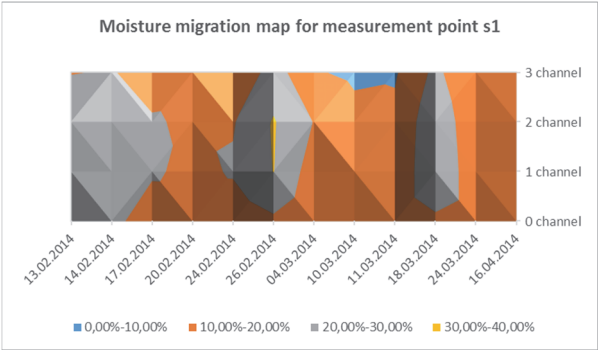


Fig.2.82.a Moisture migration map including moisture content in % in each section of AAC

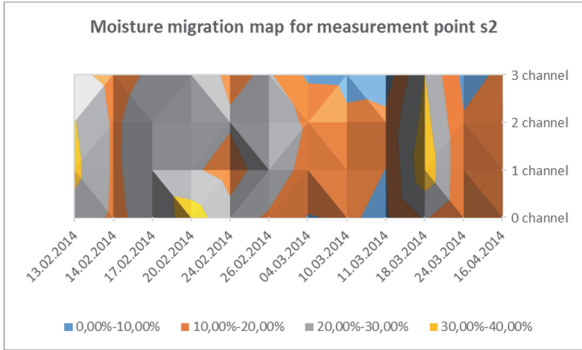


Fig.2.82.b Moisture migration map including moisture content in % in each section of AAC

The obtained results (fig.2.82.a and 2.82.b) differ significantly although the moisture content in the relevant sections s1 and s2 is similar. Therefore, it is necessary to detect masonry joints between measurement points for in situ measurements in order to obtain credible and comparable results of moisture distribution. As the joints have different structure and resistivity to the measurement frequency EIS, it may cause irregularities in the obtained results.

Test results have proved that previous assumptions about moisture distribution and its gradients in AAC masonry blocks have been correct. The blocks accumulate the moisture and the drying process begins after masonry construction is completed. The moisture gradient is pointed outwards from the centre of the cross section towards the sides of the block, which are in connection with surrounding environment (usually air, not towards other blocks and masonry joints).

2.7. Impact of finishing works on drying of AAC masonry constructions

In-situ AAC masonry constructions are usually insulated with a layer of heat insulation material (e.g. mineral wool or polystyrene). As a part of approbation of the methodology the moisture transport processes in AAC masonry wall segments with different types of insulation have been monitored.

2.7.1. Description of the experiment

For the particular experiment there were prepared three samples of AAC masonry wall construction with dimensions 1200×600×250mm (length × height × thickness). AAC with 375 kg/m³ density was used and additional layer of heat insulation was attached on two

specimen. Most popular heat insulation materials which are usually used in Latvia were used – one of the samples was insulated with 100mm thick layer of mineral wool (specimen A) and the second sample was insulated with 100mm thick polystyrene insulation (specimen B). The third specimen was left without additional heat insulation layer in order to use it as a reference sample (sample C). Afterwards both insulated specimen and the third specimen, which was left without any additional insulation were covered with plaster from the external side of the insulation (e.g. the external side of the wall construction). Thus, a model of construction phase when the cladding of the masonry construction has been finished and the external finishing of the wall has been finished was simulated (Fig.2.83 and 2.84).

In each specimen 17 bores were made in order to monitor the moisture migration in all directions of the sample by EIS. The monitoring of the drying process was performed for 12 weeks in laboratory conditions with air Rh in range of 60-80% and the average temperature in range from 18 to 25 °C. Such conditions comply with average weather conditions on construction site in Northern European summers when the building envelope is not fully closed and heating of the building has not begun. For all specimen same drying conditions were maintained.



Fig.2.83. Sample constructions on stand.



Fig.2.84. Sample constructions on stand.

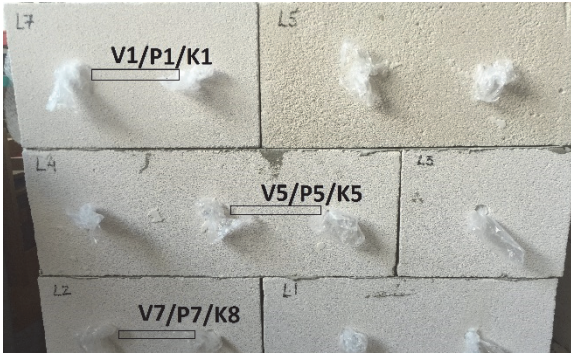


Fig.2.85. Measurement points on sample

2.7.2. Results

Initial moisture distribution throughout the cross section of the specimen constructions.

After the specimen were constructed the initial moisture distribution was determined by EIS. As the EIS measures the resistance values, the determination of the moisture content in the AAC material can be detected by application of correlation equations. Such correlation equation (2.9) between the electrical resistivity values of the respective AAC material and its moisture content has been developed by authors [23] and tested in laboratory conditions.

$$y = -0,236 \ln(x) + 3,1507 \quad (2.9)$$

The EIS measurement results provided information about the initial moisture distribution throughout the cross section of the sample constructions (Fig.2.86 to Fig.2.88)

The average moisture content of the AAC blocks at the beginning of the experiment was 25% of the dry mass of AAC. The moisture distribution throughout the cross section of all specimen was even with the exception of the channel 4, where the least moisture content was observed in all specimen. This fact can be explained with the least impact of humid construction processes (e.g. finishing mortar on sample C or insulation installation mortar on samples A and B) on the internal side of the specimen construction.

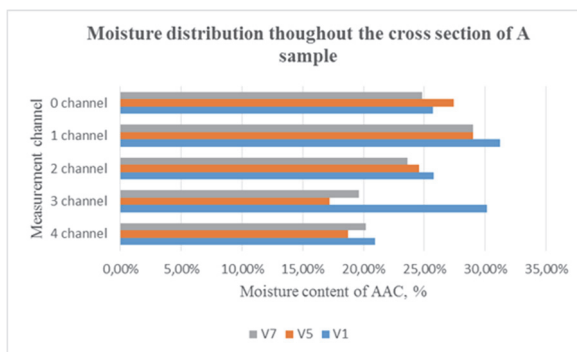


Figure 2.86. Moisture distribution throughout the cross section of the A sample measurement points at the beginning of the experiment

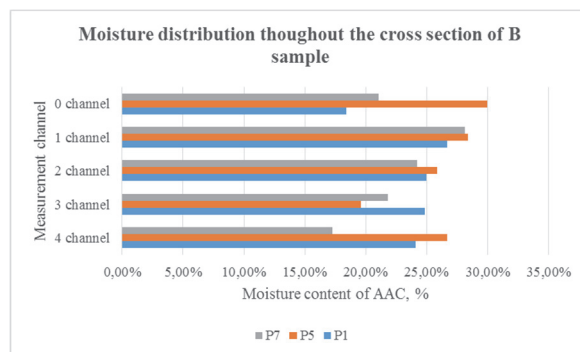


Figure 2.87. Moisture distribution throughout the cross section of the B sample measurement points at the beginning of the experiment

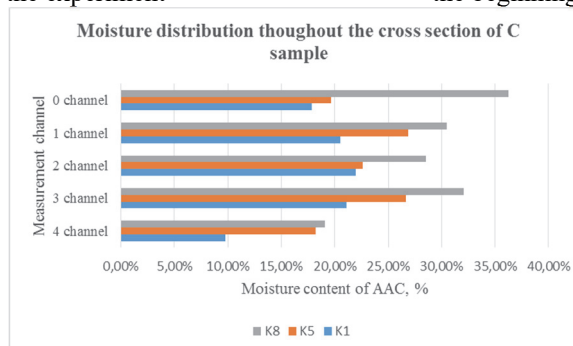


Figure 2.88. Moisture distribution throughout the cross section of the C sample measurement points at the beginning of the experiment

Further, the moisture distribution changes throughout the cross section of the specimen were monitored by application of EIS measurements three times a week and certain dynamics of drying process were established for each sample construction. Fig.2.89 to Fig.2.91 display the changes of moisture distribution throughout the cross section of the AAC samples with different external finishing. The obtained data was merged in one surface graph for each sample and the division of the data on x axis allow to follow the changes of the moisture distribution throughout the cross section of the specimen during the whole period of the experiment.

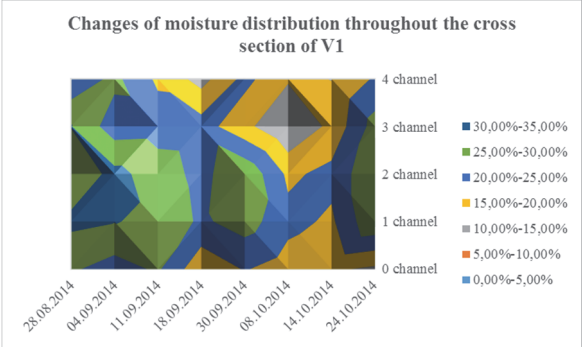


Figure 2.89. Changes of moisture distribution throughout the cross section V1 of A specimen construction during the experiment

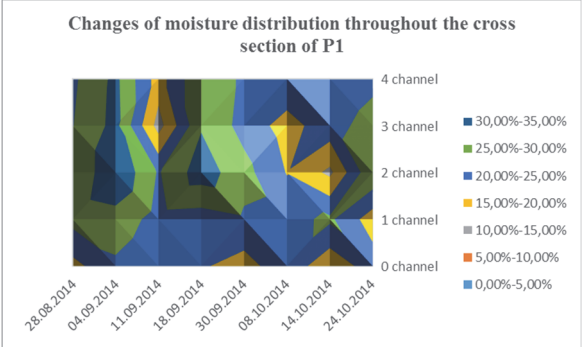


Figure 2.90. Changes of moisture distribution throughout the cross section P1 of B specimen construction during the experiment

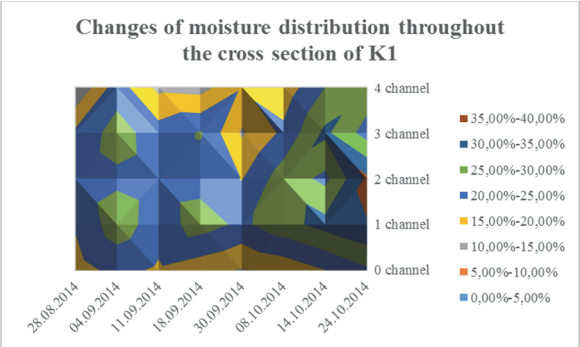


Figure 2.91. Changes of moisture distribution throughout the cross section K1 of C specimen construction during the experiment

The specimen construction A displayed the fastest drying speed in comparison with sample constructions B and C. The slowest drying speed was observed for specimen construction B. Therefore the assumption that the insulation material has significant influence on the drying speed on wall construction approved. The B specimen approved that the vapour diffusion coefficient of the insulation materials has high impact on the drying speed of the AAC wall construction.

Table 2.4

Drying speed of specimen			
Sample	Average moisture content of the cross section at the beginning of the experiment, %	Average moisture content of the cross section at the end of the experiment, %	Drying speed (% of moisture lost/obtained in 12 weeks)
Sample A	26,82%	24,07%	-2,75%
Sample B	23,79%	24,04%	0,24%
Sample C	18,24%	29,24%	11,00%

The difference in drying speed of the respective samples vary for 12,75%. The results prove that the only type of insulation, which allow decreasing of AAC masonry construction's moisture content rate, is mineral wool as in sample A. Such performance depends on two factors. Firstly, the mineral wool insulation decrease the amount of moisture, which is absorbed by the masonry construction from the mortar used for installation of the insulation and, secondly, allows the moisture to migrate through the insulation layer due to high value of the vapour diffusion coefficient. The sample B displayed a minimal increase of the average moisture content due to the fact that the low vapour diffusion coefficient of the polystyrene did not allow the moisture to migrate freely through the insulation layer and all moisture from the installation mortar was absorbed by the AAC masonry construction. The reference block (specimen C) displayed the highest absorption of moisture, which can be based on the amount of the moisture absorber from the finishing mortar and the fact that all surfaces of the reference construction were exposed to the external humidity of the premise while the other two samples had one covered surface. The fact that the changes of constructions moisture content are caused by the changes of the Rh rate in the premise are proved by Fig.7;8 which clearly indicates the increase of moisture rate in external layers of the construction starting from 30.09.2014 when the Rh rate of the premise increased as well.

3. SUMMARY OF RESULTS

The results and data obtained in experiments described in the 2nd chapter of the thesis have been analysed and summarised in order to develop further trends for application of EIS and Z-meter III device for non-destructive on-site methodology for detection of moisture distribution in AAC masonry constructions.

Following issues have impact on the accuracy of the obtained results of moisture distribution throughout the cross section of AAC and should be taken into consideration during application of this method:

The frequency analysis has a significant impact on the accuracy of moisture content measurement results obtained by EIS and Z-meter III device. The results of frequency analysis depend on the density of the AAC material and the porous structure of the material. The results of frequency analysis (paragraph 2.1.) can vary in range of 2000Hz for the saturated and non-saturated specimen. Moreover, the porous structure of the AAC material has significant impact on the results of frequency analysis. After comparing specimen with different porous structure and density (paragraph 2.1.) it can be concluded that the optimal frequency varies in range of 2000Hz as well. Therefore, it is strongly advisable to choose a measurement frequency which is at least 2000Hz higher than the minimal applicable measurement frequency for EIS.

Correlation equations between EIS measurement results and moisture content rate in AAC developed within the research performed for these thesis can be applied for all types of AAC masonry blocks. The accuracy of the universal equation is 71%, which is acceptable result as the preferable moisture content in AAC masonry constructions is 5% to 10%. Therefore the maximal deviation provided by this equation in case of moisture content of 10% is 3%. However, order to increase the accuracy of the obtained results it is necessary to determine the type of AAC and apply the equation developed for the relevant type of the AAC. The accuracy of the obtained equations vary in range from 70% to 81% if an equation for the relevant type of AAC is used. If universal equation is applied (equation 2.2) then the accuracy of the obtained results can decrease up to 17,05% in absolute values or 31% in percentage rate. The most deviation has the AAC with high densities (higher than 500kg/m³). Other types of AAC with similar density have deviation in range of 13% in absolute values or 24% in percentage rate (data from paragraph 2.2).

Porous structure of the AAC has impact on the accuracy of EIS measurement results as well. In this case not only the EIS measurement results vary by themselves but also the

correlation equation between the EIS measurement results and moisture content in AAC material vary. In case the EIS measurements are taken in different directions vs the direction of expansion of AAC the result can vary in range of 3% (paragraph 2.3.). The range is not too wide by itself, however, in combination with other factors, which cause deviations in measurement results, can decrease the accuracy of obtained data.

Conclusions

Comprehensive analysis of the results obtained during the experimental part of the research prove that the electrical impedance spectrometry can be applied on autoclaved aerated concrete masonry constructions for non-destructive measurements of moisture distribution throughout the cross section of the masonry construction. A methodology for application of EIS for non-destructive monitoring of moisture migration throughout the cross section of AAC masonry constructions with Z-meter device has been developed.

At the beginning of the research following tasks were set:

1. Determination of correlation between EIS measurement results and moisture content in AAC;
2. Determination of impact of contact surface between measurement probe and AAC masonry construction on the accuracy of the obtained results.
3. Determination of impact of the coating on measurement contact surface on the accuracy of the measurement results.
4. Determination of the impact of measurement distance on accuracy of measurement results.
5. Determination of the impact of cracks and masonry joints on accuracy of EIS measurement results.

All of the tasks stated above have been reached during the research. Answering the goals set in the beginning of the research the following statements can be made:

- EIS can be applied on AAC masonry constructions for non-destructive detection of moisture distribution throughout the cross section of the AAC masonry construction with average precision of 70%;
- Prior the application of the EIS on AAC masonry constructions a frequency analysis must be performed in order to detect most suitable EIS measurement frequency; for most common types of AAC in Latvian construction market the measurement frequency for EIS is 8000Hz;
- The contact surface between the measurement probe and AAC masonry construction must be as close as possible. However, the impact of the contact surface on the accuracy of the measurement results does not exceed 3% of the reference result;

- The most precise measurement results can be obtained without any contact surface coating between the measurement probe and the AAC;
- EIS measurements can be performed in any range of measurement distances between measurement probes. However, the measurement distance between probes has impact on the determination of the measurement frequency. For measurement distance range from 150mm to 300mm, which comply with measurement distance within borders of one masonry block, the most suitable measurement frequency is 8000Hz;
- Correlation equation between EIS measurement results and moisture content in AAC masonry constructions has been established. Correlation has logarithmic character and slightly differs depending on the type of AAC. The equation developed during the research is $y=a \ln(x) + C$;
- Large cracks and masonry joints have significant impact on the EIS measurement results, therefore EIS should not be applied for detection of moisture content in AAC sections with masonry joints in absolute means. However, EIS can be applied in such sections for non-destructive monitoring of moisture migration in relative means.

During the researches performed in the framework of these thesis following suggestions for the improvement of the Z-meter device has been developed:

- Self-drilling measurement probes should be manufactured;
- Software update for automatic frequency analysis should be developed;
- Software of the Z-meter device should be updated with the correlation equations between the EIS measurement results of most common types of AAC and moisture content rate of AAC.

Thesis for the defence:

- A following methodology for non-destructing detection of moisture distribution throughout the cross section of AAC masonry constructions with Z-meter device has been established:
 1. Choice of measurement points within the AAC masonry construction;
 2. Preparation of measurement bores, cleaning of internal surface of the measurement bores by compressed air;
 3. Frequency analysis of the AAC material (if high accuracy of the EIS measurement results is required);
 4. EIS measurements of the moisture distribution with Z-meter device;

5. Processing of the measurement results.

- Correlation between EIS measurement results and moisture content in AAC is equal to:
 $y = a \ln(x) + C$;
- Distribution of pores throughout the volume of AAC has impact on the accuracy of EIS measurement results, therefore it is advisory to detect expansion direction of the AAC prior the EIS measurements.

Annexes

Annex 1 Vocabulary

<i>No</i>	<i>Term in English / Termins angliiski</i>	<i>Term in Latvian / Termins latviski</i>
1	alterating current	maiņstrāva
2	autoclaved aerated concrete	autoklāvā izturēts gāzbetons
3	capacitance	kapacitāte
4	direct current	līdzstrāva
5	electrical impedance spectrometry	elektriskās impedances spektrometrija
6	expansion direction	izplešanās virziens (gāzbetona ražošanā)
7	gravimetric method	gravimetriskā metode
8	inductance	induktivitāte
9	moisture	mitrums
10	moisture migration	mitruma pārvietošanās
11	resistance	pretestība
12	sustainable construction	ilgtspējīga būvniecība

References

1. Adan, O.C.G. (1995). Determination of Moisture Diffusivities in Gypsum Renders. *Heron*, Vol. 40, No. 3, 201–215.
2. Ait-Mokhtar, A., et al. (2006). Relationship between the Transfer Properties of the Coating and Impedance Spectroscopy in Reinforced Cement-Based Materials. *J. Mat. Sci.* 41:6006–6014 DOI 10.1007/s10853-006-0493-x
3. Akita, H., Fujiwara, T., and Ozaka, Y. (1996). A Practical Procedure for the Analysis of Moisture Transfer within Concrete due to Drying. *Magazine of Concrete Research* 48 (6), 129–137.
4. Alexanderson, J. (1979). Relations between Structure and Mechanical Properties of Autoclaved Aerated Concrete. *Cem. Concr. Res.* 1979;9:507±14 5
5. Andrade, C., Castelo, V., Alonso, C., and Gonzalez, J.A. (1986). Corrosion Effect of Stray Currents and the Technique for Evaluating Corrosion of Rebar in Concrete. ASTM STP-906, Philadelphia.
6. Andrade, C., Keddam, M., Novoa, X.R., Perez, M.C., Rangel, C.M., and Takenouti, H. (2001). Electrochemical Behaviour of Steel Rebars in Concrete: Influence of Environmental Factors and Cement Chemistry. *Electrochim. Acta.* 2001;46:3905–3912. doi: 10.1016/S0013-4686(01)00678-8.
7. Arfvidsson, J., and Janz, M. (1994). Determination of Moisture Transport Coefficients at Very High Moisture Levels by a Series of Capillary Absorption Tests (in Swedish), Part of Report TVBH-7180, Division of Building Physics, Lund Institute of Technology.
8. Barsottelli, M., Cellai, G.F., Fratini, F., and Manganelli Del Fa, C. (2001). The Hygrometric Behaviour of Some Artificial Stone Materials Used as Elements of Masonry Walls. *Materials and Structures/Materiaux et Constructions* 34, 211–216.
9. Barsoukov, E., and McDonald, R. (2005). *Impedance Spectroscopy Theory, Experiment, and Applications*. New York, USA: John Wiley & Sons. ISBN: 0-471-64749-7 39
10. Bave, G. (1980). Aerated Light Weight Concrete-Current Technology. *Proceedings of the Second International Symposium on Lightweight Concretes*. London.
11. Bjerkeli, L. (1990). X-ray Tomography as a Method to Determine the Water Adsorption in Concrete (in Norwegian), Report STF65 A90008, FCB, SINTEF, Trondheim.
12. Bruce, R.R., and Klute, A. (1956). The Measurement of Soil Moisture Diffusivity. *Soil. Sci. Soc. Am. Proc.*, 458–462.

13. Chelidze, T.L., and Gueguen, Y. (1999). Electrical Spectroscopy of Porous Rocks: A Review – Theoretical Models. *Geophys J.Int.* 137, 1–15.
14. Christensen, B.J., Coverdale, R.T., Olson, R.A., Ford, S.J., Garboczi, E.J., Jennings, H.M., and Mason, T.O. (1994). Impedance Spectroscopy of Hydrating Cement Based materials: measurement, interpretation, and application. *J Amer Ceram Soc* 77:2789.
15. Christensen, B.J., Coverdale, R.T., Olson, R.A., Ford, S.J., Garboczi, E.J., Jennings, H.M., and Mason, T.O. (1994). Impedance Spectroscopy of Hydrating Cement-Based Materials: Measurement, Interpretation, and Application. *J Am Ceramic Soc* 77(11), 2789–2802 75.
16. Daniel, A., Vries, D.E. (1987). The Theory of Heat and Moisture Transfer in Porous Media Revisited. *Int J Heat Mass Transf* 30(7), 1343–1350.
17. Dawei, M., Chaozong, Z., Zhiping, G., Yisi, L., Fulin, A., and Quitian, M. (1986). The Application of Neutron Radiography to the Measurement of the Water Permeability of Concrete. *Proceedings of the Second World Conference on Neutron Radiography, Paris, 16–20 June, 255–262*
18. DeAngelis, K.M. (2007). Measurement of Soil Moisture Content by Gravimetric Method. *American Society of Agronomy, 1–2.*
19. Elkey, W., Sellevold, E.J. (1995). Electrical Resistivity of Concrete. Publication No. 80. Norwegian Road Research Laboratory, Oslo, Norway, 11–13.
20. Elsener, B. (1990). Ion Migration and Electric Conductivity in Concrete. Zürich: SchweizerischerIngenieur- und Architekten-Verein. In: *Korrosion und Korrosionsschutz. Tl 5. Electrochemical Protection Process for Concrete Building Structures, Symposium, 51–59.*
21. Fejfarová, M. (2013). The Application of EIS and PIV Methods to the Measurement of Aerated Flow. *EPJ Web of Conferences, Vol. 45, EFM12 – Experimental Fluid Mechanics 2012.*
22. Freitas, V. P., De Krus, M., Künzel, H., and Quenard, D. (1995). Determination of the Water Diffusivity of Porous Materials by Gamma-Ray Attenuation and NMR. *Proceeding of the International Symposium on Moisture Problems in Building Walls, Porto, 445–460.*
23. Funke, K. (1986). Debye-Hückel-Type Relaxation Processes in Solid Ionic Conductors: The Model. *Solid State Ionics* 18–19, 183–190.
24. Garboczi, E.J. (1990). Permeability, Diffusivity, Microstructural Parameters: A Critical Review. *Cement Concrete Res* 20(4), 591–601.
25. Grasley, Z., D.A.L. Relative Humidity in Concrete. *ACI Committee 236, 51–57.*

26. Gu, P., Fu, Y., Xie, P., and Beaudoin, J.J. (1993). Application of A.C. Impedance Techniques in Studies of Porous Cementitious Materials: (I): Influence of Solid Phase and Pore Solution on High Frequency Resistance. *Cem Conc Res* 23 (3), 531–540.
27. Gu, P., Fu, Y., Xie, P., and Beaudoin, J.J. (1994). Characterization of Surface Corrosion of Reinforcing Steel in Cement Paste by Low Frequency Impedance Spectroscopy. *Cem Conc Res* 24(2), 231–242.
28. Guo, X.G., and Chen, Y.M. (2008). Computational Analysis of Heat and Moisture Performance of Multilayer Wall in South China. *J Central South Univ Technol* 114(3),106–110.
29. Hachani, L., Fiaud, C., Triki, E. (1994). Characterisation of Steel/Concrete Interface by Electrochemical Impedance Spectroscopy *Br Corr J* 29, 122.
30. Hall, C. (1989). Water Sorptivity of Mortars and Concretes: A Review. *Mag Concr Res.* 41, 51–61.
31. Hedenblad, G. (1993). Moisture Permeability of Mature Concrete, Cement Mortar and Cement Paste, Report TVBM-1014, Division of Building Materials, Lund Institute of Technology.
32. Jacobs, F., and Mayer, G. (1992). Porosity and Permeability of Autoclaved Aerated Concrete. *Proceedings Advances in Autoclaved Aerated Concrete*, 71–76.
33. Janz, M. (1997). Methods of Measuring the Moisture Diffusivity at High Moisture Levels. Licentiate Thesis, Lund.
34. John DJ, Searson PC, Dawson JL (1981) Use of AC impedance technique in studies on steel in concrete in immersed conditions *Br Corr J* 16:102
35. Johnson, D.L., and Sen, P.N. (1988). Dependence of the Conductivity of a Porous Medium on Electrolyte Conductivity. *Phys Rev B* 37(7), 3502–3510.
36. Jonscher, A.K., and Reau, J.-M. (1978). Analysis of the Complex Impedance Data for beta-PbF₂. *J. Mat. Sci.* 13, 563–570.
37. Justnes, H., Bryhn-Ingebrigtsen, K., and Rosvold, G. O. (1994). Neutron Radiography: An Excellent Method of Measuring Water Penetration and Moisture Distribution in Cementitious Materials. *Advances in Cement Research* 6(22), 67–72
38. Kießel, K., and Krus, M. (1991). NMR-Measurements of Capillary Penetration Behaviour of Water and Hydrophobing Agent in Porous Stone and Derivation of New Capillary Transport Values., Report FtB-12e, Fraunhofer-Institut für Bauphysik, Holzkirchen.
39. Kopinga, K., and Pel, L. (1994). One-Dimensional Scanning of Moisture in Porous Materials with NMR. *Rev. Sci. Instrum.* 65 (12).

40. Kuenzel, H.M. (1995). *Simultaneous Heat and Moisture Transport in Building Components*. Stuttgart: IRB Verlag.
41. Künzel, H.M. (1995). *Simultaneous Heat and Moisture Transport in Building Components – One- and Two-Dimensional Calculation Using Simple Parameters*. Stuttgart: IRB Verlag.
42. Laurent, J.P., Guerre-Chaley, C. (1995). Influence of Water Content and Temperature on the Thermal Conductivity of Autoclaved Aerated Concrete. *Mater Struct* 28, 164–172.
43. Li, A. et al. (2014). Coupled Heat and Moisture Transfer in Two Common Walls. *Proceedings of the 8th International Symposium on Heating, Ventilation and Air Conditioning. Lecture Notes in Electrical Engineering*, 335–342.
44. Loudon, A.G. (1983). The Effect of Moisture Content on Thermal Conductivity of Aerated Concrete. *Proceedings of Autoclaved Aerated Concrete, Moisture and Properties*. Amsterdam: Elsevier, 131–141.
45. Luikov, A.W. (1966). *Heat and Mass Transfer in Capillary-Porous Bodies*. Oxford: Pergamon.
46. Matiasovsky, P., and Mihalka, P. (2014). Pore Structure Parameters and Drying Rates of Building Materials. *Drying and Wetting of Building Materials and Components, Building Pathology and Rehabilitation* 4, 71–90. Springer International Publishing Switzerland. DOI: 10.1007/978-3-319-04531-3_4
47. McCarter, W.J. (1996). Monitoring the Influence of Water and Ionic Ingress on Cover-Zone Concrete Subjected to Repeated Absorption. *Cement, Concrete Aggregates* 18(1), 55–63 77.
48. McCarter, W.J. (1996). The A.C. Impedance Response of Concrete during Early Dehydration. *J Mater Sci* 31(23), 6285–6292.
49. McCarter, W.J., Emerson, M., and Ezirim, H. (1995). Properties of Concrete in the Cover Zone: Developments in Monitoring Techniques. *Magazine of Concrete Research*, 47(172), 243–251.
50. McCarter, W.J., Ezirim, H., and Emerson, M. (1996). Properties of Concrete in the Cover Zone: Water Penetration, Sorptivity, and Ionic Ingress. *Magazine Concrete Res* 48(176), 149–156 76.
51. McCarter, W.J., Garvin, S. (1989). Dependence of Electrical Impedance of Cement-Based Materials on Their Moisture Condition. *Journal of Applied Physics Series D: Applied Physics* 22 (10), 1773–1776 69.

52. McCarter, W.J., Garvin, S. (1989). Dependence of Electrical Impedance of Cement-Based Materials on Their Moisture Condition. *Journal of Applied Physics Series D: Applied Physics* 22 (10), 1773–1776.
53. Mendes, N., Winkelmann, F.C., Lamberts, R. et al. (2003). Moisture Effects on Conduction Loads. *Energy Build* 35(7), 641–644.
54. Monfore, G.E. (1968). The Electrical Resistivity of Concrete. Bulletin 224, Research and Development Laboratories of the Portland Cement Association, Chicago, Illinois.
55. Multon, S.E.M. (2004). Water Distribution in Beams Damaged by Alkali-Silica Reaction: Global Weighing and Local Gammadensitometry. *Materials and Structures* 37.
56. Narayanan, N. (1998). Influence of Composition on the Structure and Properties of Aerated Concrete. M.S thesis. IIT Madras.
57. Narayanan, N., and Ramamurthy, K. (2000). Structure and Properties of Aerated Concrete: A Review. *Cement & Concrete Composites* 22, 321–329.
58. Parilkova, J. The EIS Method and a Z-meter III Device, a lecture within an event in Litice.
59. Parilkova, J., et al. (2011). Monitoring of Changes in Moisture Content of the Masonry due to Microwave Radiation Using the EIS Method. EUREKA 2011, Brno, ISBN 978-80-214-4325-9
60. Parrott, L.J. (1988). Moisture Profiles In Drying Concrete. *Adv. Cem. Res.* 1, 164–170.
61. Pel, L. (1995). Moisture Transport in Porous Building Materials. Eindhoven University of Technology.
62. Pel, L., Brocken, H., and Kopinga, K. (1996). Determination of Moisture Diffusivity in Porous Media Using Moisture Concentration Profiles. *Int J Heat Mass Transf* 39, 1273–1280.
63. Pel, L., Landman, K.A. (2004). A Sharp Drying Front Model. *Drying Technol* 22, 637–647.
64. Pel, L., Landman, K.A., and Kaasschieter, E.F. (2002). Analytic Solution for the Non-Linear Drying Problem. *Int J Heat Mass Transf* 45, 3173–3180.
65. Petrov, I., and Schlegel, E. (1994). Application of Automatic Image Analysis for the Investigation of Autoclaved Aerated Concrete Structure. *Cem Concr Res* 24, 830–40.
66. Philip, J.R., and DeVries, D.A. (1975). Moisture Movement in Porous Materials under Temperature Gradients. *Trans Am Geophys Union* 2, 222–232.
67. Phillipson, M.C., Baker, P.H., Davies, M., et al. (2007). Moisture Measurement in Building Materials: An Overview of Current Methods and New Approaches. *Build Serv Eng Res Technol*, 28(4), 303–316.

68. Physics, C. (2010). Relative humidity sensors, 1–3.
69. Prazak, J, and Lunk, P. (1992). Capillary Suction of AAC. Proceedings of Advances in Autoclaved Aerated Concrete, 119–123.
70. Prim, P., Witmann, F.H. (1983). Structure and Water Absorption of Aerated Concrete. Proceedings of Autoclaved Aerated Concrete, Moisture and Properties. Amsterdam: Elsevier, 43–53.
71. Qiankun, W., Youzhi, C., Fangxian, L., Tao, S., Bingbo, X. (2006). Microstructure and Properties of Silty Siliceous Crushed Stone-lime Aerated Concrete. Journal of Wuhan University of Technology - Mater. Sci. FA 21(2), 17–20.
72. Qin, M.H., Belarbi, R., Aït-Mokhtar, A. et al. (2009). Coupled Heat and Moisture Transfer in Multilayer Building Materials. Constr Build Mater 23(2), 967–975.
73. Quincot, G., Azenha, M., Barros, J., and Faria, R. (2011). State of the Art – Methods to Measure Moisture in Concrete. Projetos De Investigação Científica E Desenvolvimento Tecnológico, Portugal.
74. Rajabipour, F, Weiss, W.J., and Abraham, D. (2004). In Situ Electrical Conductivity Measurements to Assess Moisture and Ionic Transport in Concrete. Advances in concrete through science and engineering; Proceedings of the International RILEM Symposium, Evanston, Illinois.
75. Rajabipour, F. (2006). In Situ Electrical Sensing and Material Health Monitoring of Concrete Structures. Ph.D. Dissertation, West Lafayette, Indiana: Purdue University.
76. Rajabipour, F., and Weiss, J. (2007). Electrical Conductivity of Drying Cement Paste, Materials and Structures 40, 1143–1160. DOI 10.1617/s11527-006-9211-z 84
77. Rajabipour, F., Weiss, J., Shane, J.D., Mason, T.O., and Shah, S.P. (2005). A Procedure to Interpret Electrical Conductivity Measurements in Cover Concrete during Rewetting. Journal of Materials in Civil Engineering, 17(5), 586–594 32.
78. Revil, A, and Glover, P.W.J. (1997). Theory of Ionic-Surface Electrical Conduction in Porous Media. Phys Rev B 55(3), 1757–1773.
79. Richard, T.G. (1977). Low Temperature Behaviour of Cellular Concrete. J Am Concr Inst 47, 173–8.
80. RILEM (1991). Materials and Structures/Materiaux et Constructions, 24, 317–320.
81. RILEM recommended practice. (1993). Autoclaved aerated concrete ±Properties, testing and design. E&FN SPON.

82. Roels, S., Carmeliet, J., Hens, H., et al. (2004). A Comparison of Different Techniques to Quantify Moisture Content Profiles in Porous Building Materials. *J Therm Envelope Build Sci* 27(4), 261–276.
83. Rubene, S. et al. (2014). Determination of Humidity Level in Aerated Concrete Constructions by Non Destructive Testing Methods. Proc “Innovative Materials, Structures and Technologies”, Riga, 135–140.
84. Rubene, S., and Vilnītis, M. (2013). Application of Electrical Impedance Spectrometry for Determination of Moisture Distribution in Aerated Concrete Constructions. Proc. “1st Conference and Working Session Eureka! 7614”, Brno, Czech Republic, 124–130.
85. Rubene, S., Vilnītis, M., Noviks, J. (2014). Monitoring of the Aerated Concrete Construction Drying Process by Electrical Impedance Spectrometry. Proceedings of 4th International Conference “Advanced Construction 2014”, Lithuania, Kaunas, 9–10 October 2014. Kaunas: Kaunas University of Technology, 216–220. ISSN 2029-1213
86. Rubene, S., Vilnītis, M., Noviks, J. (2015). Frequency Analysis for EIS Measurements in Autoclaved Aerated Concrete Constructions. *Procedia Engineering* 108, 647–654. ISSN 1877-7058. Available from: doi:10.1016/j.proeng.2015.06.194
87. Rubene, S., Vilnītis, M., Noviks, J. (2015). Impact of Masonry Joints on Detection of Humidity Distribution in Aerated Concrete Masonry Constructions by Electric Impedance Spectrometry Measurements. *International Journal of Civil, Architectural, Structural and Construction Engineering* 9(1) 1089–1094. e-ISSN 1307-6892
88. Rudnai, G. (1963). *Light Weight Concretes*. Budapest: Akademi Kiado.
89. Saremi, M., Mahallati, E. (2002). A Study on Chloride-Induced Depassivation of Mild Steel in Simulated Concrete Pore Solution. *Cem Conc Res* 32(12), 1915–1921.
90. Schießl, A., Weiss, W.J., Shane, J.D., Berke, N.S., Mason, T.O., and Shah, S.P. (2002). Assessing the Moisture Profile of Drying Concrete Using Impedance Spectroscopy. *Concrete Science and Engineering* 2, 106-116.
91. Schmit, T., Rajabipour, F., and Weiss, W.J. (2005). Investigating the Use of a Diffuse Measurement Interpretation for Analyzing In Situ Electrical Measurements. The 3rd International Conference on Construction Materials: ConMat’05. Vancouver, Canada.
92. Scuderi, C.A., Mason, T.O., and Jennings, H.M. (1991). Impedance Spectra of Hydrating Cement Pastes. *J Mater Sci* 26(2), 349–353.
93. Selih, J., Sousa A.C.M., and Bremner, T.W. (1996). Moisture Transport in Initially Fully Saturated Concrete during Drying. *Transport in Porous Media* 24, 81–106.

94. Skramlik, J., and Novotny, M. (2008). One-Dimensional Moisture Transport Monitored by a Non-Destructive Method. *International Journal of Computers* 2(4).
95. Skramlik, J., et al. (2011). Determining Moisture Parameters in Building Materials. 5th Pan American Conference for NDT. 2–6 October 2011, Cancun, Mexico.
96. Sosoro, M., and Reinhardt, H.W. (1995). Thermal Imaging of Hazardous Organic Fluids in Concrete. *Materials and Structures* 28(183), 526–533.
97. Tada, S. (1986). Material Design of Aerated Concrete. An Optimum Performance Design. *Materials and Construction* 19, 21–6.
98. Tada, S. (1992). Pore Structure and Moisture Characteristics of Porous Inorganic Building Materials. *Proceedings of Advances in Autoclaved Aerated Concrete*. A.A. Balkema, 53–63.
99. Tada, S., and Nakano, S. (1983). Microstructural Approach to Properties of Moist Cellular Concrete. *Proceedings of Autoclaved Aerated Concrete, Moisture and Properties*. Amsterdam: Elsevier, 71–89.
100. Tamtsia, T., Beaudoin, J.J., and Marchand, J. (2003). A Coupled AC Impedance – Creep and Shrinkage Investigation of Hardened Cement Paste. *Journal of Materials and Structures* 36, 147–155 40
101. Valore, R.C. (1954). Cellular Concretes-Composition and Methods of Preparation. *J Am Concr Inst* 25, 773–95.
102. Valore, R.C. (1956). Insulating concretes. *J Am Concr Inst* 28, 509–32.
103. Villain, G., and Thiery, M. (2006). Gammadensimetry: A Method to Determine Drying and Carbonation Profiles in Concrete. *NDT & E International* 39(4), 328–337.
104. Vos, B.H. (1965). Non-Steady-State Method for the Determination of Moisture Content in Structures. *Humidity and Moisture* 4, 35–47.
105. Vu, T.H. (2006). Influence of Pore Size Distribution on Drying Behaviour of Porous Media by a Vontinuous Model. PhD thesis, Magdeburg: Otto von Guericke University.
106. Watson, K.L., Eden, N.B., and Farrant, J.R. (1977). Autoclaved Aerated Materials from Slate Powder and Portland Cement. *Precast Concr.*, 81–85.
107. Weiss, W.J. (1999). Prediction of Early-Age Shrinkage Cracking in Concrete. Ph.D. Dissertation, Evanston, Illinois: Northwestern University.
108. Weiss, W.J., Shane, J.D., Mieses, A., Mason, T.O., and Shah, S.P. (1999). Aspects of Monitoring Moisture Changes Using Electrical Impedance Spectroscopy. *Proceedings of the 2nd Symposium on Self-Desiccation and Its Importance in Concrete Technology*, Lund, Sweden, 78.

109. Weiss, W.J., Shane, J.D., Mieses, A., Mason, T.O., and Shah, S.P. Aspects of Monitoring Moisture Changes Using Electrical Impedance Spectroscopy. Proceedings of the 2nd Symposium on Self-Desiccation and Its Importance in Concrete Technology, Lund, Sweden.
110. Whittington, H.W., McCarter, W.J., and Forde, M.C. (1981). The Conduction of Electricity through Concrete. Magazine Concrete Res 33(114), 48–60.
111. Wiederhold, P.R. (1997). Water Vapour Measurement, Methods, and Instrumentation. NY: Marcel Dekker, Inc.
112. Wilson, M.A., Hoff, W.D., and Hall, C. (1991). Water Movement in Porous Building Materials ± Absorption from a Small Cylindrical Cavity. Build Environ 26, 143–152.
113. Woloszyn, M., and Rode, C. (2008). Tools for Performance Simulation of Heat, Air and Moisture Conditions of Whole Buildings. Build Simul 1(1), 5–24.
114. Zhang, P., Wittman, F.H., Zhao, T.J., Lehmann, E., Jin, Z.Q. (2010). Visualization and Quantification of Water Movement in Porous Cement-Based Materials by Real Time Thermal Neutron Radiography: Theoretical Analysis and Experimental Study. Science China – Technological Sciences 53(5), 1198–1207 doi: 10.1007/s11431-010-0115-3

List of publications

1. Rubene, S., Vilnītis, M. Application of Electrical Impedance Spectrometry for Determination of Moisture Distribution in Aerated Concrete Constructions. In: EUREKA 2013: 1st Conference and Working Session: Proceedings, Czech Republic, Karolinka, 30 October – 1 November 2013. Brno: VUTIUM, Brno University of Technology, 2013, pp. 124–131. ISBN 978-80-214-4735-6.
2. Rubene, S., Vilnītis, M., Noviks, J. Impact of Contact Surface on Accuracy of Humidity Distribution Measurements in Autoclaved Aerated Concrete Constructions by EIS. In: Proceedings of 1st International Conference on Civil Engineering, Water Resources, Hydraulics and Hydrology (CEWHH 2014), Greece, Athens, 28–30 November 2014. Athens: EUROPMENT, 2014, pp. 99–104. ISBN 978-1-61804-253-8.
3. Rubene, S., Vilnītis, M. Correlation between EIS Measurements and Relative Humidity Distribution in Aerated Concrete Masonry Constructions. In: Recent Advances in Civil Engineering and Mechanics. Mathematics and Computers in Science and Engineering Series 35, Italy, Florence, 22–24 November 2014. Florence: WSEAS Press, 2014, pp. 67–72. ISBN 978-960-474-403-9. ISSN 2227-4588.
4. Rubene, S., Vilnītis, M. Monitoring of Humidity Distribution Changes in Aerated Concrete Masonry Construction by EIS. In: EUREKA 2014: 2nd Conference and Working Session Proceedings, Czech Republic, Brno, 30–31 October 2014. Brno: VUTIUM Brno University of Technology, 2014, pp. 124–130. ISBN 978-80-214-4883-4.
5. Rubene, S., Vilnītis, M., Noviks, J. Monitoring of the Aerated Concrete Construction Drying Process by Electrical Impedance Spectrometry. In: Proceedings of 4th International Conference “Advanced Construction 2014”, Lithuania, Kaunas, 9–10 October 2014. Kaunas: Kaunas University of Technology, 2014, pp. 216–220. ISSN 2029-1213.
6. Rubene, S., Noviks, J., Vilnītis, M. Determination of Humidity Level in Aerated Concrete Constructions by Non Destructive Testing Methods. In: Proceedings of the International Conference “Innovative Materials, Structures and Technologies”, Latvia, Riga, 28-30 November 2013. Riga: RTU Press, 2014, pp. 141–146. ISBN 978-9934-10-583-8. e-ISBN 978-9934-10-584-5. Available from: doi:10.7250/isconstrs.2014.23

7. Rubene, S., Vilnītis, M., Noviks, J. Impact of Masonry Joints on Detection of Humidity Distribution in Aerated Concrete Masonry Constructions by Electric Impedance Spectrometry Measurements. *International Journal of Civil, Architectural, Structural and Construction Engineering*, 2015, Vol. 9, No. 1, pp. 1089–1094. e-ISSN 1307-6892.
8. Rubene, S., Vilnītis, M., Noviks, J. Impact of External Heat Insulation on Drying Process of Autoclaved Aerated Concrete Masonry Constructions. *IOP Conference Series: Materials Science and Engineering*, 2015, Vol. 96, conference 1, pp. 1–8. ISSN 1757-8981. e-ISSN 1757-899X. Available from: doi:10.1088/1757-899X/96/1/012059 (SCOPUS indexed).
9. Rubene, S., Vilnītis, M., Noviks, J. Frequency Analysis and Measurements of Moisture Content of AAC Masonry Constructions by EIS. *Procedia Engineering*, 2015, Vol. 123, pp. 471–478. ISSN 1877-7058. Available from: doi:10.1016/j.proeng.2015.10.096 (SCOPUS indexed).
10. Rubene, S., Vilnītis, M., Noviks, J. Frequency Analysis for EIS Measurements in Autoclaved Aerated Concrete Constructions. *Procedia Engineering*, 2015, Vol. 108, pp. 647–654. ISSN 1877-7058. Available from: doi:10.1016/j.proeng.2015.06.194 (SCOPUS indexed).
11. Rubene, S., Vilnītis, M. Application of Electrical Impedance Spectrometry for Measurements of Humidity Distribution in Aerated Concrete Masonry Constructions. *International Journal of Mechanics*, 2015, Vol. 9, pp. 213–219. ISSN 1998-4448. (SCOPUS indexed).
12. Rubene, S., Vilnītis, M., Noviks, J. Impact of Density and Special Features of Manufacturing Process on Drying of Autoclaved Aerated Concrete Masonry Blocks. In: *Environment.Technology.Resources*. Rezekne, Latvia: Rezekne Higher Education Institution, 2015, pp. 186–192. ISSN 1691-5402. (SCOPUS indexed).
13. Rubene, S., Vilnītis, M. Frequency Analysis and Measurements of Moisture Content of AAC Masonry Constructions by EIS. In: *Proceedings “Creative Construction Conference 2015”*. Budapest, Hungary: Diamond Congress Ltd., 2015, pp. 147–147. ISBN 978-963-269-491-7.
14. Rubene, S., Vilnītis, M. Monitoring of Water Infiltration in Autoclaved Aerated Concrete Masonry Construction Blocks by Electrical Impedance Spectrometry. In: *Recent Advances in Mechanical Engineering Series 17 “Fluids, Heat and Mass Transfer, Mechanical and Civil Engineering”*, Hungary, Budapest, 12–14 December

2015. Budapest: WSEAS Press, 2015, pp. 106–111. ISBN 978-1-61804-358-0. ISSN 2227-4596.
15. Rubene, S., Vilnītis, M. Impact of Porous Structure of the AAC Material on Moisture Distribution throughout the Cross Section of the AAC Masonry Blocks. WSEAS Transactions on Heat and Mass Transfer, 2016, Vol. 11, pp. 13–20. ISSN 1790-5044. e-ISSN 2224-3461.
16. Rubene, S., Vilnītis, M. Accuracy of Humidity Distribution Measurements in Autoclaved Aerated Concrete Constructions by Electrical Impedance Spectrometry. In: EUREKA 2015 Proceedings, Czech Republic, Jaromerice nad Rokytinou, 15–16 October, 2015. Brno: 2015, pp. 156–164. ISSN 2464-4595.

DECLARATION OF ACADEMIC INTEGRITY

I hereby declare that the Doctoral Thesis submitted for the review to Riga Technical University for the promotion to the scientific degree of Doctor of Engineering Science is my own and does not contain any unacknowledged material from any source. I confirm that this Thesis has not been submitted to any other university for the promotion to other scientific degree.

Sanita Rubene

/26.08.2016/

The Doctoral Thesis contains introduction, three chapters, conclusion, bibliography comprising 114 reference sources and one appendix. It has been illustrated by 107 figures. The volume of the Thesis is 112 pages.